

**Investigation of Factors that Limit Efficacy of Ultraviolet Disinfection in
Water and Wastewater Treatment**

by

Kerim Kollu

B.S., M.A.Sc. Environmental Engineering

A thesis submitted to the Faculty of Graduate and Postdoctoral Affairs
in partial fulfillment of the requirements for the degree of

Doctor of Philosophy

in

Environmental Engineering

Department of Civil and Environmental Engineering

Carleton University

Ottawa, Ontario

Ottawa-Carleton Institute of Civil and Environmental Engineering

©2014

Kerim Kollu

ABSTRACT

This research has been undertaken to contribute to our understanding of factors that limit and hinder ultraviolet (UV) disinfection efficacy, specifically the presence of flocs, and self-aggregation, regrowth and reactivation of microorganisms (Chapters 1 and 2). Chapter 4 aimed to provide an in-depth understanding of the effect of particles and flocs on UV disinfection by using a well-defined and well-controlled synthetic system that simulates the bioflocculation process. Results indicated that particle size had significant effects on *Escherichia coli* (*E. coli*) inactivation at high UV doses, and larger particles protected bacteria more than smaller particles. Moreover, the size of the constituent particles of flocs did not make a significant difference on inactivation levels. In Chapter 5, the bioflocculation process was monitored with a dynamic particle analyzer (DPA 4100) and UV inactivation data were assessed in light of the floc characteristics determined with the particle analyzer. Less circular and more porous flocs formed when the degree of bioflocculation was increased and larger flocs had a more heterogeneous structure. Irradiation experiments confirmed that floc size alone cannot explain how much *E. coli* are protected from UV light in the presence of particles and flocs. In Chapter 6, the DPA 4100 and an inverted microscope (Nikon Eclipse Ti) were used to examine the extent of UV-induced self-aggregation of *E. coli* after exposure to low-pressure and medium-pressure UV irradiation. All low-pressure UV doses tested yielded significant increases in particle size following UV exposure, indicating self-aggregation. In the medium-pressure UV experiments, only a dose of 80 mJ/cm² had a significant impact on the formation of aggregates upon UV exposure. In Chapter 7, the regrowth issue was addressed by studying regrowth in the absence of reactivation. Results showed

that percent regrowth of *E. coli* and indigenous wastewater bacteria were higher after UV disinfection at 40 mJ/cm² than at 15 mJ/cm². Regrowth of *E. coli* was observed even in phosphate-buffered saline with no added nutrients indicating that lysis of UV-damaged cells may provide nutrients for surviving bacteria. Overall, this research underscores the importance of addressing the aforementioned issues for improving UV disinfection performance and better protecting public health.

TABLE OF CONTENTS

ABSTRACT.....	ii
TABLE OF CONTENTS.....	iv
LIST OF TABLES.....	x
LIST OF FIGURES.....	xi
LIST OF APPENDICES.....	xvi
CHAPTER 1.....	1
INTRODUCTION.....	1
1.1. References.....	6
CHAPTER 2.....	11
LITERATURE REVIEW.....	11
2.1. UV Disinfection.....	11
2.2. Particle and Aggregation Related Issues.....	15
2.2.1. Origin and Nature of Particles and Aggregates in Water.....	16
2.2.2. Particle Measurements.....	19
2.2.3. Effect of Particles and Aggregation on UV Disinfection.....	21
2.2.4. Tailing Phenomenon.....	26
2.2.5. Enumeration.....	27
2.3. Reactivation Related Issues.....	29
2.3.1. Photoreactivation.....	29

2.3.2. Dark Repair	30
2.3.3. Review of Previous Research on Photoreactivation	31
2.3.4. Review of Previous Research on Dark Repair.....	40
2.4. Regrowth.....	41
2.5. Summary of the Literature Review	43
2.6. References.....	44
CHAPTER 3	56
MATERIALS AND METHODS.....	56
3.1. Determination of Ingredients for Synthetic Floccs.....	56
3.2. Preparation of Stock Solutions and Growth Media	59
3.3. Preparation of Synthetic Floccs	60
3.4. UV Collimated Beam Setup.....	62
3.5. UV Dose Determination	64
3.6. Bacterial Enumeration	68
3.7. Particle/Floc Size, Concentration and Shape Analyses	70
3.8. Presentation of the Inactivation Data.....	71
3.9. References.....	72
CHAPTER 4	74
EFFECT OF PARTICLES AND BIOFLOCCULATION ON ULTRAVIOLET DISINFECTION OF <i>ESCHERICHIA COLI</i>	74

4.1. Abstract	74
4.2. Introduction	75
4.3. Materials and Methods	78
4.3.1. Preparation of particle suspensions	78
4.3.2. Addition of <i>E. coli</i>	78
4.3.3. Bioflocculation of particles	79
4.3.4. UV irradiation experiments	80
4.3.5. <i>E. coli</i> enumeration	81
4.3.6. Particle and floc size measurements	82
4.3.7. Experimental design and data analysis	82
4.4. Results and Discussion	84
4.4.1. Phase I: effect of particles on UV inactivation	84
4.4.2. Phase II: effect of bioflocculation on UV inactivation	88
4.4.3. Phase III: comparison of UV inactivation of non-flocculated and flocculated samples	91
4.4.4. Implications for UV disinfection applications	95
4.5. Conclusions	96
4.6. References	98
4.7. Figures and Tables	101
CHAPTER 5	110

EFFECT OF BIOFLOCCULATION PARAMETERS ON THE SIZE AND STRUCTURE OF FLOCS.....	110
5.1. Abstract.....	110
5.2. Introduction.....	111
5.3. Materials and Methods.....	113
5.3.1. Sample Preparation.....	113
5.3.2. Bioflocculation.....	114
5.3.3. Particle and Floc Analyses.....	116
5.3.4. UV Disinfection Experiments.....	118
5.4. Results and Discussion	118
5.5. Conclusions.....	128
5.6. References.....	129
5.7. Figures and Tables	132
CHAPTER 6	140
UV-INDUCED SELF-AGGREGATION OF <i>E. COLI</i> AFTER LOW AND MEDIUM PRESSURE ULTRAVIOLET IRRADIATION	140
6.1. Abstract.....	140
6.2. Introduction.....	141
6.3. Materials and Methods.....	143
6.3.1. Sample Preparation	143

6.3.2. UV Irradiation Setups	144
6.3.3. Microscopy and Particle Count Analyses	146
6.4. Results and Discussion	147
6.4.1. Effect of LP UV irradiation	147
6.4.2. Effect of MP UV irradiation	150
6.4.3. Effect of UV light intensity and exposure time	151
6.4.4. Time resolved analysis of aggregates	152
6.4.5. Implications for UV disinfection applications.....	155
6.5. Conclusions.....	155
6.6. References.....	156
6.7. Figures and Tables	160
CHAPTER 7	173
REGROWTH POTENTIAL OF BACTERIA AFTER ULTRAVIOLET DISINFECTION IN ABSENCE OF LIGHT AND DARK REPAIR.....	173
7.1. Abstract	173
7.2. Introduction.....	174
7.3. Materials and Methods.....	176
7.3.1. Experimental design.....	176
7.3.2. Culture preparation	176
7.3.3. Water matrices	178

7.3.4. Control for light and dark repair	179
7.3.5. UV reactor setup and dose calculations	181
7.3.6. Enumeration	182
7.4. Results and Discussion	182
7.5. Conclusions.....	189
7.6. References.....	191
7.7. Figures and Tables	194
CHAPTER 8	199
CONCLUSIONS AND SUGGESTIONS FOR FUTURE RESEARCH	199
APPENDIX A: ADDITIONAL DATA FOR CHAPTER 5.....	203

LIST OF TABLES

Table 3.1: Polystyrene latex particle characteristics	58
Table 4.1: Experimental design used for different phases.....	101
Table 6.1: Percent change from before UV irradiation to after UV irradiation.....	172
Table A.1: Number concentrations of very large flocs.....	203

LIST OF FIGURES

Figure 2.1: UV induced damage to the DNA: after UV exposure adjacent thymine bases bond with each other, instead of across the ladder (Source: Allen, J., 2001).	12
Figure 2.2: A typical dose-response curve where lag and tailing are observed.....	14
Figure 2.3: Divalent cation bridging within a floc (Source: Urbain et al., 1993, Modified).	18
Figure 3.1: Low-pressure UV collimated beam setup (Source: Bolton and Linden, 2003).	63
Figure 4.1: Size distributions of 1- μm particle suspension (a), 3.2- μm particle suspension (b), 11- μm particle suspension (c), 25- μm particle suspension (d), and 45- μm particle suspension (e).....	102
Figure 4.2: <i>E. coli</i> dose-response curves in the absence of particles (a), in the presence of 3.2 μm , 11 μm and 25 μm particles (b), and in the presence of 1 μm , 11 μm , and 45 μm particles.	103
Figure 4.3: Flocs observed by flow-cell imaging during the bioflocculation of 1- μm particles at increasing calcium doses (a) and flocs of 11- μm particles observed by the naked eye at an elevated calcium concentration for better visibility (b).	104
Figure 4.4: <i>E. Coli</i> dose-response curves under increasing degrees of flocculation (from 0 mM to 15 mM Ca^{2+}) in suspensions of 3.2- μm (a), 11- μm (b), and 25- μm (c) particles.	105
Figure 4.5: <i>E. Coli</i> dose-response curves under increasing degrees of flocculation (from 0 mM to 15 mM Ca^{2+}) in suspensions of 1- μm (a), 11- μm (b), and 45- μm (c) particles..	106

Figure 4.6: Flow-cell images of non-flocculated and flocculated suspensions of 3.2- μm (a), 11- μm (b) and 25- μm (c) particles.	107
Figure 4.7: <i>E. coli</i> dose-response curves in non-flocculated (a) and flocculated (b) suspensions of 3.2, 11, and 25- μm particles.	108
Figure 4.8: Comparison of <i>E. coli</i> inactivation levels of non-flocculated and flocculated suspensions of 3.2- μm particles (a), 11- μm particles (b) and 25- μm particles (c) using box-and-whisker diagrams where the box represents the distribution of the inactivation data from the 25 th to the 75 th percentile value and the whiskers extend to the minimum and maximum inactivation values.	109
Figure 5.1: Particle size distributions at a given particle size, 3.2 μm (a), 11 μm (b) and 25 μm (c), and at calcium concentrations of 0, 5, 10 and 15 mM.	132
Figure 5.2: Floccs observed by flow-cell imaging during the bioflocculation of 25- μm particles at calcium concentrations of 0 mM (a), 5 mM (b), 10 mM (c), 15 mM (d)....	133
Figure 5.3: Analyses of floccs formed at calcium concentrations of 0, 5, 10 and 15 mM with respect to maximum diameter, circularity, area and porosity when particles used were 3.2 μm (a, b), 11 μm (c, d) and 25 μm (e, f).	134
Figure 5.4: Analyses of the twenty largest (by area) floccs formed at calcium concentrations of 0, 5, 10 and 15 mM with respect to maximum diameter, circularity, area and porosity when particles used were 3.2 μm (a, b), 11 μm (c, d) and 25 μm (e, f).....	135
Figure 5.5: Comparison of particle sizes used for making floccs with respect to flocc porosity and area at calcium concentrations of 0 mM (a), 5 mM (b), 10 mM (c) and 15 mM (d).	136

Figure 5.6: Floc porosity versus area when samples were flocculated by adding 15 mM of calcium and 3.2 μm (a), 11 μm (b) and 25 μm (c) particles.	137
Figure 5.7: Floc circularity versus area when samples were flocculated by adding 15 mM of calcium and 3.2 μm (a), 11 μm (b) and 25 μm (c) particles.	138
Figure 5.8: Log inactivation of <i>E. coli</i> when only particles were added (a), samples were flocculated by adding 15 mM of calcium (b).	139
Figure 6.1: Effect of UV irradiation on aggregate formation. Low-pressure 40 mJ/cm^2 before (a) and after (b) UV irradiation. Low-pressure 60 mJ/cm^2 before (c) and after (d) UV irradiation.	160
Figure 6.2: Effect of UV irradiation on size distribution. Low-pressure 20 mJ/cm^2 , % of particles which are $\leq 2 \mu\text{m}$ (a), $> 2 \mu\text{m}$ (b), $> 3 \mu\text{m}$ (c), $> 4 \mu\text{m}$ (d), $> 5 \mu\text{m}$ (e), $> 10 \mu\text{m}$ (f).	161
Figure 6.3: Effect of UV irradiation on size distribution. Low-pressure 40 mJ/cm^2 , % of particles which are $\leq 2 \mu\text{m}$ (a), $> 2 \mu\text{m}$ (b), $> 3 \mu\text{m}$ (c), $> 4 \mu\text{m}$ (d), $> 5 \mu\text{m}$ (e), $> 10 \mu\text{m}$ (f).	162
Figure 6.4: Effect of UV irradiation on size distribution. Low-pressure 60 mJ/cm^2 , % of particles which are $\leq 2 \mu\text{m}$ (a), $> 2 \mu\text{m}$ (b), $> 3 \mu\text{m}$ (c), $> 4 \mu\text{m}$ (d), $> 5 \mu\text{m}$ (e), $> 10 \mu\text{m}$ (f).	163
Figure 6.5: Effect of UV irradiation on size distribution. Low-pressure 80 mJ/cm^2 , % of particles which are $\leq 2 \mu\text{m}$ (a), $> 2 \mu\text{m}$ (b), $> 3 \mu\text{m}$ (c), $> 4 \mu\text{m}$ (d), $> 5 \mu\text{m}$ (e), $> 10 \mu\text{m}$ (f).	164
Figure 6.6: Size distribution before and after UV irradiation, low-pressure lamps, doses of 20 (a), 40 (b), 60 (c), and 80 (d) mJ/cm^2	165

Figure 6.7: Effect of UV irradiation on size distribution. Medium-pressure 40 mJ/cm ² , % of particles which are ≤2 μm (a), >2 μm (b), >3 μm (c), >4 μm (d), >5 μm (e), >10 μm (f).....	166
Figure 6.8: Effect of UV irradiation on size distribution. Medium-pressure 80 mJ/cm ² , % of particles which are ≤2 μm (a), >2 μm (b), >3 μm (c), >4 μm (d), >5 μm (e), >10 μm (f).....	167
Figure 6.9: Size distribution before and after UV irradiation, medium-pressure lamps, doses of 40 (a), and 80 (b) mJ/cm ²	168
Figure 6.10: Effect of UV irradiation on size distribution. Low-pressure 40 mJ/cm ² , low intensity and long exposure time experiments, % of particles which are ≤2 μm (a), >2 μm (b), >3 μm (c), >4 μm (d), >5 μm (e), >10 μm (f).....	169
Figure 6.11: Size distribution before and after UV irradiation, low-pressure lamps, dose of 40 mJ/cm ² , short exposure time (a) versus long exposure time (b).....	170
Figure 6.12: Time Resolved Sampling. Low-pressure 40 mJ/cm ² . Number concentration of particles before (a) and after (b) exposure to UV light. Mean size of the particle population before (c) and after (d) exposure to UV light.	171
Figure 6.13: Time Resolved Sampling. Low-pressure 80 mJ/cm ² . Number concentration of particles before (a) and after (b) exposure to UV light. Mean size of the particle population before (c) and after (d) exposure to UV light.	172
Figure 7.1: Experimental design.	194
Figure 7.2: Number of surviving <i>E. coli</i> in PBS over 48 hours after exposure to 15 and 40 mJ/cm ² when initial <i>E. coli</i> concentration was 5-, 7- or 9-log.....	195

Figure 7.3: Percent change in <i>E. coli</i> concentration in PBS for the 7- and 9-log samples after exposure to 15 and 40 mJ/cm ²	195
Figure 7.4: Number of surviving <i>E. coli</i> in nutrient enriched PBS over 48 hours after exposure to 15 mJ/cm ² when initial <i>E. coli</i> concentration was 5-, 7- or 9-log. Arrows show that the actual <i>E. coli</i> concentrations were higher than the measured values.....	196
Figure 7.5: Number of surviving <i>E. coli</i> in autoclaved secondary wastewater over 48 hours after exposure to 15 and 40 mJ/cm ² when initial <i>E. coli</i> concentration was 5-, 7- or 9-log.	196
Figure 7.6: Percent change in <i>E. coli</i> concentration in autoclaved wastewater for the 7- and 9-log samples after exposure to 15 and 40 mJ/cm ²	197
Figure 7.7: Number of surviving total coliform in wastewater over 48 hours after exposure to 15 and 40 mJ/cm ²	198
Figure 7.8: Percent change in total coliform concentration in wastewater over 48 hours after exposure to 15 and 40 mJ/cm ²	198

LIST OF APPENDICES

APPENDIX A: ADDITIONAL DATA FOR CHAPTER 5	203
---	-----

CHAPTER 1

INTRODUCTION

Water disinfection dates back to as early as the mid to late 1800's and has played the largest role in reducing the number of waterborne disease outbreaks (USEPA, 2000). Disinfection processes make an essential and final barrier against human exposure to pathogenic microorganisms during water and wastewater treatment processes. In fact, a significant part of the decrease in infant and total mortality rates in the developed world during the early twentieth century can be attributed to the introduction of chlorination and filtration into water treatment (Cutler and Miller, 2005). Since then, emerging health and environmental concerns, stricter regulations, and development of new technologies have continuously been shaping the design of disinfection systems and the extent of disinfection required during treatment of drinking water and wastewater. Historically, chlorine has been the most widely used disinfectant in the water treatment industry. However, recent discoveries have demonstrated that chlorination by-products and disinfectant residuals have harmful effects on humans and the environment. Therefore, some restrictions on chlorine concentration have come into effect around the world. In the Canadian Wastewater Systems Effluent Regulation (2012), for instance, total residual chlorine is defined as a "deleterious substance" (Section 5(C)) and the permissible average concentration of total residual chlorine is limited to 0.02 mg/L for wastewater effluents (Section 6(1)(C)). Water treatment facilities will therefore need to install dechlorination units or replace chlorination units by other means of disinfection in order to reduce the harmful effects related to chlorination.

Ideally, a disinfectant should cause no hazardous by-product formation at doses that would typically be encountered in water treatment. A promising example of such a system is ultraviolet (UV) radiation disinfection (Malley et al., 1995). In addition to being safe with regards to by-products, studies indicated UV light's effectiveness against chlorine resistant protozoa, specifically: *Cryptosporidium parvum* and *Giardia lamblia* (Linden et al., 2002; Shin et al., 2001; Clancy et al., 2000). These developments, along with the improvements in the UV lamp and ballast design technologies have accelerated the widespread application of UV radiation in water and wastewater treatment. Although the first UV irradiation application in drinking water treatment dates back to as early as 1910, until recently general application has been impeded because of the low cost of chlorination and operational problems with early UV disinfection equipment (USEPA, 2006). As of today; however, water disinfection by UV radiation can be considered as a competitive alternative to chlorination in terms of both cost and effectiveness against pathogens (Metcalf and Eddy Inc., 2003).

The primary goal of this research is to contribute to the field of water disinfection via UV radiation by evaluating the performance of UV disinfection in non-ideal treatment conditions and characterizing some of the response (regrowth) and resistance (self-aggregation) mechanisms of bacteria to UV disinfection. One of the biggest challenges facing the successful application of UV disinfection systems in water treatment stems from the presence of particles and flocs (aggregates). Particles and flocs present in water may effectively reduce the amount of UV radiation reaching the target organisms by absorbing, blocking or scattering the UV light (Mamane, 2008). Often, processes which

physically remove particles and flocs are included in both water and wastewater treatment systems upstream of the disinfection unit. However, some particles and flocs may still reach the disinfection stage of the treatment due to situations such as process upsets or design limitations (Templeton et al., 2008). In addition, some microorganisms have been observed to self-aggregate upon exposure to UV light (Blatchley et al., 2001), which creates conditions similar to the presence of flocs. The interaction of microorganisms with particles and flocs can enhance their survival through the disinfection process (Gerba, 1984, Parker and Darby, 1995; Gehr and Nicell, 1996; Loge et al., 1996, 1999, 2001a, 2001b; Emerick et al., 1999, 2000; Jolis et al., 2001; Madge and Jensen, 2006). On the other hand, the mechanisms behind the survival of bacteria are not fully understood as particles and flocs present in water and wastewater tend to have highly variable physical, chemical and biological characteristics and host microbial populations that are time-dependent in nature. Therefore, there is need for a stable, well-defined and well-controlled surrogate system in order to study their effects on UV disinfection.

Another concern for UV disinfection systems arises from microbial repair mechanisms (reactivation). Since UV irradiation does not result in immediate cell lysis, it is possible that a UV inactivated cell might regain viability via a repair mechanism (Malley et al., 2004), and hence the net overall inactivation efficiency is reduced. The repair potential of microorganisms has been studied widely in the literature and there is mounting evidence that there are significant levels of reactivation occurring for most organisms of concern to water and wastewater disinfection (Harris et al., 1987; Zimmer and Slawson, 2002;

Kalisvaart, 2004). However, except for a few notable studies (Lindenauer and Darby, 1994; Hu et al., 2005) researchers studying reactivation did not consider regrowth as a parameter to be controlled for. As microorganisms surviving the UV irradiation are capable of multiplying, regrowth has the potential to significantly affect the quality of the treated water and the outcomes of reactivation studies, depending on the concentration of surviving population and availability of nutrients. While regrowth is preventable by achieving a complete inactivation during disinfection, reactivation may depend on factors outside the disinfection unit such as exposure to light. Therefore, addressing regrowth related problems would be fundamentally different than dealing with reactivation related problems.

This dissertation consists of eight chapters. Chapters 4 – 7 were written as stand-alone chapters and have either been published, are under review or have been prepared for publication as peer-reviewed journal articles. Chapter 1 and 2 provide a short introduction and a general review of the literature on the topics studied in the following chapters, respectively. Chapter 3 outlines additional details concerning materials and methods. Each of the chapters from 4 to 7 also includes an introduction with a review of the literature relevant to the topic of interest in that chapter. In Chapter 8, overall conclusions and future research suggestions are presented.

In Chapter 4, the effect of particles and flocs on UV disinfection was examined by running well-controlled experiments in a stable and well-defined synthetic system that

can simulate the bioflocculation of particles and microorganisms in water and wastewater samples. Latex particles were used to represent water and wastewater particles, and *Escherichia coli* was chosen as the model bacterial strain. Synthetic bioflocs were formed by adding natural facilitators of flocculation in water (alginate and calcium) and hence they truly mimicked the physical and chemical characteristics of wastewater flocs (Sanin and Vesilind; 1996, 1999). In addition, an inverted microscope and an advanced particle counter were used in parallel for visual observations of the flocs. This chapter was published in the journal *Water Research* (Kollu and Örmeci, 2012).

Chapter 5 explored the potential of a dynamic particle counter (DPA 4100) for monitoring bioflocculation under controlled conditions and characterizing the flocs formed. Bioflocculation of samples containing latex particles of fixed sizes and shape, and *E. coli* was initiated by adding alginate and calcium. The extent of bioflocculation and the final floc size were determined by the calcium concentration. The number concentration and size distribution of the flocs were analyzed along with the flocs' area, shape, perimeter, ferret diameter and porosity. The correlation of floc size and porosity with UV inactivation was also examined.

Chapter 6 expanded on the work of Chapter 5 and used the same DPA 4100 system and an inverted microscope (Nikon Eclipse Ti) to examine and quantify the extent of UV induced self-aggregation of *E. coli* upon exposure to low-pressure and medium-pressure UV radiation. Effect of UV dose, intensity and exposure time were investigated by

analyzing the samples' particle size distribution and particle concentration, as well as the light transmittance and area of the flocs before and after UV irradiation.

Finally, in Chapter 7, the regrowth potential of *E. coli* and indigenous wastewater bacteria after UV disinfection was investigated. The regrowth potential was studied in the absence of light and dark repair and under different nutrient conditions. Light repair was prevented by keeping the samples in the dark after UV exposure. Dark repair was controlled for by varying the initial and surviving bacteria concentrations, and achieving complete inactivation and no growth in control samples. In this way, it was possible to observe the relative importance of regrowth versus reactivation. This chapter was submitted to the *The Journal of Environmental Engineering* and is currently under review.

1.1. References

Blatchley, E. R., Dumontier, N., Halaby, T. N., Levi, Y. and Laine, J. M. (2001). Bacterial responses to ultraviolet irradiation. *Water Science and Technology*, 43(10), 179-186.

Canadian Wastewater Systems Effluent Regulations (2012). SOR/2012-139, FISHERIES ACT.

Available at: <http://laws-lois.justice.gc.ca/eng/regulations/SOR-2012-139/FullText.html>

Clancy, J. L., Bukhari, Z., Hargy, T. M., Bolton, J. R., Dussert, B. W. and Marshall, M. M. (2000). Using UV to inactivate *Cryptosporidium*. *Journal of American Water Works Association*, 92(9), 97-104.

Cutler, D. and Miller, G. (2005). The role of public health improvements in health advances: the twentieth-century United States. *Demography*, 42(1), 1-22.

Emerick, R. W., Loge, F. J., Thompson, D. and Darby, J. L. (1999). Factors influencing ultraviolet disinfection performance part II: association of coliform bacteria with wastewater particles. *Water Environment Research*, 71(6), 1178-1187.

Emerick, W. R., Loge, F. J., Ginn, T. and Darby, J. L. (2000). Modeling the inactivation of particle-associated coliform bacteria. *Water Environment Research*, 72(4), 432-438.

Gehr, R. and Nicell, J. (1996). Pilot studies and assessment of downstream effects of UV and ozone disinfection of a physicochemical wastewater. *Water Qual. Res. J. Can.*, 31 (2), 263-281.

Gerba, C. P. (1984). Virus survival and transport in groundwater. *Developments in Industrial Microbiology*, 24, 247-251.

Harris, G. D., Adams, V. D., Sorensen, D. L. and Dupont, R. R. (1987). The influence of photoreactivation and water quality on ultraviolet disinfection of secondary municipal wastewater. *Journal of Water Pollution Control Federation*, 59 (8), 781-787.

Hu, J. Y., Chu, X. N., Quek, P. H., Feng, Y. Y. and Tan X. L. (2005). Repair and regrowth of *Escherichia coli* after low- and medium-pressure ultraviolet disinfection. *Water Science and Technology: Water Supply*, 5 (5), 101-108.

Jolis, D., Lam, C. and Pitt, P. (2001). Particle effects on ultraviolet disinfection of coliform bacteria in recycled water. *Water Environment Research*, 73 (2), 233-236.

Kalisvaart, B. F. (2004). Re-use of wastewater: preventing the recovery of pathogens by using medium-pressure UV lamp technology. *Water Science and Technology*, 50 (6), 337-344.

Kollu, K. and Örmeci, B. (2012). Effects of particles and bioflocculation on ultraviolet disinfection of *Escherichia coli*. *Water Research*, 46 (3), 750-760.

Linden, K. G., Shin, GA.,Faubert, G., Cairns, W. and Sobsey, M. D. (2002). UV disinfection of *Giardialambli*a cysts in water. *Environmental Science and Technology*, 36(11), 2519-2522.

Lindenauer, K. G. and Darby, J. L. (1994). Ultraviolet disinfection of wastewater: effect of dose on subsequent photoreactivation. *Water Research*, 28(4), 805-817.

Loge, F. J., Darby, J. L. and Tchobanoglous, G. (1996). UV disinfection of wastewater: a probabilistic approach to design. *Journal of Environmental Engineering*, 122(12), 1078-1084.

Loge, F. J., Emerick, R. W., Thompson, E. D., Nelson, D. C. and Darby, J. L. (1999). Factors influencing ultraviolet disinfection performance part I: light penetration to wastewater particles. *Water Environment Research*, 71(3), 377-381.

Loge, F. J., Bourgeois, K., Emerick, R. W. and Darby, J. L. (2001a). Variations in wastewater quality influencing UV disinfection performance: relative impact on filtration. *Journal of Environmental Engineering*, 127 (9), 832-837.

Loge, F. J., Emerick, R. W., Ginn, T. R. and Darby, J. L. (2001b). Association of coliform bacteria with wastewater particles impact of operational parameters of the activated sludge process. *Water Research*, 36, 41-48.

Madge, B. A. and Jensen, J. N. (2006). Ultraviolet disinfection of fecal coliform in municipal wastewater: effects of particle size. *Water Environment Research*, 78, 294-304.

Malley, J. P., Shaw, J. P. and Ropp, J. R., 1995. Evaluation of By-products Produced by Treatment of Groundwaters with Ultraviolet Irradiation. The Foundation and American Water Works Association, Denver, CO.

Malley, J. P., Ballester, N. A., Margolin, A. B., Linden, K. G., Mofidi, A., Bolton, J. R., Crozes G., Cushing B., Mackey, E., Laine J. M. and Janex M. L. (2004). Inactivation of Pathogens with Innovative UV Technologies. American Water Works Association Research Foundation, USA.

Mamane, H. (2008). Impact of particles on UV disinfection of water and wastewater effluents: a review. *Reviews in Chemical Engineering*, 24 (2-3), 67-157.

Metcalf and Eddy Inc., 2003. *Wastewater Engineering: Treatment and Reuse*. McGraw-Hill, Boston, MA.

Parker, J. A. and Darby, J. L. (1995). Particle-associated coliform in secondary effluents: shielding from ultraviolet light disinfection. *Water Environment Research*, 67(7), 1065-1075.

Sanin, D. F. and Vesilind, A. P. (1996). Synthetic sludge: a physical/chemical model in understanding bioflocculation. *Water Environment Research*, 68(5), 927-933.

Sanin, D. F. and Vesilind, A. P. (1999). A comparison of physical properties of synthetic sludge with activated sludge. *Water Environment Research*, 71(2), 191-196.

Shin, G.A., Linden, K. G., Arrowood, M. J. and Sobsey, M. D. (2001). Low-pressure UV inactivation and DNA repair potential of *Cryptosporidium parvum* oocysts. *Applied Environmental Microbiology*, 67(7), 3029-3032.

Templeton, M. R., Andrews, R. C. and Hofmann R. (2008). Particle-associated viruses in water: impacts on disinfection processes. *Environmental Science and Technology*, 38, 137-164.

USEPA (2000) The history of drinking water treatment. Office of Water (4606) EPA 816-F-00-006.

USEPA (2006) Ultraviolet disinfection guidance manual for the final long term 2 enhanced surface water treatment rule. Office of Water (4601) EPA 815-R-06-007.

Zimmer, J. L. and Slawson, R. M. (2002). Potential repair of *Escherichia coli* DNA following exposure to UV radiation from both medium and low pressure UV sources in drinking water treatment. *Applied Environmental Microbiology*, 68 (7), 3293-3299.

CHAPTER 2

LITERATURE REVIEW

In this chapter, a review of the literature on UV disinfection related problems is presented. First, basic information on UV disinfection is provided. Then, the literature addressing the effects of particles and aggregation, and reactivation and regrowth on UV irradiation is summarized.

2.1. UV Disinfection

UV radiation occurs in the portion of the electromagnetic spectrum from 100 to 400 nm, yet practical germicidal activity in water is limited to radiation mainly in the UV-C and UV-B range: at wavelengths between 200 and 300 nm (USEPA, 2006). The most common type of lamps employed for producing UV radiation are mercury lamps. For mercury lamps, three different lamp arrangements exist, namely: low-pressure low-intensity, low-pressure high-intensity, and medium-pressure high-intensity systems. In most laboratory scale experiments, and water and wastewater treatment applications, low-pressure (LP) UV mercury vapour lamps which generate essentially monochromatic radiation at a wavelength of 254 nm, and medium-pressure (MP) UV mercury vapour lamps which produce polychromatic radiation between the 220 and 300 nm germicidal UV range and beyond, are used (USEPA, 2006). This wavelength range is considered highly germicidal due its proximity to the point at which DNA's absorbance reaches its peak (260 nm).

UV light is considered a physical rather than a chemical disinfecting agent, as no chemicals are added to water. Therefore, under most circumstances chemical changes do not occur and no formation of disinfection by-products is observed.

The inactivation of microorganisms by UV light is achieved via damage to the cell DNA (or RNA). Once a sufficient amount of radiation is absorbed by the DNA, thymine and cytosine dimerization takes place (Figure 2.1), which inhibits cell replication (Bolton and Linden, 2003). An organism that cannot reproduce is not capable of infecting a host, and will eventually lyse and die (Malley et al., 2004).

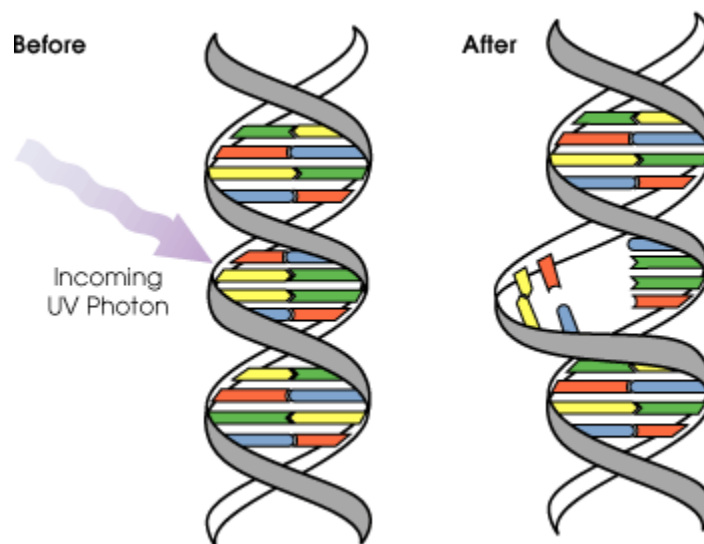


Figure 2.1: UV induced damage to the DNA: after UV exposure adjacent thymine bases bond with each other, instead of across the ladder (Source: Allen, J., 2001).

By far the most important parameter that controls the extent of UV disinfection is the UV dose. Similar to the case of chlorination where efficacy is based on contact time and concentration, the effectiveness of UV disinfection is based on exposure time and radiation intensity, the product of which gives the UV dose. The intensity is usually reported in units of milliwatts per square centimetre (mW/cm^2) and the exposure time in units of seconds (s). Therefore, the UV dose is reported in units of millijoules per square centimetre (mJ/cm^2).

Typically, the rate and extent of inactivation achieved after UV exposure is analyzed by plotting a dose-response curve, which is a plot of the logarithm of the ratio of number of surviving bacteria to the initial number of bacteria versus the UV dose applied. In cases where inactivation of a sample containing only dispersed bacteria is of concern, the dose-response curve is expected to follow first order kinetics (Farnood, 2004). On the other hand, in most cases a lag or shoulder effect at low doses due to self-aggregation of microbes (Severin et al, 1983) or cellular repair mechanisms (Jagger, 1967), and a tailing effect at high doses due to shielding of bacteria by particles (Qualls et al, 1983) are observed. These phenomena are demonstrated in Figure 2.2.

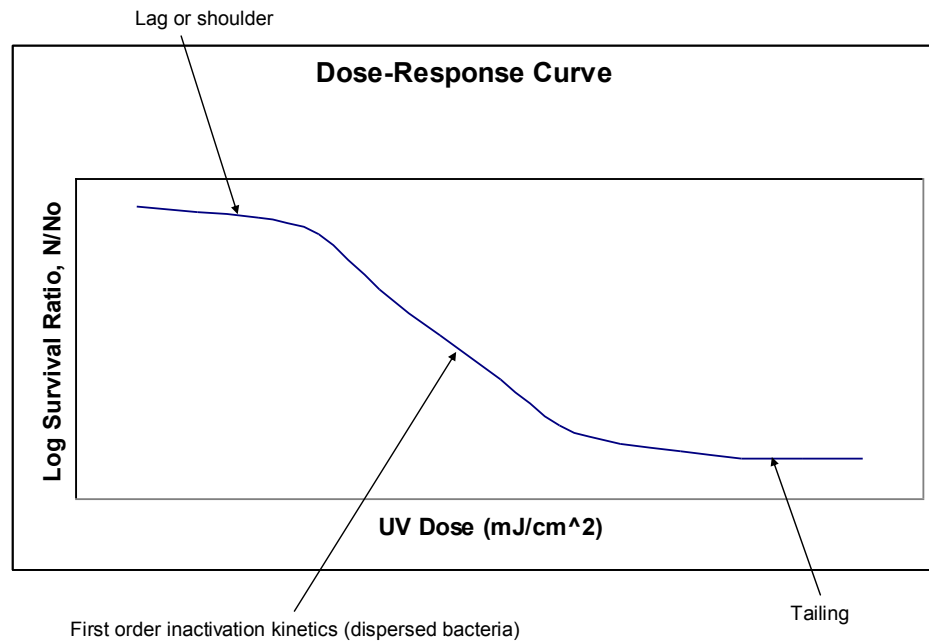


Figure 2.2: A typical dose-response curve where lag and tailing are observed.

Theoretically, any type of water can be UV disinfected to any degree desired, provided that adequate amounts of UV energy reach the target organisms. Therefore, the main concern in water disinfection by UV radiation has always been to ensure delivery of UV light to the target organisms with minimum loss of energy to the other constituents present in the system or to the water itself. With that regard, the transmittance of UV light throughout the system becomes the determining factor as to how much of the dose produced by the lamps is actually delivered to the target organisms. In other words, any interference in the form of absorption or scattering of the UV light resulting from the liquid medium itself (colour, dissolved substances) or the other materials present (suspended solids) will have a defining effect on the outcomes of UV disinfection. In

addition, since UV irradiation does not result in immediate cell lysis, it is possible that a UV inactivated cell might regain viability via a repair mechanism, and hence the net overall inactivation efficiency is reduced. As these issues are the subject of recent and ongoing studies, including those in this thesis, a detailed review of the related literature is provided in the following sections.

2.2. Particle and Aggregation Related Issues

As mentioned previously, UV light is used for disinfection purposes in both water and wastewater treatment applications. Thus, various water types such as secondary and tertiary wastewater effluents, stabilizations ponds, combined sewer overflows, filtered and unfiltered surface waters and ground waters are all subjects of UV related research. The limitations of UV disinfection heavily depend on water characteristics. One of the water characteristics that is of particular concern is the presence of particles. In water sources, particles may exist in a dispersed state, as single entities; or in the form of aggregates, as flocs. The same principle also applies to microorganisms. Microorganisms may either be dispersed (free swimming) or in aggregates together with other particles and/or microorganisms. If the target organisms are free swimming, it is expected that the UV light will reach the target by a direct path and inactivation problems are unlikely to occur. However, when target organisms exist in self-aggregates, or within flocs together with other microorganisms and particles, the UV light will have to penetrate a certain distance of UV absorbing material before reaching some of the target organisms. This means some (or all) of the light energy will be lost before being utilized for inactivation. And hence, the effectiveness of UV disinfection will decrease. Moreover, aggregation of

microorganisms also adversely affects the reliability of traditional plate count methods, which are widely used for the determination of pathogen concentrations in the water treatment industry (Templeton et al., 2005). There has been extensive research on the effect of particles and aggregation on UV disinfection and the most significant ones with regards to this study are summarized in the following sections.

2.2.1. Origin and Nature of Particles and Aggregates in Water

Particles in water may be of either organic or inorganic origin. Organic particles can be further broken down into those that are nonliving and that are living. Inorganic particles mainly constitute of iron and alumina oxides, and clays, whereas organic living particles include microorganisms, and organic nonliving particles include cellular debris or dead microbial cells (Wilkinson et al., 1997; Mamane 2008).

Furthermore, microorganisms show an affinity to form aggregates among themselves and with other particles due to favourable environmental conditions such as better food assimilation and protection from environmental stresses (Liss et al., 1996; Gerba and Mcleod, 1976). Such aggregates are collectively termed flocs. Flocs are reported to be significantly different from their constituent particles and microorganisms in size, shape, porosity, density and composition (Droppo, 2001).

If the aggregation is not artificially enhanced by the addition of chemical coagulants, a more appropriate term for flocs found in water would be bioflocs. Bioflocculation is defined as the natural process of microorganisms aggregating into flocs (Sobeck and Higgins, 2002). Different organisms present in water (bacteria, fungi, viruses and protozoa) together with the other organic and inorganic constituents form flocs in a polymeric network holding them together. This polymeric network is referred to as the extracellular polymeric substances (EPS) and mainly originates from the microorganisms and/or the water itself (Friedman et al., 1969; Pavoni et al., 1972; Horan and Eccles, 1986; Urbain et al., 1993). It has been shown that EPS play a key role in bioflocculation and the total mass of EPS can be as high as 80% of the total mass of the floc (Frolund et al., 1996). It has also been reported that due to the presence of negatively charged functional groups (such as carboxyl groups) within the EPS, the net charge of flocs tends to be negative (Horan and Eccles, 1986; Frolund et al., 1996). Therefore, the flocs formed by bioflocculation (bioflocs) are considerably different in their physical and chemical nature than chemical flocs achieved through flocculation induced via inorganic chemical addition, such as alum or ferric chloride.

In addition to EPS, cations have also been shown to play an important role in bioflocculation primarily due to the net negative charge of bioflocs. The divalent cation bridging (DCB) theory suggests that divalent cations [specifically calcium (Ca^{2+}) and magnesium (Mg^{2+}) ions due to their abundance in natural aquatic systems] have an overall promoting effect on floc formation as they enhance bridging between negatively charged functional groups within the EPS (Tezuka, 1969). According to this theory, it is

this bridging mechanism that facilitates aggregation and stabilization of biopolymers and microorganisms. Monovalent cations (Na^+ , NH_4^+ , and K^+), on the other hand, have been shown to have a deteriorating effect on biofloc formation as they displace divalent cations (Higgins and Novak, 1997). Bruus et al. (1992) found that when calcium ions are present, alginate which is a polysaccharide formed by two monosaccharide units starts forming alginate gels. The fact that extracellular polymers extracted from activated sludge have a greater affinity toward calcium ions than magnesium ions led to the conclusion that alginate is an important component of EPS (Bruus et al., 1992). The role of divalent cations within a floc is demonstrated in Figure 2.3.

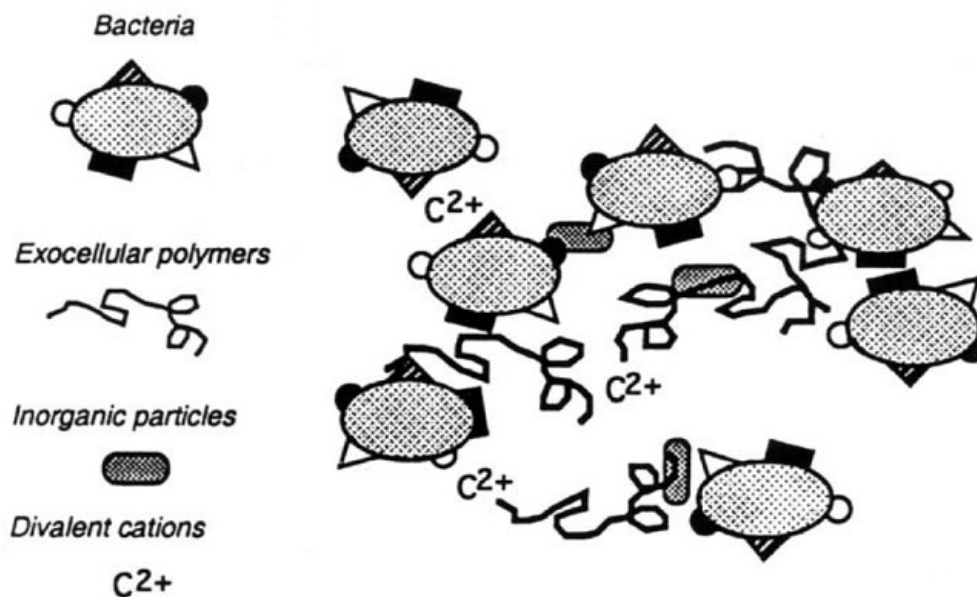


Figure 2.3: Divalent cation bridging within a floc (Source: Urbain et al., 1993, Modified).

2.2.2. Particle Measurements

Particle characteristics of water can be analyzed in various ways. Some of the techniques employ instruments like microscopes and advanced particle counters, which utilize image analysis, and yield in-depth information on parameters such as size, shape, light transmittance (porosity and density) of individual entities present in water. Other techniques such as separation methods (sedimentation, serial membrane filtration etc.), turbidity, and total solids measurements, on the other hand, yield only an overall estimation of particle characteristics in water.

It is particularly difficult to size and shape bioflocs as they tend to have a very fragile structure. Flocs can easily break up upon sampling. Therefore, it is crucial to use a measurement methodology that allows for a non-destructive direct sampling and observation of flocculated material such as microscopy techniques that allow for visualization in water (Droppo et al., 1997).

Furthermore, the lack of control over their composition and their time-dependent highly variable nature make bioflocs in natural systems hard to work with, in controlled experiments. For example, samples taken from a wastewater treatment plant on the same day may exhibit completely different characteristics. Samples may also develop significantly different properties over a shorter period of time than the duration of the laboratory analyses making the data very difficult if not impossible to reproduce (Sanin and Vesilind, 1999). A stable, well-defined and well-controlled surrogate that can

simulate the particle characteristics, and coagulation-flocculation properties of water/wastewater samples would aid researchers with this problem.

Sanin and Vesilind (1996) created a stable chemical surrogate for activated sludge by using polystyrene latex particles, alginate and calcium ions. In this system, alginate simulated the extracellular material and calcium ions facilitated the bridging between the negatively charged functional groups as discussed previously. They reported formation of visible flocs physically very similar to activated sludge flocs immediately following calcium addition. The synthetic matrix, called synthetic sludge, was prepared by addition of latex particles first, followed by alginate addition and mixing to provide adsorption of alginate onto particle surfaces. Within time periods as short as 5 seconds after calcium addition visible floc formation was observed to take place at calcium concentrations of 10 and 15 mM. As well, no visible floc formation was observed when initial calcium concentration was set at 5 mM and a faster visible floc formation was seen at higher calcium concentrations (20 and 25 mM). This observation verified the importance of calcium in bridging and kinetics of bioflocculation.

A further study of Sanin and Vesilind (1999) investigated the suitability of synthetic sludge in terms of its physical properties as a surrogate for wastewater sludge. The study concluded that synthetic sludge may serve as a good surrogate material in experiments dealing with physical properties of sludge especially when reproducibility is of concern.

2.2.3. Effect of Particles and Aggregation on UV Disinfection

Mechanisms which are important when evaluating the effect of particles and aggregation on UV disinfection are shielding (shading) and enmeshment (embedding). In a well-mixed system, shielding would be unlikely to significantly affect disinfection efficiency, as the shielding of a particular target organism would only be a temporary situation (Parker and Darby, 1995). Furthermore, the cumulative amount of light energy lost to particle shielding (estimated by measuring the UV absorbance of the sample) should be accounted for while calculating the UV dose (Bolton and Linden, 2003). Effects of enmeshment on microbial inactivation, on the other hand, depend on the presence of light pathways permitting penetration of UV light through aggregates. Thus, mixing would not provide significant improvements for the inactivation of enmeshed microorganisms. Moreover, since the UV absorbance within an aggregate would be undoubtedly different than the overall UV absorbance of the solution, it cannot be accounted for during dose calculations.

Generally, the impact of particles on UV disinfection has been studied by adding clays or natural particles to increase water turbidity and seeding microorganisms into the sample. Thus, until recently the main study parameter for examining the particle effect has been turbidity in most of the previous research. Turbidity is widely used in regulations as a water quality parameter and is a simple way of measuring particles content of a sample by detecting the intensity of light scattered (AWWA, 1999). However, turbidity is a lumped parameter that does not provide any information on particle size, distribution of the individual particles in the water or particle shape (Mamane, 2008). Furthermore, it is

poorly correlated with number concentration of particles as light scattering depends on the particle size (Huber and Frost, 1998).

Passantino et al. (2004) investigated the effects of turbidity and algae on UV inactivation of *MS2* bacteriophage with medium-pressure UV lamps. Turbidity levels up to 12 NTU and algal concentrations up to 42 $\mu\text{g/L}$ were examined by using suspensions of montmorillonite clay particles and *Chlorella vulgaris* cells. The study was conducted by spiking turbidity and the *MS2* into a sample water and no steps were taken to facilitate particle-association. The results of this study indicated that there was no significant difference in inactivation at doses of 40 and 80 mJ/cm^2 with changing turbidity or chlorophyll concentration in synthetic samples. This was attributed to minor interference of particles with the UV light and to the lack of association of *MS2* with the particles. Batch et al. (2004) conducted a similar study as Passantino et al. (2004). They examined the effect of turbidity, and additionally the particle count and size on UV disinfection of *MS2* bacteriophage. This study focused on natural turbidities found in filtered waters from different water treatment plants, hence the range of turbidities investigated were relatively low (<0.3 NTU). The results showed no significant decrease in inactivation of *MS2* with increasing turbidity over the range of UV doses employed (10, 30, 60, and 100 mJ/cm^2) when both low-pressure and medium-pressure UV lamps were used. Amoah et al. (2005) also found that UV inactivation of dispersed *C. Parvum* and *Giardia* cysts was not affected by adding natural turbidity up to a level of 10 NTU.

The main similarities between these studies are that the tested suspensions essentially represented surface waters, but a coagulation/flocculation step enhancing enmeshment of the spiked organisms within floc matrices was missing. Thus, the studies were essentially focused on the effects of increased UV absorbance of the bulk solution (shielding/shading) on inactivation performance rather than impacts of enmeshment. In addition, since the absorbance values of the solutions examined and the other corrections suggested in Bolton and Linden (2003) were properly factored into the calculation of delivered UV dose, the effects of shading had potentially been accounted for.

Bitton et al. (1972), Templeton et al. (2005), Mamane and Linden (2006) and Liu et al. (2007) all reported no significant impact of particles (measured in terms of turbidity) on UV disinfection efficiency when study conditions were similar to the above mentioned research.

On the other hand, studies focusing on wastewater effluents (Parker and Darby, 1995; Gehr and Nicell, 1996; Loge et al., 1996, 1999, 2001a, 2001b; Emerick et al., 1999, 2000; Jolis et al., 2001; Madge and Jensen, 2006) found significant impacts on UV disinfection. This was generally attributed to the presence of naturally occurring aggregates in wastewater effluents, and hence enmeshment of target organisms within floc structures. In fact, a large portion of bacterial groups (60-70%) in secondary wastewater effluents were observed to be associated with small flocs (Morgan-Sagastume, 2008).

In their study of light penetration into wastewater flocs, Loge et al. (1999) found that absorbance can occur to such a degree that the transmission of UV light is completely blocked if the entire incident light was to hit the solid material. Therefore, it was concluded that the observed penetration of UV light, as indicated by persistent inactivation of organisms located within flocs at higher UV doses, is due to the porous structure of wastewater flocs. The main implications of this finding are that it is not only the size of a floc that controls or limits the inactivation of target organisms but also the structure, and that the spatial distribution of microbes within a floc determines to what degree they will be protected from UV irradiation. In accordance with these implications, it was also hypothesized by Loge et al. (1999) that a highly porous floc with pathways for light penetration would not necessarily provide more protection to an organism embedded deep within the floc than a smaller floc would provide to an organism located closer to the floc surface but lacking a light pathway.

Farnood (2005) addressed the same issue of light penetration. In the first part of the study, actual wastewater samples were used to investigate the effect of floc size on UV disinfection performance. The results of the first part indicated a noticeable decrease in inactivation with increasing floc size. Moreover, the dose-response curves showed a more prominent tailing effect for larger flocs implying a higher ratio of completely protected microbes to the total concentration of microbes. When the inactivation rates of floc samples were compared to that of free fecal coliform, it was observed that even at very low UV doses a large difference in concentration of surviving organisms existed. This observation strongly suggests that most of the coliform bacteria present in the samples

were associated with particles. The second part of the study concentrated on the role of floc composition. As in the case of Loge et al. (1999) it was hypothesized that the intensity of UV light within a floc depends not only on the size of the flocs but also on their composition. With that regard, particular attention was given to the EPS content of the flocs and how their spatial distribution affects the UV penetration. Absorbance measurements on EPS extracted from pure cultures of *Klebsiella sp.* were used to model three idealized cases of EPS distribution within flocs. It was hypothesized that depending on whether the EPS was concentrated in the centre of a floc, uniformly distributed within a floc, or around the floc forming a coating layer; the reduction in the intensity of UV light could vary from less than 1% to as much as 55%.

Templeton et al. (2005) examined the effect of particles with different characteristics (inorganic clay particles, and organic humic acid and activated sludge particles) on UV disinfection of viruses. The study found strong evidence for the importance of floc and particle composition on UV inactivation: the highest degree of protection was observed with the organic humic acid particles rather than the same size inorganic clay particles or the larger sized activated sludge particles. This was attributed to the high UV absorbing characteristics of humic acid particles. Another important indication of the study's results was that induced flocculation through the addition of alum or ferric chloride coagulants did not lead to a statistically significant reduction of virus inactivation. This led to the hypothesis that viruses might have attached to the particles primarily through electrostatic attraction (self-attachment), and only to a lesser extent by the aid of coagulants. Finally, it was also suggested that the degree of association, that is whether the microbes were only

surface-attached, or partially or completely enmeshed within particles, may have played an important role on the inactivation efficiency. The evidence for this suggestion originated from the experiments with activated sludge particles. In these experiments, the reduction in inactivation as a result of particle-association was more distinct at higher UV doses implying that surface-attached microbes were likely to be inactivated at lower doses, whereas, the completely enmeshed ones were unlikely to be inactivated even at higher doses, thereby limiting the overall level of inactivation.

2.2.4. Tailing Phenomenon

In some cases of UV disinfection, some of the microorganisms remain intact even at very high UV doses. This is commonly referred to as tailing. Tailing implies that a residual of microorganisms would be present in the water systems at very high UV doses, which is a potential public health concern. Interpretation of the tailing phenomenon can be classified under two different approaches: (1) vitalistic approach assumes that individual organisms in a population cultured from a pure colony are not identical with respect to disinfection, and (2) mechanistic approach assumes that resistance of individuals in a population are similar but other factors affect their level of inactivation (Mamane, 2008). If all individuals in a population have identical resistance to disinfection, then tailing could occur due to the following:

1. Modification of cell resistance occurs during disinfection due to a natural resistance mechanism possessed by the organisms, such as self-aggregation of microorganisms (Cerf, 1977; Blatchley et al., 2001)

2. Local variations of disinfectant concentration/dose within a sample volume (Cerf, 1977)
3. Enumeration errors at low concentrations of surviving organisms (Cerf, 1977)
4. Microbe-particle association, or enmeshment (Loge et al., 2001)

All of the above mechanisms need further investigation, except for the second one, to better understand the tailing phenomenon and its potential effects on UV disinfection efficiency.

2.2.5. Enumeration

The two most commonly used methods for enumeration of fecal coliform in wastewater analyses are the membrane filtration (MF) and the multiple tube fermentation (MTF) techniques as described in Standard Methods: [American Public Health Association (APHA), American Water Works Association and Water Pollution Control Federation, 2005]. Both of these methods work best for analyzing suspensions of dispersed bacteria (also called free-swimming bacteria) that are not associated with particles or self-aggregated (clumped). However, coliform bacteria have been found to be frequently particle-associated in wastewater. Since particle-associated and clumped bacteria are counted as single colonies when these techniques of enumeration are directly used, usually the organism concentrations are underestimated (Parker and Darby, 1995).

Several methods of treatment prior to enumeration have been suggested to overcome this problem. Various physical and chemical techniques to extract (free) organisms from particles, flocs and other organisms were shown to be effective at varying degrees (Örmeci and Linden, 2005). Mamane and Linden (2006a) employed vortex mixing to release spores from spore-spore and spore-particle aggregates and concluded that sufficient extraction was achieved. Borst and Selvakumar (2003) investigated the effect of 1-minute and 2-minute blending on microbial enumeration with standard MF method. It was reported that increasing the blending time from 1 to 2 minutes caused an increase in the detected concentration of fecal coliform, whereas, no significant change occurred in the case of *E. coli* and total coliform enumerations.

The extent of underestimation of the measured microbial concentration was reported to reach such levels that enumeration following extraction resulted in concentrations up to 340 times greater than enumeration without any extraction. This was shown to be more significant for samples irradiated at higher UV doses as the ratio of particle-associated organisms to total organisms is expected to increase with increasing applied UV dose (Parker and Darby, 1995). Therefore, microbial analysis techniques that do not include an extraction step prior to enumeration might lead to flawed conclusions by underestimating the microbial concentration.

2.3. Reactivation Related Issues

Mainly, the inactivation of microorganisms by UV light is achieved by absorption of UV radiation by the nucleic acids of the target organisms. Once a sufficient amount of radiation is absorbed, thymine and cytosine dimerization takes place (pyrimidine dimer formation), which in turn inhibits replication or causes death of the cell (Bolton and Linden, 2003). However, since UV irradiation does not immediately result in cell lysis it is possible that some of the UV inactivated organisms regain viability through a repair mechanism (Malley et al., 2004). In fact, many organisms in nature have evolved mechanisms for reversing UV damage (Jagger, 1967). There are two different types of such mechanisms: (1) photoreactivation (photorepair) and (2) dark repair. These mechanisms are explained in more detail in the following sections.

2.3.1. Photoreactivation

Photoreactivation involves specific enzymes which are capable of repairing damaged DNA segments when a sufficient amount of light energy is present and the wavelength of the light is within the absorption spectra of the enzymes. The enzyme responsible for DNA repair in this manner is named photolyase. Photoreactivation can be described as a two-step enzymatic reaction where the first step involves binding of photolyase with a dimer pair to form an enzyme-substrate complex, and the second step involves breaking up of dimers via utilizing the energy of light at wavelengths between 310 and 490 nm (Friedberg et al., 1995). The first step is light-independent and hence can occur under dark conditions as well. The second step, on the other hand, is completely dependent on the light energy available. Most bacteria have been shown to possess the necessary

enzymes to repair UV induced damage whereas, viruses lack them. However, viruses are still capable of repair by using a host cell's enzymes.

2.3.2. Dark Repair

The repairing of UV radiation induced DNA damage can also be carried out in the absence of light (Hanawalt et al., 1979). Unlike photorepair which does not occur in the absence of light, dark repair can occur both in the absence and the presence of light. Dark repair appears to be accomplished by two mechanisms: (1) excision repair and (2) recombination repair. In excision repair, enzymes remove the damaged section of the DNA, and in recombination repair the damaged DNA is regenerated using a complimentary strand of DNA. As such, dark repair can occur only with double stranded DNA and RNA. Contrary to photoreactivation, which has high selectivity for pyrimidine dimers, dark repair can act on various kinds of damage in the genome. Many researchers have shown that dark repair tends to be much slower and less effective than photorepair (Kashimida et al., 1996; Knudson, 1985; Scheible et al., 1986; Schoenen and Kolch, 1992; Sommer et al., 2000; Whitby et al., 1984; Zimmer and Slawson, 2002). However, some researchers have observed equal or comparable degrees of repair under dark and light conditions (Mechsner et al., 1991; Gehr and Nicell, 1996; Chan and Killick 1995). The extent of dark repair varies with the microorganism. In bacteria and protozoa, dark repair enzymes start to act immediately following exposure to UV light; therefore reported dose-response data are assumed to account for dark repair (Sinha and Hader, 2002).

2.3.3. Review of Previous Research on Photoreactivation

Photorepair is believed to play an important role, especially in wastewater disinfection, where the potential of being exposed to sunlight following UV treatment is high (Bohrerova and Linden, 2007). Many factors such as; the UV dose, the photoreactivating lamp type, the light intensity and the exposure time, the type of UV lamp, the type of organisms, the quality of the water, and the post UV exposure conditions, can affect the rate of photoreactivation in water following UV disinfection. These factors are discussed further in the following sections.

2.3.3.1. Effect of UV Dose on Photoreactivation

The effect of UV dose on photoreactivation is not very clear. More DNA damage is expected to occur at higher UV doses, and consequently additional time is required for maximum photoreactivation as the number of active photolyase enzymes is limited (Martin and Gehr, 2007). Lindenauer and Darby (1994) studied the effect of UV dose on subsequent photoreactivation extensively. In their study, the reactivation rates of total coliform were measured following UV irradiation experiments which consisted of a wide range of UV doses (30-239 mJ/cm²). It was concluded that an increase in UV dose is very important in minimizing photoreactivation rates. This finding was attributed to the fact that when sufficiently high doses of UV energy were provided, the DNA of the organisms was damaged to an extent that could not be repaired. Another major implication of the study was about the potential benefits of applying a UV dose in excess of what is required for the desired level of inactivation. It was observed that the excess

UV dose may be beneficial for the disinfection process by decreasing the potential for photoreactivation by causing further damage to the organisms' DNA.

Similar to the work of Lindenauer and Darby (1994), Gehr and Nicell (1996) and Kashimida et al. (1996) also observed less photoreactivation at higher UV doses. On the other hand, Scheible et al. (1986) and Whitby and Palmateer (1993) found no correlation between the level of photoreactivation and the applied UV dose. Lindenauer and Darby (1994) attributed this controversy to the different methods used for the quantification of photoreactivation. The degree of reactivation can be quantified by either calculating the fraction of inactivated cells that have been reactivated as suggested by Kelner (1951) and Lindenauer and Darby (1994), or by measuring the difference in log survival before and after reactivation. The log difference method can be misleading because the degree of reactivation quantified this way is very much dependent on how much inactivation occurs in the first place. For instance, at low UV doses the log inactivation will be low and so will be the reactivation because there are only so much of the injured bacteria that can be reactivated, meanwhile the fractional reactivation might be close to 100%. At high UV doses, when log inactivation is very high, numerically a large sum of the bacteria might be repaired even though the fraction of the reactivated bacteria to the total inactivated is actually low.

2.3.3.2. Photoreactivating Lamp Type and Spectrum of the Lamp

It appears that photoreactivation does not depend on the lamp type but on the spectrum of the light emitted by the lamp (Bohrerova and Linden, 2007). The protein that is responsible for triggering photorepair, photolyase, was reported to be activated by light wavelengths ranging from 310-490 nm (Friedberg et al., 1995). Therefore, the lamp used for photoreactivation experiments must be emitting some portion of its light in this range of wavelengths. Although what fraction of the total emitted reactivating light falls in this particular range does not necessarily matter, it is important to make sure that the fraction in the germicidal range is small as the lethal effects of the light used might overshadow the effects of repair. For instance, the study by Bohreroova and Linden (2007) found that upon exposure to sunlight for more than a certain amount of time, the lethal effects of the sunlight did actually become more dominant than the photoreactivation processes in the study samples and as a result the bacteria counts decreased during exposure.

2.3.3.3. Light Intensity and Exposure Time

There is agreement in literature that photoreactivation depends mainly on the photoreactivating light exposure time and the intensity of the photoreactivating light source. However, increased light intensity will likely increase merely the photoreactivation rate and the ultimate level of photoreactivation will remain the same, regardless of light intensity (Martin and Gehr, 2007). On the other hand, when the exposure time to photoreactivating light is sufficiently long, all the dimers formed during inactivation can be repaired (Harm, 1975).

For instance, Kashimida et al. (1996) and Bohrerova and Linden (2007) reported that maximum photoreactivation took place after 15 minutes in the sun (high intensity), significantly faster than the photoreactivation rate for artificial light (low intensity) exposed samples. However, the final photoreactivation levels were not different in either case. It was also reported that, beyond 15 minutes, photoreactivation levels decreased in the samples exposed to the sun to a level below that of the samples exposed to artificial light, probably as a result of inactivation by germicidal UV irradiation from the sun. It was hypothesized that UV-A portion of the sun light may be responsible for irreparable damage to the organisms.

Although Zimmer and Slawson (2002) reported no photoreactivation below a certain intensity, Bohrerova and Linden (2007) observed photorepair at all intensities tested (the intensities tested in the study of Bohrerova and Linden (2007) were lower than the intensities tested in the study of Zimmer and Slawson (2002)). However, it was shown that the rate at which photorepair occurs is well correlated with the light intensity and higher intensities yield higher rates of repair. Some other studies also showed that photoreactivation rate is proportional to the intensity of the photoreactivating light and that the photoreactivation level typically reaches a maximum within 3 hours (Zimmer and Slawson, 2002; Schoenen and Kolch, 1992; Whitby et al., 1984).

In the study of Martin and Gehr (2007) photoreactivation of fecal coliforms was achieved using three different light sources (sunlight, high-intensity halide grow bulb, or a bank of fluorescent lights). No statistically significant difference was found between levels of light repair for samples exposed to low-intensity fluorescent lamps or to the high-intensity metal halide bulb. Furthermore, there was no statistically significant difference within each type of treatment for samples exposed to artificial light and sunlight. This result along with results of the other researchers indicates that above a certain minimum illuminance, the ultimate level of photoreactivation will be constant.

2.3.3.4. Fluence-Based Photorepair

According to Bohrerova and Linden (2007), photorepair depends on the photoreactivating light intensity and the exposure time together (not independently from each other). Therefore, they suggested that these two parameters be evaluated together under the term fluence. In fact, exposure time, light intensity, spectra of emission, the distance from the lamp to the sample surface and the sample depth can all be combined together under fluence. Using a fluence term when reporting photoreactivation data would make it easier to compare results from different studies.

2.3.3.5. Type of UV Lamps Used (Medium-Pressure versus Low-Pressure)

Oguma et al. (2002), and Zimmer and Slawson (2002) reported decreased levels of photoreactivation when medium-pressure UV lamps were used instead of low-pressure UV lamps. In both studies, *E. coli* exposed to monochromatic low-pressure UV light

were able to repair themselves whereas *E. coli* exposed to polychromatic medium-pressure UV light were unable to repair themselves. It was hypothesized by Oguma et al. (2005) that the difference observed in the level of photoreactivation was due to the simultaneous exposure of the organisms to both UV and visible light under medium-pressure UV lamps.

Zimmer and Slawson (2002) hypothesized that the wide variety of wavelengths emitted by medium-pressure UV lamps, especially UV-A (320 to 400 nm) and UV-B (290 to 320 nm), might have played a major role in lowering the level of photoreactivation. This would be true if biological molecules other than the DNA absorb UV light at different wavelengths and become damaged accordingly. Specifically, if the repair enzymes themselves are damaged, a complete repair inhibition might be achieved. Another mechanism of irreparable damage might be due to alteration of cell membranes and membrane functions. In this case photorepair by photolyase enzymes would not function. Oguma et al. (2002) also reported that wavelengths between 220 and 300 nm reduced the subsequent photorepair by causing a disorder in endogenous photolyase.

2.3.3.6. Type of Organisms

The ability to perform photorepair depends on whether the organism has the enzyme photolyase. Most strains of *Escherichia coli* are known to be able to perform photoreactivation. This ability has been shown to occur in bacteria, plants, and animals, but evolutionarily allied species need not necessarily show similar photoreactivation

characteristics (Friedberg et al., 1995). Therefore, it is necessary to investigate the ability of photoreactivation for each organism individually.

In the case of pathogenic parasites, the effects of photoreactivation are unclear. Based on infectivity studies, it was reported that the oocysts of *C. parvum* did not undergo photoreactivation (Shin et al., 2001). In another study, it was reported that repair of the pyrimidine dimers did occur in oocysts of *C. parvum* (Oguma et al., 2001). What appears to be happening is that the repair of DNA following UV irradiation may not be sufficient for the organism to regain its infectivity.

In the study of Oguma et al. (2001), photorepair of *E. coli* and *C. parvum* were investigated by an endonuclease sensitive site (ESS) assay, which can determine the number of UV-induced pyrimidine dimers in the genomic DNA as the number of ESS. This assay proved to be effective both for the comparative study of the UV sensitivity of different kinds of organisms and for the quantitative investigation of DNA repair mechanisms. During this study, Oguma et al. (2001) found that while *E. coli* was being exposed to fluorescent light, pyrimidine dimers were continuously repaired and the colony-forming ability gradually recovered. It was also shown that a high correlation between the ESS remaining ratio and the colony-forming ability ratio existed. This indicated that during the exposure of *E. coli* to fluorescent light irradiation, the repair of pyrimidine dimers in the genomic DNA contributed to the recovery of colony-forming ability. In the same study, Oguma et al. (2001) reported that a gradual repair of

pyrimidine dimers was observed during the exposure of *C. parvum* to fluorescent light irradiation, as well. The ESS remaining ratio, defined as the ratio of the number of ESS during fluorescent light irradiation to the total number of ESS induced by UV irradiation, was calculated for *E. coli* and *C. parvum* in order to compare these microorganisms from a photorepair point of view. The ratio of ESS remaining in *C. parvum* after 120 min of exposure to fluorescent light irradiation was almost the same as that in *E. coli*. This suggests that the photorepair ability of *C. parvum* is almost the same as that of *E. coli*. However, while *E. coli* clearly demonstrated a recovery of colony-forming ability after photoreactivation, recovery of the infectivity of *C. parvum* was not observed as determined by an animal infectivity assay. This was also reported by Shin et al. (2001): there was no phenotypic evidence of either photoreactivation or dark repair of the infectivity of *C. parvum* after UV inactivation. This suggests that the vitality of the oocysts would not always reflect their infectivity, as some of the viable oocysts would not be able to infect the hosts. As the repair of pyrimidine dimers in the genomic DNA did not contribute to the recovery of infectivity of *C. parvum*, it is likely that UV irradiation produces not only pyrimidine dimers in the DNA of *C. parvum* but also other kinds of damage in the DNA or other parts of the cell. The damage other than pyrimidine dimers would not be repaired by photoreactivation and should be playing an important role in its infectivity.

2.3.3.7. Water Quality Parameters

With respect to water quality, several studies have looked into the effect of COD, UV Transmittance (UVT), suspended solids concentration, turbidity, initial bacteria

concentration (N_0) and surviving bacteria concentration (N) on photoreactivation levels. One of the main ideas is that many of the constituents found in wastewater can absorb UV and photoreactivating light and therefore the amount of light energy available for either disinfection or photoreactivation will be reduced (Lidenauer and Darby, 1994).

A slightly significant interaction was reported to exist between suspended solids concentration and light repair levels and no interaction between COD or UVT and photoreactivation by Martin and Gehr (2007). On the other hand, Chan and Killick (1995) and Lindenauer and Darby (1994) reported higher levels of photoreactivation when the water quality was poor (i.e. high suspended solids concentration and low UVT), while Whitby and Palmateer (1993) observed no statistically significant correlation between suspended solids concentration or UVT and photoreactivation. According to the study of Lindenauer and Darby (1994), water quality improvements consistently resulted in improved initial inactivation and less subsequent photoreactivation, possibly due to increased DNA damage. However, at very high UV doses the effects of water quality on photoreactivation were found to be insignificant.

Lindenauer and Darby (1994) found no correlation at any dose tested in their study (30 to 239 mWs/cm²) between initial coliform numbers (N_0) and photoreactivation. However, number of surviving bacteria was found to be strongly correlated with the level of photoreactivation achieved. Increased number of survival led to increased number of photoreactivated bacteria.

2.3.3.8. Effects of post UV Exposure Conditions

As previously mentioned, the ability for an organism to repair itself appears to depend on a number of factors including UV dose, UV wavelength, UV light intensity, and exposure time to photoreactivating light (Martin and Gehr, 2007). Yet another major factor on photoreactivation might be the time disinfected water spends in the absence of light, it appears that if reclaimed water that has undergone UV disinfection is subsequently kept in the dark for approximately 3 hours, the reactivation potential is reduced significantly (Martin and Gehr, 2007). In their study, Martin and Gehr (2007), kept their UV-treated samples in the dark for 3 hours before photoreactivating light exposure to simulate the photoreactivation conditions of the Montreal Wastewater Treatment Plant effluent (which passes through a 4-km outfall tunnel with approximately 3 hours of detention time). After this period, photoreactivation levels were found to be close to zero. Hence, it was concluded that the effects of photoreactivation may be diminished by delaying exposure of the disinfected wastewater to light.

2.3.4. Review of Previous Research on Dark Repair

Sinha and Hader (2002) stated that dark repair is less effective and much slower than photoreactivation. In fact, the reported levels of dark repair in literature are often negligible compared to photoreactivation. For instance, Oguma et al. (2001) observed neither the repair of pyrimidine dimers nor the recovery of colony forming ability when *E. coli* was kept under dark conditions following UV exposure. Due to these lower levels of reactivation observed through dark repair, the factors affecting dark repair have not been researched as in a detailed way as the factors affecting photoreactivation have been.

Nonetheless, Mechsner et al. (1991), and Mofidi and Linden (2004) observed significantly high levels of dark repair after several days of incubation. The ability for dark repair is also known to differ greatly from one species to another. Therefore, it would be necessary to investigate the ability of dark repair in each organism individually. Martin and Gehr (2007) observed no significant effect of any water quality parameter on dark repair.

2.4. Regrowth

Previous studies generally used the terms “reactivation” and “regrowth” interchangeably. However, it is important and necessary to distinguish these two terms from each other. Reactivation can be defined as the ability of an organism to repair itself by means of either photoreactivation or dark repair and thus regain the ability to multiply and possibly to infect, after being induced with UV damage. Regrowth, on the other hand, should refer to the population growth due to healthy organisms that survive the disinfection process without any significant damage. Provided suitable conditions, both regrowth and reactivation can take place after UV disinfection. However, the rate and level of regrowth and reactivation would be governed by different parameters and mechanisms. For instance, while light exposure is a major factor in reactivation, availability of nutrients would be the primary drive for regrowth.

It appears that in the vast majority of previous research on reactivation and regrowth, the researchers focused on reactivation only and did not control for regrowth. In fact, only

two studies investigating reactivation touched on regrowth: Lindenauer and Darby (1994) and Hu et al. (2005). While Hu et al. (2005) found insignificant levels of regrowth, Lindenauer and Darby (1994) assumed regrowth would be insignificant without any testing. Hu et al. (2005) reported a 4-log repair versus a 0.3-log regrowth at a UV dose of 10 mJ/cm². Conversely, the way regrowth was defined in their study excluded the regrowth that might be happening during repair and focused solely on the regrowth occurring due to disinfection by-products (DBPs) formed during UV irradiation. As such, the control sample was distilled water with nitrogen and phosphorus, and without acetic acid and formaldehyde (DBPs typically found in water after UV applications). The reported 0.3-log regrowth was achieved by deducting all the growth that occurred in the control sample from the actual regrowth results. Considering that the actual study sample was *E. coli* suspended in a sodium chloride solution containing acetic acid and formaldehyde with no nitrogen or phosphorus source available for the bacteria, deducting growth occurring in a solution containing nitrogen and phosphorus may be quite misleading. What is more, wastewater samples would naturally contain some amounts of nitrogen and phosphorus. Another source of nutrients for the bacteria surviving the UV disinfection may come from lysing cells. Although cells do not immediately lyse after UV inactivation (Malley et al., 2004), Villarino et al. (2003) observed cell lysis within the first 24 h after irradiation when the UV dose was high (80 mJ/cm²). Concurrently, an increase in the number of culturable cells was detected, which according to the authors was due to the nutrients released from the lysing cells. As opposed to reactivation, which decreases with increasing UV dose (Lindenauer and Darby, 1994), Villarino et al. (2003) noted that the regrowth observed at 80 mJ/cm² did not occur when the samples were

exposed to 4 mJ/cm² of UV radiation. This inverse relationship might have major implications on the efficacy of UV irradiation and the operational strategies followed for achieving disinfection goals.

2.5. Summary of the Literature Review

The literature on UV disinfection provides a large amount of information on issues that challenge the efficacy of UV disinfection systems. For the case of particles and flocs, it has been shown that particles are not the main concern and that the real problems arise from the presence of flocs which effectively protect target organisms from UV light. It was also observed that certain floc characteristics (size, density and porosity) are correlated with the efficacy of UV disinfection. However, to what extent floc characteristics are important and exactly how they are related with the efficacy were not fully understood. A good knowledge of these factors will greatly help determine the reliability of UV disinfection systems under prevailing water and treatment conditions and justify the enforcement of upstream treatment units in cases where disinfection criteria cannot be met due to system performance upsets. In addition, the self-aggregation mechanisms that are exhibited by certain microorganisms upon exposure to UV light were shown to create conditions similar to the presence of flocs. As is the case for flocs, the relationship between these mechanisms and, UV dose and UV disinfection efficacy were not fully explored either. A good understanding of this matter is crucial in improving the overall efficiency of UV disinfection systems as well as in determining the limits of the level of inactivation that can be achieved by UV. Last but not least, the reactivation issue has been studied extensively in the literature and has been shown to

significantly reduce levels of inactivation achieved by a UV irradiation system in relatively short times. Yet, regrowth of microorganisms, which would simultaneously occur with reactivation provided that there are organisms that survive the UV irradiation, was largely ignored while studying reactivation. The rate and level of regrowth and reactivation would be governed by different parameters and mechanisms. Thus, their relative significance would be a determining factor as to what operational option should be followed in order to achieve a certain disinfection goal.

2.6. References

Allen, J. (September 6, 2001). Ultraviolet radiation: how it affects life on earth. Retrieved from: <http://earthobservatory.nasa.gov/Library/UVB/printall.php>

Amoah, K., Craik, S., Smith, D. W. and Belosevic, M. (2005). Inactivation of *Cryptosporidium oocysts* and *Giardia cysts* by ultraviolet light in the presence of natural particulate matter. *Journal of Water Supply Research and Technology AQUA*, 54 (3), 165-178.

American Public Health Association (APHA), American Water Works Association and Water Pollution Control Federation, 2005. *Standard Methods for the Examination of Water and Wastewater*. APHA/AWWA, Washington DC.

American Water Works Association (AWWA), 1999. *Water Quality and Treatment: A Handbook of Community Water Supplies*. McGraw-Hill, New York, N.Y.

American Water Works Association (AWWA), American Society of Civil Engineers, 2005. Water Treatment Plant Design. McGraw-Hill, New York, N.Y.

Batch, L. F., Schulz, R. C. and Linden, K. G. (2004). Evaluating water quality effects on UV disinfection of MS2 coliphage. Journal of American Water Works Association, 96(7), 75-87.

Bitton, G., Henis, Y. and Lahav N. (1972). Effect of several clay minerals and humic acid on the survival of *Klebsiella aerogenes* exposed to ultraviolet irradiation. Applied Microbiology, 23, 870-874.

Blatchley, E. R., Dumontier, N., Halaby, T. N., Levi, Y. and Laine, J. M. (2001). Bacterial responses to ultraviolet irradiation. Water Science and Technology, 43(10), 179-186.

Bohrerova, Z. and Linden, K. (2007). Standardizing photoreactivation: comparison of DNA photorepair rate in *Escherichia coli* using four different fluorescent lamps. Water Research, 41, 2832-2838.

Bolton, J. R. and Linden, K. G. (2003). Standardization of methods for fluence (UV dose) determination in bench-scale UV experiments. Journal of Environmental Engineering, 129(3), 209-215.

Borst, M. and Selvakumar, A. (2003). Particle-associated microorganisms in stormwater runoff. Water Research, 37(1), 215-223.

Bruus, J. H., Nielsen, P. H. and Keiding, K. (1992). On the stability of activated sludge flocs with implications to dewatering. Water Research, 26(12), 1597-1604.

Bydzovska, O. and Merka, V. (1981). Disinfecting properties of performic acid against *Bacteriophage-PHI X-174* as a model of small envelope free viruses. *Journal of Hygiene Epidemiology Microbiology and Immunology*, 25 (4), 414-423.

Cerf, O. (1977). Tailing of survival curves of bacterial spores. *Journal of Applied Microbiology*, 42, 1-19.

Chan, Y. Y. and Killick, E. G. (1995). The effect of salinity, light and temperature in a disposal environment on the recovery of *E. coli* following exposure to ultraviolet radiation. *Water Research*, 29 (5), 1373-1377.

Droppo, I. G., Leppard, G. G., Flannigan, D. T. and Liss, S. N. (1997). The freshwater floc: a functional relationship of water and organic and inorganic floc constituents affecting suspended sediment properties. *Water Air and Soil pollution*, 99 (1-4), 43-53.

Droppo, I. G. (2001). Rethinking what constitutes suspended sediments. *Hydrological Processes*, 15 (9), 1551-1564.

DVGW. (2006). UV Disinfection Devices for Drinking Water Supply Requirements and Testing. DVGW W294-1, -2, and -3. German Gas and Water Management Union (DVGW), Bonn, Germany.

Emerick, R. W., Loge, F. J., Thompson, D. and Darby, J. L. (1999). Factors influencing ultraviolet disinfection performance part II: association of coliform bacteria with wastewater particles. *Water Environment Research*, 71(6), 1178-1187.

Emerick, W. R., Loge, F. J., Ginn, T. and Darby, J. L. (2000). Modeling the inactivation of particle-associated coliform bacteria. *Water Environment Research*, 72(4), 432-438.

Farnood, R. (2004). Investigation of factors affecting the ultraviolet disinfection of biological aggregates. PARTEC 2004, Nuremberg, Germany.

Farnood, R. (2005). Floccs and ultraviolet disinfection. In I. G. Droppo, G. G. Leppard, S. N. Liss & T. G. Milligan (Eds.), *Flocculation in Natural and Engineered Environmental Systems* (385-395). CRC Press, Boca Raton, FL.

Friedberg, E. R., Walker, G. C. and Siede, W. (1995). *DNA Repair and Mutagenesis*, p. 92-107. ASM Press, Washington, D.C.

Friedman, B. A., Dugan, P. R., Pfister, R. M. and Remsen, C. C. (1969). Structure of exocellular polymers and their relationship to bacterial flocculation. *Journal of Bacteriology*, 98(3), 1328-1334.

Frolund, B., Palmgren, R., Keiding, K. and Nielsen, P. H. (1996). Extraction of extracellular polymers from activated sludge using a cation exchange resin. *Water Research*, 30(8), 1749-1758.

Gehr, R. and Nicell, J. (1996). Pilot studies and assessment of downstream effects of UV and ozone disinfection of a physicochemical wastewater. *Water Qual. Res. J. Can.*, 31 (2), 263-281.

Gerba, C. P. and Mcleod, J. S. (1976). Effect of sediments on survival of *Escherichia coli* in marine waters. *Applied and Environmental Microbiology*, 32 (1), 114-120.

Hanawalt, P. C., Cooper, P. K., Ganesan, A. K. and Smith, C. A. (1979). DNA repair in bacteria and mammalian cells. *Annual Review of Biochemistry*, 48, 783-836.

Harm, W. (1975). *Molecular Mechanisms for Repair of DNA, Part A*. Plenum Press, New York.

Higgins, M. J. and Novak, J. T. (1997). The effect of cations on the settling and dewatering of activated sludges: laboratory experience. *Water Environment Research*, 69, 215-224.

Horan, N. J. and Eccles, C. R. (1986). Purification and characterization of extracellular polysaccharide from activated sludges. *Water Research*, 20(11), 1427-1432.

Hu, J. Y., Chu, X. N., Quek, P. H., Feng, Y. Y. and Tan X. L. (2005). Repair and regrowth of *Escherichia coli* after low- and medium-pressure ultraviolet disinfection. *Water Science and Technology: Water Supply*, 5 (5), 101-108.

Huber, E. and Frost, M. (1998). Light scattering by small particles. *Aqua*, 47(2), 87-94.

Jagger, J., 1967. *Introduction to research in ultraviolet photobiology*. Prentice-Hall, Eaglewood Cliffs, N.J.

Jolis, D., Lam, C. and Pitt, P. (2001). Particle effects on ultraviolet disinfection of coliform bacteria in recycled water. *Water Environment Research*, 73 (2), 233-236.

Kashimida, K., Kamiko, N., Yamamoto, K. and Ohgaki, S. (1996). Assessment of photoreactivation following ultraviolet light disinfection. *Water Science and Technology*, 33, 261-269.

Kelner, A. (1951). Action spectra for photoreactivation of ultraviolet irradiated *Escherichia coli* and *Streptomyces griseus*. *Journal of General Physiology*, 34 (6), 835-852.

Knudson, G. B. (1985). Photoreactivation of UV irradiated *Legionella pneumophila* and other *Legionella* species. *Applied Environmental Microbiology*, 49 (4), 975-980.

Linden, K. G. and Darby, J. L. (1997). Estimating effective germicidal dose from medium pressure UV lamps. *ASCE Journal of Environmental Engineering*, 123 (11), 1142-1149.

Lindenauer, K. G. and Darby, J. L. (1994). Ultraviolet disinfection of wastewater: effect of dose on subsequent photoreactivation. *Water Research*, 28(4), 805-817.

Liss, S. N., Droppo, I. G., Flannigan, D. T. and Leppard, G. G. (1996). Floc architecture in wastewater and natural riverine systems. *Environmental Science and Technology*, 30, 680-686.

Liu, G., Slawson, R. M. and Huck, P. M. (2007). Impact of flocculated particles on low pressure UV inactivation of *E. coli* in drinking water. *Journal of Water Supply Research and Technology*, 56, 153-162.

Loge, F. J., Darby, J. L. and Tchobanoglous, G. (1996). UV disinfection of wastewater: a probabilistic approach to design. *Journal of Environmental Engineering*, 122(12), 1078-1084.

Loge, F. J., Emerick, R. W., Thompson, E. D., Nelson, D. C. and Darby, J. L. (1999). Factors influencing ultraviolet disinfection performance part I: light penetration to wastewater particles. *Water Environment Research*, 71(3), 377-381.

Loge, F. J., Bourgeois, K., Emerick, R. W. and Darby, J. L. (2001a). Variations in wastewater quality influencing UV disinfection performance: relative impact on filtration. *Journal of Environmental Engineering*, 127 (9), 832-837.

Loge, F. J., Emerick, R. W., Ginn, T. R. and Darby, J. L. (2001b). Association of coliform bacteria with wastewater particles impact of operational parameters of the activated sludge process. *Water Research*, 36, 41-48.

Madge, B. A. and Jensen, J. N. (2006). Ultraviolet disinfection of fecal coliform in municipal wastewater: effects of particle size. *Water Environment Research*, 78, 294-304.

Malley, J. P., Ballester, N. A., Margolin, A. B., Linden, K. G., Mofidi, A., Bolton, J. R., Crozes G., Cushing B., Mackey, E., Laine J. M. and Janex M. L. (2004). Inactivation of Pathogens with Innovative UV Technologies. American Water Works Association Research Foundation, USA.

Mamane, H. (2008). Impact of particles on UV disinfection of water and wastewater effluents: a review. *Reviews in Chemical Engineering*, 24 (2-3), 67-157.

Mamane, H. and Linden, K. G. (2006a). Impact of particle aggregated microbes on UV disinfection. I: Evaluation of spore-clay aggregates and suspended spores. *Journal of Environmental Engineering*, 132(6), 596-606.

Mamane, H. and Linden, K. G. (2006b). Impact of particle aggregated microbes on UV disinfection. II: proper absorbance measurement for UV fluence. *Journal of Environmental Engineering*, 132(6), 607-615.

Martin, N. and Gehr, R., (2007). Reduction of photoreactivation with the combined UV/Peracetic acid process or by delayed exposure to visible light. *Water Environment Research*, 79 (9), 991-999.

Mechsner, K., Fleischmann, T., Mason, C. A. and Hamer, G. (1991). UV disinfection: short term inactivation and revival. *Water Science and Technology*, 24 (2), 339-342.

Mofidi, A. A., and Linden, K. G. (2004). Disinfection effectiveness of UV light for heterotrophic bacteria leaving biologically active filters. *Journal of Water Supply Research and Technology - AQUA*, 53 (8), 553-566.

Morgan-Sagastume, F., Larsen P., Nielsen, J. L. and Nielsen P. H. (2008). Characterization of the loosely attached fraction of activated sludge bacteria. *Water Research*, 42, 843-854.

Morowitz, H. J. (1950). Absorption effects in volume irradiation of microorganisms. *Science*, 111, 229-230.

Oguma, K., Katayama, H., Mitani, H., Morita, S., Hirata, T. and Ohgaki S. (2001). Determination of pyrimidine dimers in *Escherichia coli* and *Cryptosporidium parvum* during UV light inactivation, photoreactivation, and dark repair. *Applied and Environmental Microbiology*, 67(10), 4630-4637.

Oguma, K., Katayama H. and Ohgaki, S. (2002). Photoreactivation of *Escherichia coli* after low or medium pressure UV disinfection determined by an edonuclease sensitive site assay. *Applied Environmental Microbiology*, 68 (12), 6029-6035.

Oguma, K., Katayama, H. and Ohgaki, S. (2005). Spectral impact of inactivating light on photoreactivation of *Escherichia coli*. *Journal of Environmental Engineering and Science*, 4, S1-S6 (Supplement: Suppl. 1).

ÖNORM. (2001). Plants for the Disinfection of Water Using Ultraviolet Radiation Requirements and Testing Part 1: Low Pressure Mercury Lamp Plants. ÖNORM M 5873-1. Österreichisches Normungsinstitut, Vienna, Austria.

Örmeci, B., Ducoste, J. J. and Linden K. G. (2005). UV disinfection of chlorinated water: impact on chlorine concentration and UV dose delivery. *Journal of Water Supply Research and Technology – AQUA*, 54 (3), 189-199.

Örmeci, B. and Linden, K. G. (2005). Comparison of physical and chemical methods for extraction of coliform from wastewater particles and flocs. *Environmental Engineering Science*, 22(4), 459-471.

Parker, J. A. and Darby, J. L. (1995). Particle-associated coliform in secondary effluents: shielding from ultraviolet light disinfection. *Water Environment Research*, 67(7), 1065-1075.

Passantino, L., Malley, J. Jr., Knudson, M., Ward, R. and Kim, J. (2004). Effect of low turbidity and algae on UV disinfection performance. *Journal of American Water Works Association*, 96(6), 128-137.

Pavoni, J. L., Tenney, M. W. and Echelberger, W. F. Jr. (1972). Bacterial exocellular polymers and biological flocculation. *Journal of Water Pollution Control Federation*, 44(3), 414-429.

- Pennell, K. G., Aronson, A. I. and Blatchley, E. R. (2007). Phenotypic persistence and external shielding ultraviolet radiation inactivation kinetic model. *Journal of Applied Microbiology*, 104 (4), 1192-1202.
- Qualls, R. G., Flynn, M. P. and Johnson, J. D. (1983). The role of suspended particles in ultraviolet disinfection. *Journal of Water Pollution Control Federation*, 55(10), 1280-1285.
- Sanin, D. F. and Vesilind, A. P. (1996). Synthetic sludge: a physical/chemical model in understanding bioflocculation. *Water Environment Research*, 68(5), 927-933.
- Sanin, D. F. and Vesilind, A. P. (1999). A comparison of physical properties of synthetic sludge with activated sludge. *Water Environment Research*, 71(2), 191-196.
- Scheible, O. K., Casey, M. and Forndran, A. (1986). Ultraviolet disinfection of wastewaters from secondary effluents and combined sewer overflows, EP-600/2-86/005. U.S. Environmental Protection Agency, Cincinnati, Ohio.
- Schoenen, D. and Kolch, A. (1992). Photoreactivation of *Escherichia coli* depending on light intensity after UV irradiation. *Zentralblatt Fur Hygiene und Umweltmedizin*, 192 (6), 565-570
- Severin, B. F., Suidan, M. T. and Engelbrecht, R. S. (1983). Kinetic modeling of UV disinfection of water. *Water Research*, 17(11), 1669-1678.
- Shin, G.A., Linden, K. G., Arrowood, M. J. and Sobsey, M. D. (2001). Low-pressure UV inactivation and DNA repair potential of *Cryptosporidium parvum* oocysts. *Applied Environmental Microbiology*, 67(7), 3029-3032.

- Sinha, R. P. and Hader, D. P. (2002). UV-induced DNA damage and repair: a review. *Photochemical and Photobiological Sciences*, 1 (4), 225-236.
- Sobeck, D. C. and Higgins, M. J. (2002). Examination of three theories for mechanisms of cation-induced bioflocculation. *Water Research*, 36(3), 527-538.
- Sommer, R., Lhotsky, M., Haider, T. and Cabaj, A. (2000). UV inactivation, liquid-holding recovery and photoreactivation of *Escherichia coli* O157 and other pathogenic *Escherichia coli* strains in water. *Journal of Food Protection*, 63 (8), 1015-1020.
- Templeton, M. R., Andrews, R. C. and Hofmann R. (2005). Inactivation of particle-associated viral surrogates by ultraviolet light. *Water Research*, 39(15), 3487-3500.
- Tezuka, Y. (1969). Cation-dependent flocculation in a Flavobacterium species predominant in activated sludge. *Applied Microbiology*, 17(2), 222-226.
- USEPA (2006) Ultraviolet disinfection guidance manual for the final long term 2 enhanced surface water treatment rule. Office of Water (4601) EPA 815-R-06-007.
- Urbain, V., Block, J. C. and Manem, J. (1993). Bioflocculation in activated sludge: an analytic approach. *Water Research*, 27(5), 829-838.
- Villarino, A., Rager, M. N., Grimont, P. A. D., Bouvet, O. M. M. (2003). Are UV-induced nonculturable *Escherichia coli* K-12 cells alive or dead? *European Journal of Biochemistry*, 270 (12), 2689-2695.
- Whitby, G. E. and Palmateer, G. (1993). The effect of UV transmission, suspended solids and photoreactivation on microorganisms in wastewater treated with UV light. *Water Science and Technology*, 27 (3-4), 379-386.

Whitby, G. E., Palmateer, G., Cook, W. G., Maarschalkerweerd, J., Huber D. and Flood, K. (1984). UV disinfection of secondary effluent. *Journal of Water Pollution Control Federation*, 56 (7), 844-849.

Wilkinson, K. J., Negre, J. C. and Buffle, J. (1997). Coagulation of colloidal material in surface waters: the role of natural organic matter. *Journal of Contaminant Hydrology*, 26, 229-243.

Zimmer, J. L. and Slawson, R. M. (2002). Potential repair of *Escherichia coli* DNA following exposure to UV radiation from both medium and low pressure UV sources in drinking water treatment. *Applied Environmental Microbiology*, 68 (7), 3293-3299.

CHAPTER 3

MATERIALS AND METHODS

Chapters 4 through 7 each has its own materials and methods section. However, due to the limits imposed by journals on the number of pages a paper can have, some specific details on materials and methods are not provided in the relevant chapters, and are discussed here instead.

3.1. Determination of Ingredients for Synthetic Floes

The aim of the synthetic floes created for Chapters 4 and 5 was not to simulate actual wastewater floes with all of their chemical and biological constituents, but rather to create a simple flocculation matrix with the essential constituents that could be used to evaluate one parameter at a time. With the objective of assessing the effects of particles and floes on UV disinfection of bacteria, the essential constituents included in the matrix were particles, flocculating agents and the bacteria themselves. As well, the flocculating agents added to the matrix were limited to cations and extracellular polymers with the intention of maintaining the synthetic system simple and keeping key parameters such as UV absorbance of the solution under control.

The experiments presented in Chapters 4 and 5 were highly sensitive to the particle concentration and particle size distribution properties of water. For that reason, the source deionized water was analyzed with the particle counter prior to use and the background particle concentrations were maintained below 100 particles/mL.

There were two promising particle alternatives considered for the experiments: clay particles and polystyrene latex particles. The clay option was abandoned as polystyrene latex particles presented a better alternative due to their size specific availability and relatively higher uniformity with respect to both size and shape.

Five different sizes of latex particles having the same physical and chemical properties were selected: 1 μm , 3.2 μm , 11 μm , 25 μm , and 45 μm . The particles were obtained from Duke Scientific Corporation (CA, USA) and their characteristics are given in Table 3.1. The 1 and 3.2 μm particles were used to represent small particles being close to the size of *Escherichia coli* (1x2 μm). The 11 μm particles resembled the hypothesized minimum particle size (on the order of 10 μm for wastewater) controlling the capability of particles to shield bacteria from UV light (Emerick et al., 2000). The 25 and 45 μm particles served the purpose of testing with larger size particles that may be present in wastewater and provide complete protection from UV irradiation.

Table 3.1: Polystyrene latex particle characteristics.

<i>Physical/Chemical Properties</i>	<i>1 μm</i>	<i>3.2 μm</i>	<i>11 μm</i>	<i>25 μm</i>	<i>45 μm</i>
Particle Composition	Polystyrene	Polystyrene	Polystyrene	Polystyrene	Polystyrene
Particle Density	1.05 g/cm ³				
Solubility in Water	Insoluble	Insoluble	Insoluble	Insoluble	Insoluble
Size Uniformity	≤ 3%	≤ 45%	≤ 18%	≤ 15%	≤ 15%
Refractive Index	1.6	1.6	1.6	1.6	1.6

Flocculating agents were chosen based on previous studies on synthetic wastewater sludge (Sanin and Vesilind, 1996; Örmeci and Vesilind, 2000). It was decided that alginate would be used as the extracellular polymer and calcium as the divalent cation (or bridging agent). The applied concentrations of alginate and calcium were determined based on the aforementioned studies as well as preliminary experiments.

For the bacterial seeding *Escherichia coli* (*E. coli*) (ATCC®23631™) from the fecal coliform family was chosen, as it is one of the most commonly used indicator organisms of fecal contamination in waters.

3.2. Preparation of Stock Solutions and Growth Media

The stock solutions used throughout the experiments included: magnesium chloride solution, phosphate buffer solution, calcium chloride solution and alginic acid solution. In addition to these stock solutions, Difco™ M-Endo Agar LES (Becton, Dickinson & Company, MD, USA) and Bacto™ Tryptic Soy Broth (Becton, Dickinson & Company, MD, USA) were continually used as the growth media for membrane filtration (MF) tests and *E. coli* stock preparation, respectively.

The phosphate buffered saline (PBS) is recommended as a dilution solution to be used during MF analyses in Standard Methods. Magnesium chloride and phosphate buffer solutions together form the contents of PBS. For the preparation of phosphate buffer, 34 g of potassium dihydrogen phosphate (KH_2PO_4) was dissolved in 500 mL deionized water, and then the pH of the solution was adjusted to 7.2 ± 0.5 by titrating with 1 N sodium hydroxide (NaOH). After titration the volume of the solution was brought up to 1 L with deionized water. Magnesium chloride solution on the other hand was simply prepared by dissolving 81.1 g of magnesium chloride hexahydrate ($\text{MgCl}_2 \cdot 6\text{H}_2\text{O}$) in 1 L deionized water. Finally, PBS was prepared by adding 1.25 mL stock phosphate buffer solution and 5 mL magnesium chloride solution to 1 L of deionized water. The prepared PBS solutions were sterilized by autoclaving at 121°C for 15 minutes, before use.

Anhydrous calcium chloride salt (CaCl_2) was used for the preparation of the calcium stock solution. In order to yield a stock with a concentration of 1 M Ca^{2+} , 22.2 g of

anhydrous salt was added into 200 mL of deionized water and completely dissolved by mixing. This stock solution was the primary source of calcium applied to initiate flocculation at different degrees throughout the experiments in Chapters 4 and 5.

Alginate solution was prepared by mixing alginic acid (in the form of alginic acid sodium salt derived from brown algae, obtained from Sigma Chemical Company, MO, USA) in water at a concentration of 5g/L. In order to ensure that alginate is completely dissolved in water, the stock solution was thoroughly mixed and let stand for at least 24 h before it was used.

Both M-Endo Agar LES and Tryptic Soy Broth were prepared following the directions provided by the suppliers on the product containers. M-Endo Agar LES was prepared in batches that would be used within less than 2 weeks and Tryptic Soy Broth was prepared as needed in required amounts and used directly after preparation for revival of frozen bacterial stock.

3.3. Preparation of Synthetic Floccs

Extreme care was taken to have practically particle free water (< 100 particles/mL) prior to the addition of specific size particles at desired number concentrations. To increase the consistency of particle number concentration and size distribution within a set of experiments, stock particle solutions were prepared in large volumes at the beginning of

an experiment set and preserved by keeping the containers tightly sealed, therefore allowing for the same particle-stock solution to be used throughout a set of experiments. Prior to initiation of each UV exposure trial (specific particle size, alginate concentration and calcium concentration) a 200 mL sample was taken from the previously prepared particle-stock solution and dispensed into a 1 L beaker which had been rinsed with particle-free deionized water. After that point the beaker was continuously mixed with magnetic stirring rods and always kept covered unless a sample was to be withdrawn from the beaker or a material was to be added into the beaker.

The initial particle number concentration was selected as 6,000 ($\pm 5\%$) particles/mL for all particle sizes. Previous studies reported particle number concentrations in secondary wastewater effluents as 1000 to 2000 particles/mL for particles larger than 10 μm (Emerick et al., 2000; Örmeci and Linden, 2002), and as 13,000 to 18,000 for particles larger than 2 μm (Örmeci and Linden, 2002). When particles less than 2 μm in size are considered, the number concentration reaches 10^6 to 10^7 particles/mL (Parker et al., 1971). Hence, it is not possible to identify a single number concentration that would apply to all particle sizes selected for this study. However, in order to be able to investigate the effect of particle size only the number concentration of different sized particles had to be kept the same. The rationale for the chosen concentration of 6000 particles/mL is that it fell within the ranges indicated in the literature. Another reason for the chosen concentration was to make the analysis of the suspensions with the particle size analyzer without dilution possible. Dilution of samples is highly undesirable as it might cause significant deviations from the original composition of a sample by changing

the solution's ionic strength and composition (Örmeci and Linden, 2002). This is particularly critical for floc analysis as wastewater flocs tend to be fragile and can break apart easily upon handling (Mamane and Linden, 2006).

The particle stock solutions were prepared by injecting small amounts of concentrated polystyrene latex particle suspensions (10% solids content) into a continuously mixed beaker containing deionized water and simultaneously checking the concentration of particles in the beaker with the particle counter, until the desired concentration was achieved.

3.4. UV Collimated Beam Setup

The UV setup consisted of a set of low-pressure mercury lamps (Phillips UV-C germicidal lamps) emitting nearly monochromatic ultraviolet light at 253.7 nm for the experiments in Chapters 4 through 7. In Chapter 6, a medium-pressure UV setup was also used. To achieve collimation of light in the low-pressure setup, baffles with holes of varying sizes were placed successively along the light path. In the medium-pressure setup, the collimation of light was achieved via a collimation tube. Stirring is crucial for assuring equal UV dose delivery to all microorganisms in the solution during inactivation (Bolton and Linden, 2003), therefore a stirring mechanism was placed at the bottom of the UV reactor and the samples were continuously and gently mixed with micro stirring rods to avoid vortex formation. The low-pressure UV apparatus is depicted in Figure 3.1.

The medium-pressure UV apparatus was very similar in principal, with the only major difference being how the collimation of light was achieved, as described earlier.

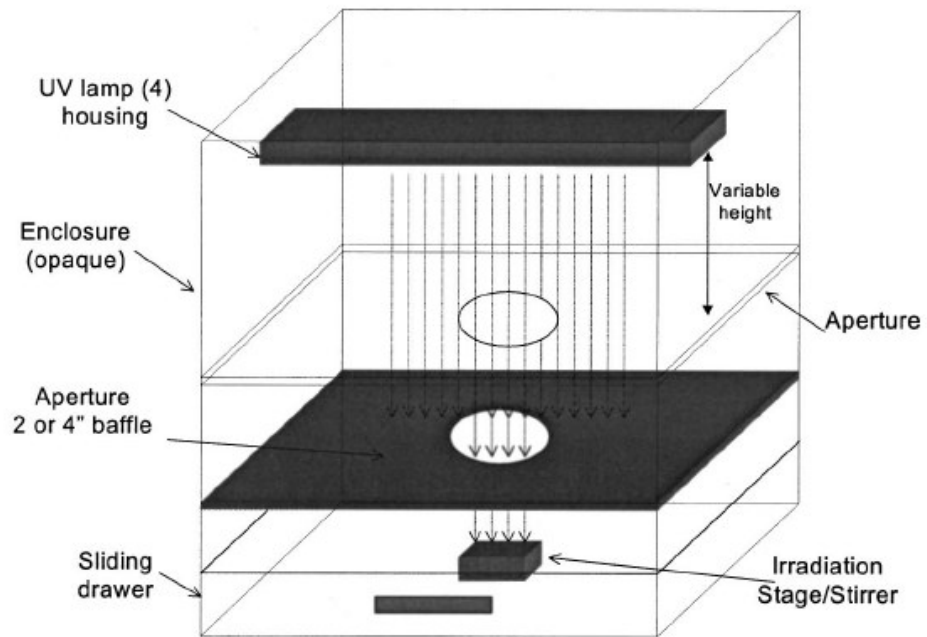


Figure 3.1: Low-pressure UV collimated beam setup (Source: Bolton and Linden, 2003).

3.5. UV Dose Determination

In order to calculate the required exposure times to reach the desired UV doses, procedures outlined by Bolton and Linden (2003) were followed. For low-pressure UV lamps these procedures include the following four necessary corrections to be included in the calculation of the actual germicidal irradiance throughout the sample volume:

- 1) Reflection Factor
- 2) Petri Factor
- 3) Water Factor
- 4) Divergence Factor

Medium-pressure UV lamps require two more correction factors in addition to the four listed above: sensor factor and germicidal factor. The additional factors are necessary to account for the broadband UV radiation generated by medium-pressure UV lamps. The sensor factor corrects for the sensitivity of the detector for the range of wavelengths encountered, and the germicidal factor weights the relative germicidal effectiveness of UV light generated at each wavelength.

The depth of the sample to be irradiated is also an important factor in the calculation of true irradiance. In order to keep corrections as simple as possible, the sample volume was kept at 60 mL or less yielding a sample depth of less than 2 cm. When a sample's depth is

less than 2 cm that sample is referred to as a shallow sample and the exposure times are calculated accordingly (Bolton and Linden, 2003).

The most important inputs for the calculation of exposure times were the incident irradiance values (mW/cm^2) measured with a radiometer (International Light, MA, USA) at the surface of the sample to be irradiated. Since the intensity of light emitted by UV lamps fluctuates, extreme care was taken to obtain a truly representative intensity for each sample to be tested. For this reason, the intensity was measured immediately before each exposure, and the exposure times were calculated accordingly. Other inputs required for the calculation of exposure times included: the distance between the UV lamps and the top of the sample surface, the Petri dish diameter and the sample volume, and the absorption coefficient of the sample. The distance between the UV lamps and the top of the sample surface is related to the divergence factor, and was fixed at 48.5 cm for all the low-pressure UV experiments and at 30 cm for all the medium-pressure UV experiments. The Petri dishes used for the entire set of experiments had a diameter of 6.5 cm and the sample volume was 60 mL or less, leading to a sample depth of 1.8 cm or less. These two values (Petri dish diameter and sample volume) were required for the calculation of Petri factor, divergence factor and water factor. Calculation of water factor requires measuring the absorption coefficient (absorbance for a 1 cm path length) of the solution to be irradiated. For low-pressure UV experiments, the absorption coefficient of each sample solution was measured at 254 nm in a UV-visible spectrophotometer (Varian Model Cary 100BIO, Victoria, Australia), which had previously been balanced by deionized water in the same cuvette as the one used for the samples. For medium-pressure UV experiments,

the UV absorbance measurements involved an absorbance scan of the sample solution from 200 nm to 300 nm to reflect the solution's absorbance characteristics within the critical range of wavelengths generated by the lamps. The scans were conducted with the same UV-visible spectrophotometer and the absorbance coefficients of the samples were measured against a background cuvette containing deionized water in the reference cell.

The reflection factor is calculated by subtracting the fraction of light that is reflected upon entry to water medium from air medium. As the fraction reflected (R) is a constant between these two media such that $R = 0.025$, the reflection factor is also equal to a constant value of $0.975 (1 - R)$.

The Petri factor accounts for the non-uniformity of the irradiance field over the sample and is calculated by averaging the intensity measured at different points within the irradiance field. However, the UV apparatuses employed in this project provided virtually uniform irradiance fields and thus, Petri factor was taken as unity (1).

The water factor is defined as:

$$\text{Water Factor} = \frac{1 - 10^{-al}}{al \ln(10)}$$

where a = absorbance for a 1 cm path length (cm^{-1}) and ℓ = vertical path length (cm) of the water in the Petri dish. Since water factor is a function of UV absorbance, it had a different value for every different condition tested.

The divergence factor is defined as:

$$\text{Divergence Factor} = \frac{L}{(L + \ell)}$$

where L = the distance between the UV lamps and the top of the sample surface (cm) and as in the water factor ℓ = vertical path length (cm) of the water in the Petri dish.

Thus, the average irradiance (E'_{avg} , mW/cm^2) in the water is defined by:

$$E'_{avg} = E_0 \times \text{Reflection Factor} \times \text{Petri Factor} \times \text{Water Factor} \times \text{Divergence Factor}$$

where E_0 = radiometer reading (intensity, mW/cm^2) at the centre of the sample's surface.

Finally, dose is defined as:

$$\text{Dose} = E'_{avg} \times \text{Exposure Time}$$

Therefore, once the average irradiance was calculated the exposure times were achieved simply by dividing the desired doses by the average irradiance values.

3.6. Bacterial Enumeration

In the experiments in Chapters 4 and 5, UV exposed samples were first deflocculated in centrifuge tubes on a vortex mixer (Baxter Diagnostics Inc., IL, USA) for 45 s in order to break apart particle-associated and clumped bacteria for more accurate enumeration. Different vortex mixing times were tested ranging from 15 s to 2 min and best results were achieved for 45 s of vortex mixing. Since the time elapsed both after the UV exposure and the deflocculation is crucial, each sample was taken immediately to the vortex mixer directly following UV irradiation and membrane filtration was carried out immediately after deflocculation.

Bacterial enumeration was carried out by following Standard Total Coliform Membrane Filter Procedure (Protocol 9222 B.) given in Standard Methods (APHA, 2005). M-Endo Agar LES medium was used as a selective growth medium and three replicates were made at each dilution. The filtration was carried out using glass filtration units by applying suction through 0.45- μm Millipore (MA, USA) filter paper. The volumes filtered were recorded and all the bacterial concentration values were adjusted accordingly to report the units as number of colony forming units per 100 mL (CFU/100mL).

Dilutions were performed in 100 mL graduated cylinders filled with required amounts of PBS and the time spent by bacteria in the dilution water was minimized in order to prevent death or growth of bacteria during dilution. To ensure that the bacterial concentration in any dilution cylinder remained homogeneous, the cylinders were sealed with parafilm and shaken at least 5 times prior to the next dilution step or filtration.

Additionally, control samples were prepared and filtered in between the actual sample filtrations against possible causes of error from contamination of stock solutions or the deionized water. These control samples included the deionized water itself, PBS, magnesium chloride stock solution, phosphate buffer stock solution, calcium stock solution and alginate stock solution.

Once the samples of a certain set were all filtered and the filter papers were placed appropriately on the growth media, they were put in the incubator (HACH BOD Incubator, CO, USA) and incubated for 24 (\pm 3 hours) at 37°C for experiments involving *E. coli* (ATCC[®]23631[™]), and at 35°C for experiments conducted with indigenous wastewater coliform bacteria. The bacterial counts were repeated at least three times, more in cases where the number counted varied between different counts.

In order to ensure the accuracy and reproducibility of results, it is important to have a stable bacterial count in the synthetic matrix during UV inactivation tests. This was

especially important for the regrowth studies in Chapter 7, as bacteria concentrations were monitored over prolonged periods of time. For this reason, a trial study was conducted where the survival of bacteria was monitored in PBS for 24 h. The trial was carried out at room temperature and the change in CFU was measured by the MF technique. The results indicated a considerably stable bacterial concentration in PBS over time, with only a 6.9% reduction in total concentration in 24 h.

3.7. Particle/Floc Size, Concentration and Shape Analyses

Particle size counts were performed with the help of DPA4100 Particle Analysis System (BrightWell Technologies, Ottawa, ON). Since the concentrations worked with fell within the range of allowable concentrations during the course of the experiments, dilution was not deemed necessary in order to carry out particle analyses for any sample. This provided a major advantage since dilution may impact the size and distribution of particles/flocs. Depending on the availability of the solution to be tested 5 to 10 mL samples were injected into the sampling syringe of the instrument and sufficient mixing was provided through a stirring rod. Due to the sensitivity of the measurements care was taken to keep the instrument and the environment clean any time a sample was being analyzed. The analyses were undertaken in volume based analysis and time-resolved analysis modes. Several trials were conducted for the stock-particle solution preparations to come up with the desired particle number concentrations. For the analysis of flocculated samples in Chapter 5, flocculation was initiated inside the sampling syringe (calcium ions were injected into the sampling syringe) to minimize any error that might

result from the disruption of flocs during their transfer from one container to another and also to keep the flocculation time constant for each sample.

Particle count tests explained above analyzed particle number concentration, and particle size distribution characteristics of the samples. In addition, for qualitative as well as quantitative analyses of flocculation and flocs, the image capturing tool of the software was utilized. This tool is capable of capturing images of particles/flocs satisfying a chosen criterion (such as size) during the analysis of the sample. Later the captured images can be analyzed via the DPA4100 software and parameters pertaining to individual flocs in the captured images reported. These parameters included equivalent circular diameter, maximum diameter, circularity, area, perimeter, and transparency.

3.8. Presentation of the Inactivation Data

The inactivation data are presented in the form of dose-response curves which were plotted using the following method of calculation. Mean concentration (CFU/100 mL) of *E. coli* spiked in solutions before UV irradiation was taken as the initial bacterial concentration, N_0 . For each UV dose, the arithmetic mean of the replicates of *E. coli* concentration was calculated, and taken as the surviving bacterial concentration, N . The \log_{10} transformation of N/N_0 (Log Survival) was plotted against the UV dose generating a dose-response curve.

3.9. References

American Public Health Association (APHA), American Water Works Association and Water Pollution Control Federation, 2005. Standard Methods for the Examination of Water and Wastewater. APHA/AWWA, Washington DC.

Bolton, J. R., and Linden, K. G. (2003). Standardization of methods for fluence (UV dose) determination in bench-scale UV experiments. *Journal of Environmental Engineering*, 129(3), 209-215.

Emerick, W. R., Loge, F. J., Ginn, T. and Darby, J. L. (2000). Modeling the inactivation of particle-associated coliform bacteria. *Water Environment Research*, 72(4), 432-438.

Mamane, H., and Linden, K. G. (2006). Impact of particle aggregated microbes on UV disinfection. I: Evaluation of spore-clay aggregates and suspended spores. *Journal of Environmental Engineering*, 132(6), 596-606.

Örmeci, B., and Vesilind, A. P. (2000). Development of an improved synthetic sludge: a possible surrogate for studying activated sludge dewatering characteristics. *Water Research*, 34(4), 1069-1078.

Örmeci, B., and Linden, K. G. (2002). Comparison of UV and Chlorine Inactivation of Particle and Non-Particle-Associated Coliform. *Water Supply*, 2(5-6), 403-410.

Parker, D. S., Jenkins, D., and Kaufman, W. J. (1971). Physical conditioning of the activated sludge floc. *Journal of Water Pollution Control Federation*, 43, 1897.

Sanin, D. F., and Vesilind, A. P. (1996). Synthetic sludge: a physical/chemical model in understanding bioflocculation. *Water Environment Research*, 68(5), 927-933.

CHAPTER 4

EFFECT OF PARTICLES AND BIOFLOCCULATION ON ULTRAVIOLET DISINFECTION OF *ESCHERICHIA COLI*

4.1. Abstract

Presence of particles is known to decrease the effectiveness of ultraviolet (UV) disinfection by shielding the targeted microorganisms from UV light. This study aims to provide an in-depth understanding of the effect of particles and flocs on UV disinfection by using a stable, well-defined and well-controlled synthetic system that can simulate the bioflocculation of particles and microorganisms in water and wastewater samples. The synthetic system was created by using *Escherichia coli*, latex particles (1, 3.2, 11, 25, and 45 μm), alginate, and divalent cations; and the bioflocculation of particles was achieved naturally, as it would occur in the environment, without using chemical coagulants. *E. coli* was quantified before and after UV disinfection using membrane filtration. Even in the absence of particles, some of the self-aggregated *E. coli* could survive a UV dose of 90 mJ/cm^2 . *E. coli* inactivation levels measured in the presence of particles were lower than the inactivation levels measured in the absence of particles. At low UV doses ($<9 \text{ mJ}/\text{cm}^2$), neither particle size nor degree of flocculation had a significant effect on the inactivation of *E. coli*. Particle size had a significant effect on the inactivation of *E. coli* only at high UV doses (80 mJ/cm^2), and larger particles (e.g., 25 μm) protected bacteria more compared to smaller particles (e.g., 3.2 and 11 μm). What size of particles the flocs were made of (3.2, 11, and 25 μm) did not make a significant difference on the inactivation levels of *E. coli*. For 3.2 μm particles, there was no significant difference in

E. coli inactivation between non-flocculated and flocculated samples at any UV dose. For 11 and 25 μm particles, there was a significant difference in *E. coli* inactivation between non-flocculated and flocculated samples at 80 mJ/cm^2 . Degree of flocculation became a significant factor in determining the number of surviving bacteria only at high UV doses and only for larger particles.

Keywords: Bacteria, Bioflocculation, Disinfection, Floc, Particle, Ultraviolet.

4.2. Introduction

The effectiveness of UV disinfection is closely related to the water quality parameters, and inactivation of microorganisms has been shown to decrease in the presence of particles (Qualls et al., 1985; Parker and Darby, 1995; Loge et al., 1999; Emerick et al., 2000; Örmeci and Linden, 2002; Christensen and Linden, 2003; Templeton et al., 2005; Wu et al., 2005; Farnood, 2005; Mamane and Linden, 2006). For an effective UV disinfection, it is necessary that a sufficient amount of UV light penetrates through the water and is delivered to the target organisms. Particles impact UV disinfection performance by interfering with the penetration and transmittance of UV light within the system. The interference usually occurs by different mechanisms: scattering, absorption, reflection and diffusion of incident UV light (Batch et al., 2004). When UV light is scattered by particles, it is still capable of inactivating microbes. UV light that is absorbed by particles, on the other hand, is no longer available for inactivation (Huber and Frost, 1998; Mamane, 2008). Particles can also shield the target organisms from UV light

through particle-microbe association and decrease the overall level of inactivation (Örmeci and Linden, 2002; Christensen and Linden, 2003; Passantino et al., 2004).

Due to their highly variable physical, chemical and biological characteristics and time-dependent nature of microbial populations, it is not possible to carry out controlled and reproducible experiments when natural water and wastewater samples are used. Therefore, for studying the effect of particles and flocs on UV disinfection, there is a need for a stable, well-defined and well-controlled surrogate system where the particle characteristics, size and distribution, as well as the particle-association and the degree of flocculation can be well-controlled. If the flocculation can be initiated as it would occur naturally in environmental samples, without the addition of chemical coagulants, the system would be more representative of natural water and wastewater samples and provide additional insights to the factors that limit UV disinfection efficiency. Chemical coagulants are likely to influence the UV disinfection efficiency by absorbing the UV light and changing the size and structure of the final flocs.

Bioflocculation is defined as the natural process of microorganisms and particles aggregating into flocs. The polymeric network, which is made of extracellular polymeric substances originating from water and wastewater bacteria, holds the constituents of a floc together (Urbain et al., 1993). Cations such as Ca^{2+} and Mg^{2+} also play an important role in bioflocculation by enhancing bridging between the negatively charged surfaces of bacteria, extracellular polymers, and particles and have an overall promoting effect on

floc formation (Tezuka, 1969). A stable chemical surrogate for bioflocculation was created by using polystyrene latex particles, alginate and calcium ions and was shown to serve as a good surrogate material when reproducibility was a concern (Sanin and Vesilind, 1996, 1999; Örmeci and Vesilind, 2000).

It was hypothesized in this study that with some modifications to the model suggested by Sanin and Vesilind (1996), a well-controlled system of latex particles and bacteria can be created for studying the effects of particles and bioflocculation on UV disinfection performance. Latex particles have a very uniform size distribution and they are perfectly spherical. Their surface characteristics, such as surface charge and hydrophobicity, can be selected to represent those of natural particles in water and wastewater. Using latex particles provides several advantages and most importantly enables to study the effect of a single particle size on UV disinfection performance which cannot be achieved with natural water samples or with other synthetic systems (e.g., clay, activated carbon, goethite). The main objective of this study was to provide an in-depth understanding on how and to what extent particles and flocs limit the efficiency of UV disinfection, and to establish a relationship between the size of the particles, the degree of flocculation and the UV disinfection performance using a well-controlled synthetic system.

4.3. Materials and Methods

4.3.1. Preparation of particle suspensions

Five different sizes of latex particles having the same physical and chemical properties were selected: 1 μm , 3.2 μm , 11 μm , 25 μm , and 45 μm . The particles were obtained from Thermo Scientific (CA, USA). The initial particle number concentration in samples was selected as 6000 ($\pm 5\%$) particles/mL based on the particle counts measured in surface waters and secondary effluent. The particle stock suspensions were prepared by injecting small amounts of polystyrene latex particle suspensions into a continuously mixed beaker containing particle-free deionized water, which was immediately followed by a particle concentration check with the particle counter until the desired number concentration of 6000 ($\pm 5\%$) was achieved.

4.3.2. Addition of *E. coli*

Escherichia coli (ATCC[®] 23631[™]) was chosen as the testing organism and was obtained from Cedarlane Laboratories (Hornby, ON). The bacteria came in the form of a pellet and were revived following the procedures suggested by the main supplier (ATCC). In brief, the procedures involved rehydrating the pellet in 0.5 mL of TYG broth (ATCC Medium #603) and transferring this aliquot into a tube containing 6 mL of TYG medium which then was incubated at 37 °C for 24 h. This culture formed the primary stock of *E. coli* for the experiments and was stored in a deep-freezer at a temperature of -20 °C or below. For use in the experiments, a new batch of culture was started from this stock by first incubating the culture overnight at 37 °C to allow for the bacteria to recover from

freezing. Then, 1 mL of this culture was added to 100 mL of tryptic soy broth in a flask and incubated at 37 °C for 4-5 h to bring the bacteria to a late exponential growth phase. Different growth phases were found to result in different levels of *E. coli* resistance to UV light (Malley et al., 2004). Thus, cultures were always brought to late exponential growth phase prior to their use in the inactivation experiments.

After the particle suspensions with desired numbers of particles were prepared, magnesium chloride (MgCl₂) and phosphate buffer stock (KH₂PO₄) solutions were added to the samples to provide a stable environment for the bacteria. The bacteria were added in amounts yielding an initial concentration of about 2 x 10⁷ colony forming units per 100 mL (CFU/ 100 mL).

4.3.3. Bioflocculation of particles

Flocculating agents were chosen based on previous studies on bioflocculation (Sanin and Vesilind, 1996; Örmeci and Vesilind, 2000) but with some modifications. Alginate was used as the extracellular polymer, latex particles as water/ wastewater particles, and calcium as the divalent cation, or bridging agent, to initiate the bioflocculation process. Anhydrous calcium chloride salt (CaCl₂) was used to prepare a 1 M calcium stock solution from which desired Ca²⁺ concentrations in the samples were achieved. Alginate solution was prepared by mixing alginic acid (in the form of alginic acid sodium salt derived from brown algae, obtained from Sigma Chemical Company, MO, USA) in deionized water at a concentration of 5 g/L. In order to ensure complete dissolution of

alginate in water, the stock solution was thoroughly mixed and let stand for at least 24 h before it was used.

Bioflocculation was achieved by addition of alginate first and then calcium ions (flocculating agents) to samples already containing bacteria and particles. It should be noted that flocculation is a time-dependent process (i.e., the floc size increases with time), therefore each sample was flocculated for the same period of time prior to UV exposure for an accurate comparison of flocculation effects on the inactivation of bacteria. The preliminary experiments indicated that visible flocs started forming within 5 min at the lowest concentrations of calcium (5 mM) and alginate (10 mg/L) tested, thus a 5-min waiting time was applied to all samples prior to irradiation.

4.3.4. UV irradiation experiments

The UV collimated-beam setup consisted of four low-pressure mercury lamps (Phillips UV-C germicidal lamps, TUV 15W/G15 T8) emitting monochromatic ultraviolet light at 253.7 nm. The collimation of light was achieved by successively placed baffles along the UV light path. UV irradiation experiments were conducted according to the procedures outlined in Bolton and Linden (2003), and they were irradiated in a random order of UV doses (0-100 mJ/cm²).

For the low UV doses tested, it was ensured that the exposure times were longer than 30 s. The 6.5-cm Petri dishes used for the inactivation experiments allowed for a sample solution depth of 0.6 cm when sample volume was 20 mL. The samples were continuously mixed at low speeds with micro stirring rods to avoid vortex formation. The incident UV intensity was measured by a radiometer (International Light, MA, USA, IL 1400) before samples were exposed to UV light.

The UV doses used in this study ranged between 0 and 100 mJ/cm². The UV doses were chosen to represent a wide range of UV doses used in practice by water and wastewater treatment plants. Low UV dosage values range from 5 to 15 mJ/cm² and are considered sufficient to inactivate *Cryptosporidium parvum* and *Giardia*, and majority of *E. coli* bacteria are also inactivated in this dose range. A UV dose of 40 mJ/cm² is typically the minimum requirement for drinking water disinfection plants, whereas recommended design UV doses can go up to 100 mJ/cm² for reclaimed water systems depending on the upstream treatment application.

4.3.5. *E. coli* enumeration

After UV irradiation, the samples were first vortexed (Baxter Diagnostics Inc., IL, USA) for 45 s in order to break apart particle-associated and clumped bacteria before enumeration. When culture-based enumeration methods are used, aggregated or clumped microorganisms might lead to the underestimation of actual bacteria numbers in samples. Membrane filtration was used to enumerate the *E. coli* according to Protocol 9222 B

given in Standard Methods (APHA et al., 2005), and m-Endo Agar LES medium (Becton, Dickinson & Company, MD, USA) was used as the selective growth medium. For each enumeration, at least three different dilutions were used and three replicates were made at each dilution. After filtration, the samples were incubated for 24 (± 3) hours at 35 °C.

4.3.6. Particle and floc size measurements

Particle and floc size measurements were conducted using the DPA4100 Particle Analysis System (BrightWell Technologies, Ottawa, ON), which utilizes Micro-Flow Imaging™ technology to analyze particle populations in fluids. Since the particle concentrations worked with fell within the instrument's range, dilution of samples was not necessary. This provided an advantage in accurately determining the size and distribution of particles as well as flocs. Samples of 10 mL were injected into the sampling syringe of the instrument, and particle number concentrations and particle size distribution of the samples were measured. In addition, images of particles and flocs were captured when they were passing through the flow cell for qualitative analysis and confirmation of the degree of flocculation. The software of the instrument also provided other relevant parameters such as area, volume, and density of the flocs formed.

4.3.7. Experimental design and data analysis

Experiments were conducted in three phases. Phase I focused on the effect of particle size alone on the UV inactivation of *E. coli* by using uniformly sized and shaped latex

particles. No flocculating agents were added and the samples were composed of particles and bacteria in PBS. In Phase II, bioflocculant agents alginate and Ca^{2+} were used to study the effect of flocculation on UV inactivation of *E. coli*. Samples contained bacteria and the selected size of particles, and the degree of flocculation was controlled by changing the Ca^{2+} concentration (0-15 mM in 5 mM increments) at a fixed alginate concentration (10 mg/L). In Phase III, experiments were designed to compare the UV inactivation levels between non-flocculated and well-flocculated samples. Flocculation was achieved at the highest Ca^{2+} and alginate concentrations (15 mM Ca^{2+} and 10 mg/L alginate) used in this study. The general experimental matrix used in the three phases is given in Table 4.1.

Preliminary experiments indicated that the effect of flocculation on UV disinfection could be different at low and high UV dose ranges, so the experiments were designed to cover both the low UV (0-15 mJ/cm^2 in 5 increments of 3 mJ/cm^2) and high UV (0-100 mJ/cm^2 in 10 increments of 10 mJ/cm^2) dose ranges for Phase I and Phase II. The experiments were carried out with 3 replicates for each dilution. In Phase III, UV exposures were carried out for both flocculated and non-flocculated samples at 15, 40, and 80 mJ/cm^2 . The UV exposures were repeated 5 times with 3 dilution replicates for each exposure yielding a total of 15 replicates for each UV dose tested. This allowed advanced statistical analysis of the data and increased the accuracy of results for well-flocculated samples.

For data analysis in Phase I and Phase II, the average UV inactivation was plotted against UV dose, with error bars indicating the standard deviation. For Phase III, box-and-whisker diagrams were used to plot the data. Single and two factor ANOVA analyses were carried out to determine the significance of particle size and flocculation effects on the inactivation of bacteria at UV doses of 15, 40 and 80 mJ/cm².

4.4. Results and Discussion

4.4.1. Phase I: effect of particles on UV inactivation

Phase I aimed to investigate the effect of particles and particle size on UV disinfection. In addition, UV inactivation of *E. coli* alone, without any particles, was determined for comparison of inactivation levels in the absence and presence of particles. Five different sizes of latex particles were selected: 1 µm, 3.2 µm, 11 µm, 25 µm, and 45 µm. The 1-µm and 3.2-µm particles were used to represent small particles that are close to the size of bacteria. The 11-µm particles were chosen based on the reported minimum 10-µm particle size that can effectively shield bacteria from UV light (Emerick et al., 2000). The 25-µm and 45-µm particles allowed testing with large and very large size particles that can provide almost complete shielding from UV. The initial particle number concentration in samples was selected as 6000 (±5%) particles/mL based on the typical particle numbers present in surface waters and secondary effluent. Another advantage of the selected particle concentration was that no dilution was required during particle count analyses which enabled a higher accuracy for the measured parameters. Dilution of samples results in substantial changes in particle size and count due to the changes in

solution properties and should be avoided when possible. Turbidity measurements were not used to adjust the initial particle numbers in samples since a preselected turbidity value would result in different particle counts for small (e.g., 1 μm) and large particles (e.g., 45 μm). Although turbidity measurements are usually directly proportional to mass concentration of particles, they are poor indicators of number concentration since equal numbers of different sized particles do not result in equal turbidities as light scattering depends on the particle size (Huber and Frost, 1998).

After the preparation of particle suspensions, the particle concentrations and distributions were checked for each suspension to ensure that the total particle count was approximately 6000 ($\pm 5\%$) and the particles were in the desired particle size range after they were added in water (Figure 4.1). The polystyrene latex particles are insoluble in water, so they are not expected to dissolve or disintegrate. However, minor aggregation might occur, even in the absence of coagulants, due to the interaction of particles with each other. The results of the particle size analysis showed that the polystyrene particles achieved their purpose, and the majority of particles in water were in the same size range and their particle size distribution was very narrow. For small particle sizes, such as 1, 3.2, and 11 μm , the size uniformity of the particles was excellent (Figure 4.1a-c). The larger particles, such as 25 μm and 45 μm , had slight deviations in their uniformity (Figure 4.1d and e), which was expected based on the C.V. (coefficient of variation) information provided by the manufacturer (e.g., C.V. $\leq 3\%$ for 1 μm particles versus C.V. $\leq 15\%$ for 45 μm particles).

The results from UV inactivation tests are illustrated in Figure 4.2. Inactivation of *E. coli* in the absence of particles was achieved rapidly, and 4.5 log inactivation was attained in the first 20 mJ/cm² of UV dose (Figure 4.2a). No significant improvement was observed in the inactivation of *E. coli* between 20 and 90 mJ/cm², and complete inactivation of *E. coli* was achieved at 100 mJ/cm². This indicated that free-swimming bacteria were inactivated very quickly in the first 20 mJ/cm², but some of the self-aggregated bacteria could resist UV inactivation even at very high UV doses. It was also reported by Blatchley et al. (2001) that self-aggregation of bacteria might be sufficient to provide complete protection from UV light.

In the presence of 3.2, 11, and 25 µm particles, inactivation levels were lower compared to the inactivation levels observed in the absence of particles (Figure 4.2a and b). The dose-response curves were not smooth, and some scatter of the data was observed beyond 40 mJ/cm² in spite of the small magnitude error bars (Figure 4.2b). The irradiations were repeated for a second time, and a similar scatter in the data was observed. The general trend, however, showed that the inactivation levels were slower in the presence of 25 µm particles compared to the inactivation levels measured in the presence of 3.2 µm particles. The scatter in the UV inactivation data started at 40 mJ/cm², at which point 4 to 5 log inactivation was already achieved depending on the particle size (5 log for 3.2 µm, 4.2 for 11 µm and 3.8 for 25 µm). This suggests that the majority of the bacteria could be inactivated rapidly at 40 mJ/cm² and were likely not associated with particles. Bacteria that were protected by particles could not be inactivated even after exposure to high UV doses.

When 1, 11, and 45 μm particles were present in samples, no significant difference was observed between the inactivation levels in the UV dose range of 0-15 mJ/cm^2 (Figure 4.2c). The UV dose was increased in increments of 3 mJ/cm^2 in order to allow multiple data points and clear observation of the inactivation patterns. Overall, the particle size did not appear to be a significant factor affecting the level of UV inactivation achieved between 0 and 15 mJ/cm^2 , and the inactivation levels were almost identical. In addition, there was no scatter in the data until 12 mJ/cm^2 . Based on the results shown in Figure 4.2b and c, it appeared that the scatter in the inactivation data started after the majority of the free-swimming or non-particle-associated bacteria were inactivated. Even though no biofloculation agents were used in these experiment sets, it should be noted that self-aggregation of bacteria and particles might still have occurred to a certain extent. In certain cases, self-aggregation process was reported to be more effective in protecting microbes from UV irradiation than particle-microbe association (Mamane and Linden, 2006). It was reported that mechanisms such as electrostatic attraction and adsorption might promote the self-attachment of microbes onto particles on their own, and this can be more prevailing than attachment achieved through induced flocculation (Templeton et al., 2005). Further supporting the importance of self-attachment processes, Wu et al. (2005) reported that attachment of microbes onto particles, to a degree significant enough to affect the efficiency of UV disinfection, was achieved simply by allowing the samples to be mixed for sufficient amounts of time.

4.4.2. Phase II: effect of bioflocculation on UV inactivation

The goal of Phase II was to study the effect of bioflocculation on UV disinfection by using alginate and Ca^{2+} as bioflocculant agents. Alginate concentration was kept constant (10 mg/L) for all samples, and bioflocculation of particles and bacteria was achieved by varying the Ca^{2+} concentration (0, 5, 10, and 15 mM). Increasing the Ca^{2+} concentration increased the degree of bioflocculation and resulted in larger flocs. The flocculation process and the final floc size could be controlled by simply varying the Ca^{2+} concentration.

Figure 4.3a illustrates the images captured by the particle counter when 1 μm particles were flocculated by adding Ca^{2+} in the presence of 10 mg/L alginate. At 5 mM Ca^{2+} concentration, no significant flocculation was observed in the first 5 min of flocculation. Visible flocs were immediately formed when Ca^{2+} concentration was increased to 10 mM. Increasing the Ca^{2+} concentration further to 15 mM resulted in larger and denser flocs. A photograph of the flocs formed is presented in Figure 4.3b. The flocs were similar to natural flocs that form in environmental water samples.

In the next set of experiments, 3.2 μm (Figure 4.4a), 11 μm (Figure 4.4b), and 25 μm (Figure 4.4c) particle suspensions were flocculated by increasing the Ca^{2+} concentration from 0 to 15 mM in 5 mM increments, and the inactivation of *E. coli* was measured in a UV dose range of 0-100 mJ/cm^2 in increments of 10 mJ/cm^2 . The particle suspensions also included alginate and bacteria as previously explained. The inactivation curves

exhibited significant scatter for all particle sizes (3.2 μm , 11 μm , and 25 μm) and at all flocculation levels (0, 5, 10, 15 mM Ca^{2+}). Selected data sets were repeated again, and similar results were obtained. The small magnitude of the error bars indicated that the observed phenomenon was caused by the samples themselves and was not likely due to an experimental error. A clear trend on the effect of flocculation rate (0, 5, 10, 15 mM Ca^{2+}) on UV inactivation for a given particle size (3.2 μm , 11 μm , or 25 μm) could not be observed. However, when inactivation levels between different particle sizes and their flocs were compared, the inactivation levels achieved in the presence of 25 μm particles and their flocs (Figure 4.4c) were lower than those achieved in the presence of 11 μm and 3.2 μm particles and their flocs (Figure 4.4a and b). It should be noted that the scatter in the data was also observed for the non-flocculated samples which had no Ca^{2+} (0 mM). However, the samples contained 10 mg/L alginate, which is a natural biopolymer that can reduce the UV inactivation by coating the bacteria as well as inducing self-aggregation. Farnood (2005) stated that the distribution of extracellular polymers within a floc structure could result in between less than 1% and 55% reduction in the UV light intensity delivered to the microorganisms. Templeton et al. (2005) reported that coating of the viruses with humic acid might provide a high degree of protection from UV light. Presence of bacterial aggregates has also been observed to negatively affect the disinfection efficacy of both UV and chlorine disinfectants (Bohrerova and Linden, 2006).

At low UV doses (0-15 mJ/cm^2 in increments of 3 mJ/cm^2), no scatter in the dose-response curves was observed when 1 μm (Figure 4.5a), 11 μm (Figure 4.5b), and 45 μm

particles (Figure 4.5c) were flocculated with increasing concentrations of Ca^{2+} . The shoulder effect (Severin et al., 1983) was visible and beyond that the inactivation rate was linear with increased UV dose until 12 mJ/cm^2 for non-flocculated samples (0 mM Ca^{2+}) and until 9 mJ/cm^2 for flocculated samples ($5, 10$ and 15 mM Ca^{2+}). Between 0 and 9 mJ/cm^2 , no significant difference in inactivation levels was observed between samples flocculated at different levels ($0, 5, 10$ and 15 mM Ca^{2+}) for a given particle size ($1 \text{ }\mu\text{m}$, $11 \text{ }\mu\text{m}$, or $45 \text{ }\mu\text{m}$). Starting at 12 mJ/cm^2 , inactivation rate of *E. coli* slowed down, and minor differences in the inactivation of flocculated samples could be seen at 15 mJ/cm^2 . For 11 and $45 \text{ }\mu\text{m}$ particles, increased flocculation achieved at higher concentrations of Ca^{2+} resulted in lower inactivation of bacteria at 15 mJ/cm^2 (inactivation at $15 \text{ mM Ca}^{2+} < 10 \text{ mM Ca}^{2+} < 5 \text{ mM Ca}^{2+} < 0 \text{ mM Ca}^{2+}$). There was approximately 1 log difference in inactivation levels between 0 mM (non-flocculated) and 15 mM Ca^{2+} (flocculated) samples.

These results indicated that at low UV doses ($<9 \text{ mJ/cm}^2$), neither particle nor floc size had a significant effect on the overall inactivation level of bacteria. Majority of the *E. coli* that were inactivated at these low UV doses were not likely associated with particles and could be inactivated very quickly. The effect of flocculation could be seen at higher UV doses, but flocculation itself resulted in a scattered UV dose response. This is not surprising since the presence of particles and more importantly the flocs would make the system highly heterogeneous. In particular, mixing of samples during UV irradiation would result in a continuous deflocculation and reflocculation of particles, and therefore a random process for the protection of microorganisms from UV light. Hence, the

inactivation tests would no longer generate consistent results unless exposure and replicate numbers are increased such that the effect of outliers can be minimized. In order to clearly demonstrate the effect of flocculation on UV disinfection, it was necessary to work with a larger number of replicates that would allow more advanced statistical analysis of the data, and to determine the span of the variability of the inactivation results as well as the statistically significant changes between different UV doses, particle and floc sizes, and inactivation levels. This task was carried out in Phase III.

4.4.3. Phase III: comparison of UV inactivation of non-flocculated and flocculated samples

In Phase III, experiments focused on comparison of UV inactivation levels between non-flocculated and flocculated samples. Each UV exposure was repeated 5 times with 3 replicates yielding a total of 15 replicates for each dose. In addition, particle suspensions were flocculated at the highest Ca^{2+} concentration (15 mM) to generate well-flocculated samples. This would allow observing the effects of flocculation under amplified conditions so that the scatter in the data would not mask a possible inactivation pattern that is a consequence of the flocculation process. Images of the non-flocculated (0 mM Ca^{2+}) and flocculated samples (15 mM Ca^{2+}) for each particle size (3.2, 11, and 25 μm) are presented in Figure 4.6.

Figure 4.7a and b shows the inactivation results from non-flocculated and flocculated particle suspensions containing 3.2, 11, and 25 μm particles at UV doses of 15, 40, and

80 mJ/ cm². The data points are the average of 15 replicates and the error bars show the standard deviations. The UV doses were selected to cover the range of low (15 mJ/cm²), average (40 mJ/ cm²), and high (80 mJ/cm²) UV doses that can be used for disinfection of water and wastewater.

One of the first observations was that standard deviations of the non-flocculated (particle only) samples were approximately 1 log (Figure 4.7a), whereas the standard deviations of the flocculated samples spanned over 2 logs (Figure 4.7b). Flocculation increased the variability of the inactivation results for an additional 1 log. This also explained the scatter in the data observed in Figure 4.4a-c with one exposure and three replicates. The findings emphasize the importance of increasing the exposure numbers when working with samples containing particles and flocs. Even 1 log variability is significant in disinfection studies and can change the interpretation of results. The results also showed that complete inactivation of *E. coli* was not achieved for any of the non-flocculated and flocculated samples even at high UV doses.

For non-flocculated samples (Figure 4.7a), a two-factor ANOVA test indicated significant differences among the data set. Thus, subsequent one-factor ANOVA tests were conducted at each UV dose (15, 40, and 80 mJ/cm²) to detect significant differences among particle sizes. The results showed that at 15 and 40 mJ/cm², there was no significant difference between the inactivation levels of 3.2, 11, and 25 µm particle suspensions ($\alpha = 0.05$, $p = 0.87$ and $p = 0.28$ respectively). However, at 80 mJ/cm² the

inactivation levels in 3.2, 11 and 25 μm particle suspensions were significantly different ($\alpha = 0.05$, and $p < 0.05$ for all), and the larger the particle size was the lower the inactivation. This showed that once particles were present in water, the particle size did not have a significant impact on the overall inactivation of bacteria at lower UV doses. The particle size became a significant factor in determining the number of surviving bacteria at high UV doses when the majority of the free-swimming bacteria have been inactivated and the larger particles better protected the remaining bacteria from UV light. It should be noted that the inactivation levels in the presence of particles, regardless of size, were always lower than the inactivation levels obtained in the absence of particles (Figs. 2a and 7a). For flocculated samples (Figure 4.7b), the two factor ANOVA indicated that no significant differences were present between the different particle sizes ($\alpha = 0.05$ and $p = 0.38$). Therefore, no further statistical analysis was pursued. Once similar size flocs were formed at 15 mM Ca^{2+} , what size of particles the flocs were made of did not make a significant difference on the inactivation levels.

Figure 4.8 shows the box-and-whisker diagrams where a rectangular box represents the distribution of the inactivation data from the 25th to the 75th percentile value, and the extended vertical lines on the top and bottom of the box represents the minimum and maximum inactivation values at a given UV dose. Figure 4.8 allows seeing the distribution of the data as well as the outliers, and also enables a direct comparison between flocculated and non-flocculated samples of the same sized particles (3.2, 11, and 25 μm). For 3.2 μm particles (Figure 4.8a), the one-factor ANOVA indicated no signifi-

cant differences between non-flocculated and flocculated samples at any of the three UV doses (15, 40, and 80 mJ/cm²).

For 11 µm particles (Figure 4.8b), the one-factor ANOVA indicated no significant difference at 15 mJ/cm² and significantly different results at 40 and 80 mJ/cm² between non-flocculated and flocculated samples (*p*-values of 0.043 and 0.019, respectively). Finally, for 25 µm particles (Figure 4.8c), the one-factor ANOVA indicated no significance at UV doses of 15 and 40 mJ/cm² and a significant difference between non-flocculated and flocculated samples at 80 mJ/cm² (*p*-value of 0.0003). For larger particles, flocculation became a significant factor in determining the number of surviving bacteria only at high UV doses. Comparison of inactivation levels between flocculated and non-flocculated samples of 11 and 25 µm particles at 80 mJ/cm² also indicated that flocculation may sometimes lead to better inactivation. During flocculation, large numbers of individual particles are aggregated into a small number of flocs resulting in improved light transmittance, decreased scattering of light and decreased shielding of bacteria by individual particles.

This study focused on the effect of particle size and degree of flocculation on the UV inactivation of *E. coli* bacteria. It should be noted that there might be several additional factors that may affect the UV inactivation of bacteria in the presence of particles. These include the attachment characteristics of bacteria on particles; total available surface area for attachment; differences in the shielding of bacteria based on the particle size

differences; scattering of UV light; self-aggregation of bacteria; enmeshment and spatial distribution of bacteria in flocs; flocculation characteristics of particles; the amount of UV absorbed by extracellular polymers and other floc constituents; differences in the porosity and structure of flocs, and changes in the light transmission pathways. One study cannot address all of these factors, and there is a need for future research to explore the above aspects of particle and microbe association using well-controlled systems.

4.4.4. Implications for UV disinfection applications

Turbulence created by reactor hydraulics in full-scale UV reactors and mixing conditions in collimated-beam studies cause continuous deflocculation and reflocculation of particles and bacteria, and contributes to the randomness of particle-bacteria association during UV exposure. This results in a large variability in the UV inactivation results for each UV exposure replicate, spanning over 2-log differences when large particles and flocs are present. The findings of this study show that it is necessary to have multiple replicates of UV exposures in addition to multiple dilution replicates of each exposure to have an acceptable level of accuracy in inactivation results in the presence of particles and flocs. This is important for lab-scale collimated-beam experiments as well as for the validation and operation of full-scale UV reactors. This also implies that less than 1 log differences in inactivation may not be a significant difference in UV studies.

In this work, some of the self-aggregated *E. coli* could survive very high UV doses even in the absence of particles. Furthermore, for samples containing particles and flocs,

complete inactivation of *E. coli* was not achieved for any of the samples at any of the UV doses tested including 100 mJ/cm². The UV doses used in this study are higher than the UV doses that are typically used at treatment plants, and considering that *E. coli* is one of the less resistant microorganisms to UV disinfection, the survival rates of more UV resistant bacteria and viruses in treated water would be higher. This could be a concern particularly for wastewater disinfection where there are higher numbers of particles and higher bioflocculation rates due to the presence of a large group of bacteria and extracellular polymers.

4.5. Conclusions

The conclusions from this study can be summarized as follows:

1. At UV doses lower than 9 mJ/cm², neither particle size nor degree of flocculation had a significant effect on the inactivation of *E. coli*. Majority of the *E. coli* inactivated at these low UV doses were likely free-swimming (non-particle-associated) bacteria that had full exposure to UV. Free-swimming bacteria are much higher in numbers compared to the particle-associated bacteria and their level of inactivation would dominate the observed inactivation levels of *E. coli*.
2. The effect of particles and bioflocculation on UV disinfection of *E. coli* was statistically significant only at high UV doses and for larger particles and well-flocculated samples. Presence of particles and the degree of flocculation did not have a significant effect on UV disinfection until majority of the free-swimming bacteria were inactivated at higher UV doses. After the majority of the free-

swimming bacteria were inactivated, the bacteria that were shielded by particles or enmeshed in aggregates determined the level of inactivation.

3. Some of the self-aggregated *E. coli* could survive a UV dose of 90 mJ/cm² even in the absence of particles. Association of *E. coli* with particles and flocs, however, provided a higher level of protection and resulted in lower inactivation levels for the particle sizes tested.
4. In addition to the size of particles and flocs, several other factors related to microbe, particle, and solution characteristics play a role in determining the overall efficiency of UV disinfection. Flocculation may sometimes lead to better inactivation.
5. When samples contain significant numbers of particles and flocs, it is necessary to have multiple replicates of UV exposures in addition to multiple dilution replicates of each exposure to have an acceptable level of accuracy in inactivation results.
6. Using well-defined latex particles, alginate and Ca²⁺ ions, a synthetic system that mimics the natural bioflocculation of particles and bacteria was created. This system enables well-controlled experiments in studying the effects of particles and bioflocculation on UV disinfection.

4.6. References

American Public Health Association (APHA), American Water Works Association and Water Pollution Control Federation, 2005. Standard Methods for the Examination of Water and Wastewater. APHA/AWWA, Washington DC.

Batch, L. F., Schulz, R. C., and Linden, K. G. (2004). Evaluating water quality effects on UV disinfection of MS2 coliphage. *Journal of American Water Works Association*, 96(7), 75-87.

Blatchley, E. R., Dumontier, N., Halaby, T. N., Levi, Y., and Laine, J. M. (2001). Bacterial responses to ultraviolet irradiation. *Water Science and Technology*, 43(10), 179-186.

Bohrerova, Z., and Linden, K. G. (2006). Ultraviolet and chlorine disinfection of *Mycobacterium* in wastewater: Effect of aggregation. *Water Environment Research*, 78(6), 565-571.

Bolton, J. R., and Linden, K. G. (2003). Standardization of methods for fluence (UV dose) determination in bench-scale UV experiments. *Journal of Environmental Engineering*, 129(3), 209-215.

Christensen, J. and Linden, K.G. (2003). How particles affect UV light in the UV disinfection of unfiltered drinking water. *J. Am. Water Works Assoc.* 95 (4), 179–189.

Emerick, W. R., Loge, F. J., Ginn, T., and Darby, J. L. (2000). Modeling the inactivation of particle-associated coliform bacteria. *Water Environment Research*, 72(4), 432-438.

Farnood, R. (2005). Floccs and ultraviolet disinfection. In I. G. Droppo, G. G. Leppard, S. N. Liss and T. G. Milligan (Eds.), *Flocculation in Natural and Engineered Environmental Systems* (385-395). CRC Press, Boca Raton, FL.

Huber, E., and Frost, M. (1998). Light scattering by small particles. *Aqua*, 47(2), 87-94.

Loge, F. J., Emerick, R. W., Thompson, E. D., Nelson, D. C., and Darby, J. L. (1999). Factors influencing ultraviolet disinfection performance part I: light penetration to wastewater particles. *Water Environment Research*, 71(3), 377-381.

Malley, J. P., Ballester, N. A., Margolin, A. B., Linden, K. G., Mofidi, A., Bolton, J. R., Crozes G., Cushing B., Mackey, E., Laine J. M. and Janex M. L. (2004). *Inactivation of Pathogens with Innovative UV Technologies*. American Water Works Association Research Foundation, USA.

Mamane, H. (2008). Impact of particles on UV disinfection of water and wastewater effluents: a review. *Reviews in Chemical Engineering*, 24 (2-3), 67-157.

Mamane, H., and Linden, K. G. (2006). Impact of particle aggregated microbes on UV disinfection. I: Evaluation of spore-clay aggregates and suspended spores. *Journal of Environmental Engineering*, 132(6), 596-606.

Örmeci, B., and Vesilind, A. P. (2000). Development of an improved synthetic sludge: a possible surrogate for studying activated sludge dewatering characteristics. *Water Research*, 34(4), 1069-1078.

Örmeci, B., and Linden, K. G. (2002) Comparison of UV and chlorine inactivation of particle and non-particle-associated coliform. *Water Science and Technology: Water Supply*, 2 (5-6), 403-410.

Parker, J. A., and Darby, J. L. (1995). Particle-associated coliform in secondary effluents: shielding from ultraviolet light disinfection. *Water Environment Research*, 67(7), 1065-1075.

Passantino, L., Malley, J. Jr., Knudson, M., Ward, R., and Kim, J. (2004). Effect of low turbidity and algae on UV disinfection performance. *Journal of American Water Works Association*, 96(6), 128-137.

Qualls, R.G., Ossoff, S.F., Chang, J.C.H., Dorfman, M.H., Dumais, C.M., Lobe, D.C., Johnson, J.D. (1985). Factors controlling sensitivity in ultraviolet disinfection of secondary effluents. *J. Water Poll. Cont. Fed.* 57 (10), 1006–1011.

Sanin, D. F., and Vesilind, A. P. (1996). Synthetic sludge: a physical/chemical model in understanding bioflocculation. *Water Environment Research*, 68(5), 927-933.

Sanin, D. F., and Vesilind, A. P. (1999). A comparison of physical properties of synthetic sludge with activated sludge. *Water Environment Research*, 71(2), 191-196.

Severin, B. F., Suidan, M. T., and Engelbrecht, R. S. (1983). Kinetic modeling of UV disinfection of water. *Water Research*, 17(11), 1669-1678.

Templeton, M. R., Andrews, R. C., and Hofmann R. (2005). Inactivation of particle-associated viral surrogates by ultraviolet light. *Water Research*, 39(15), 3487-3500.

Tezuka, Y. (1969). Cation-dependent flocculation in a Flavobacterium species predominant in activated sludge. *Applied Microbiology*, 17(2), 222-226.

Urbain, V., Block, J. C., and Manem, J. (1993). Bioflocculation in activated sludge: an analytic approach. *Water Research*, 27(5), 829-838.

Wu, Y., Clevenger, T., and Deng B. (2005). Impacts of goethite particles on UV disinfection of drinking water. *Applied and Environmental Microbiology*, 71(7), 4140-4143.

4.7. Figures and Tables

Table 4.1: Experimental design used for different phases.

	Particle size (μm)	UV dose (mJ/cm^2)	Alginate (mg/L)	Calcium (mM)
Phase I	3.2, 11, 25	0, 10, 20, 30, 40, 50, 60, 70, 80, 90, 100	0	0
	1, 11, 45	0, 3, 6, 9, 12, 15	0	0
Phase II	3.2, 11, 25	0, 10, 20, 30, 40, 50, 60, 70, 80, 90, 100	10	0, 5, 10, 15
	1, 11, 45	0, 3, 6, 9, 12, 15	10	0, 5, 10, 15
Phase III	3.2, 11, 25	15, 40, 80	0, 10	0, 15

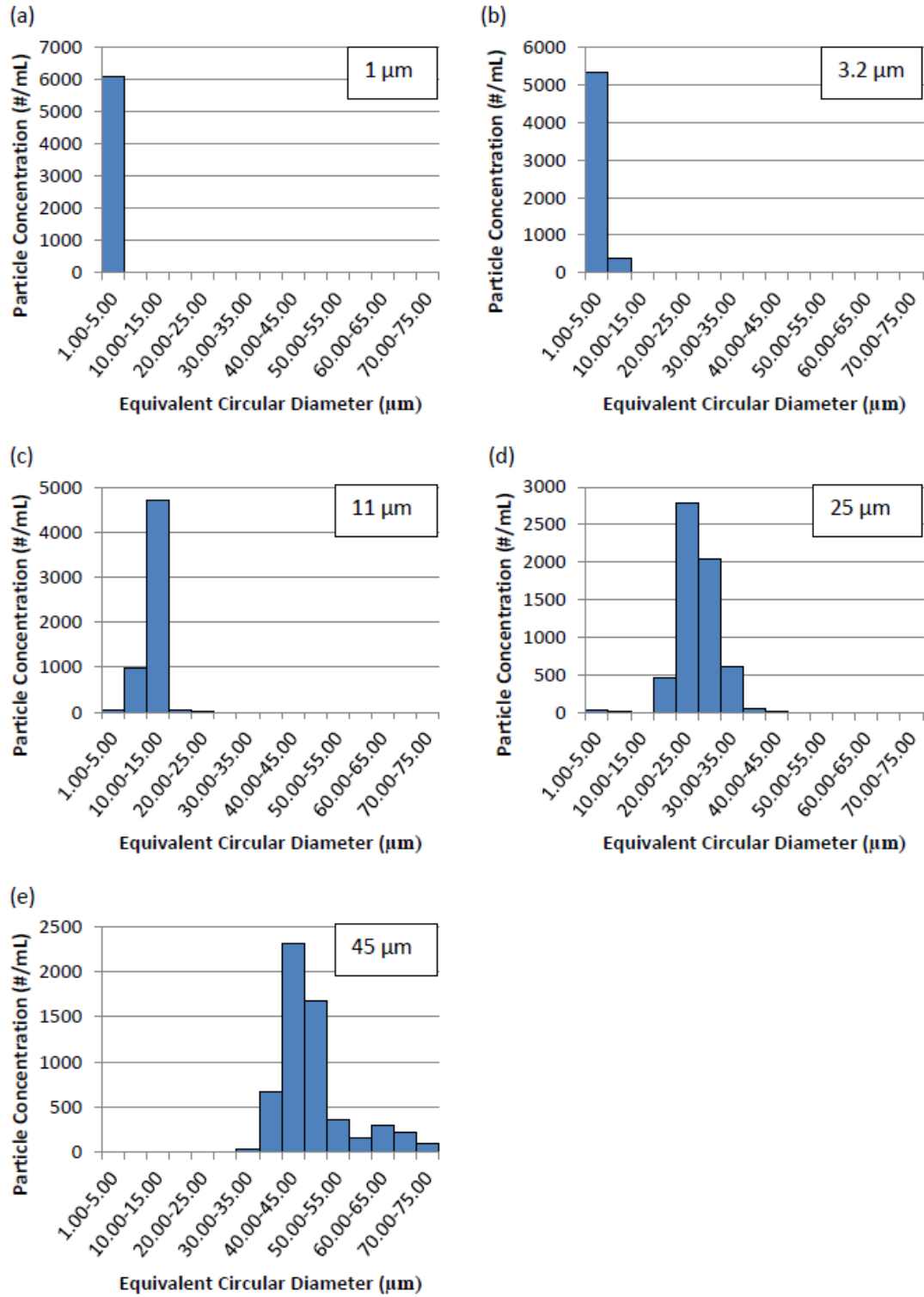


Figure 4.1: Size distributions of 1- μm particle suspension (a), 3.2- μm particle suspension (b), 11- μm particle suspension (c), 25- μm particle suspension (d), and 45- μm particle suspension (e).

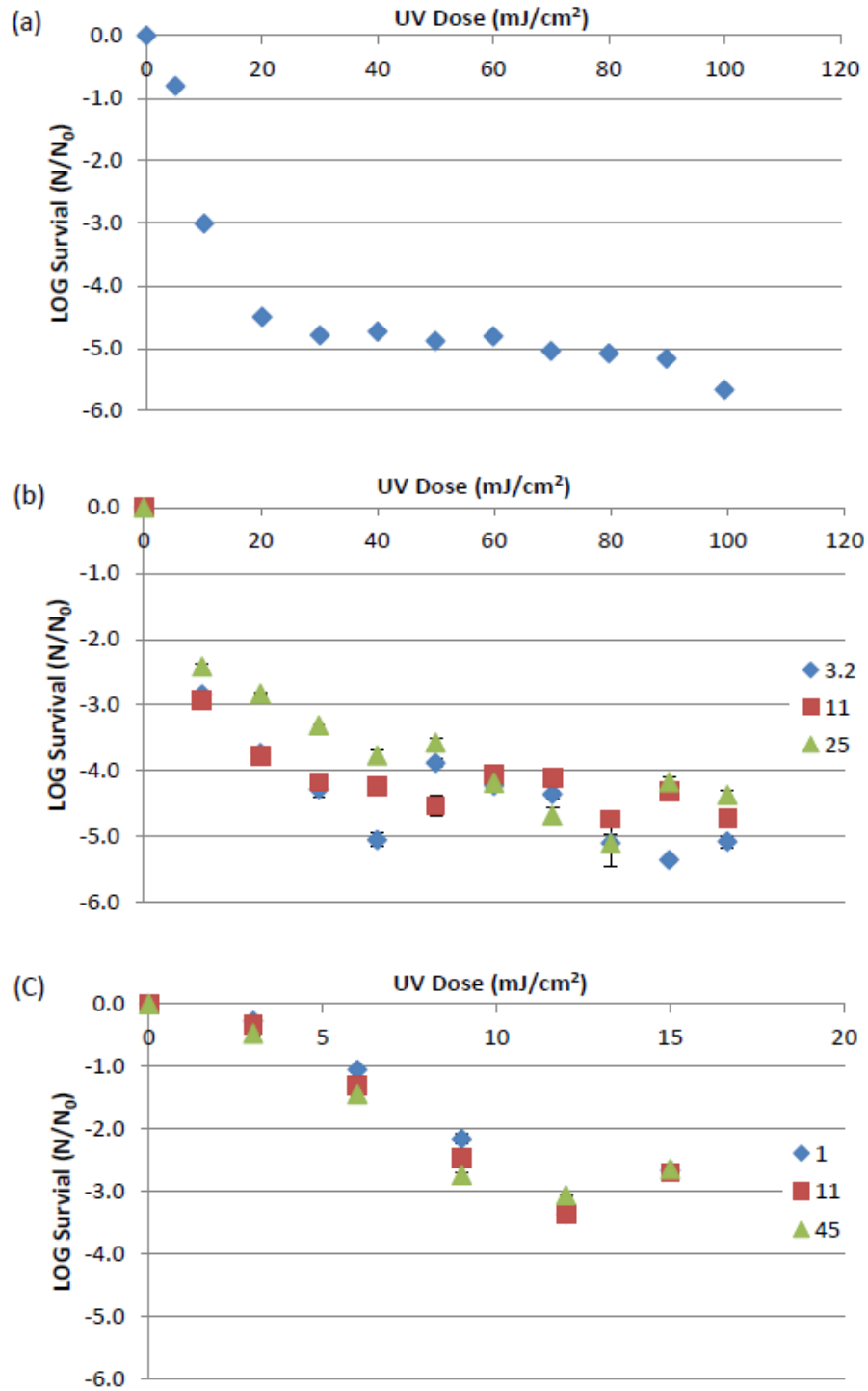


Figure 4.2: *E. coli* dose-response curves in the absence of particles (a), in the presence of 3.2 μm , 11 μm and 25 μm particles (b), and in the presence of 1 μm , 11 μm , and 45 μm particles.

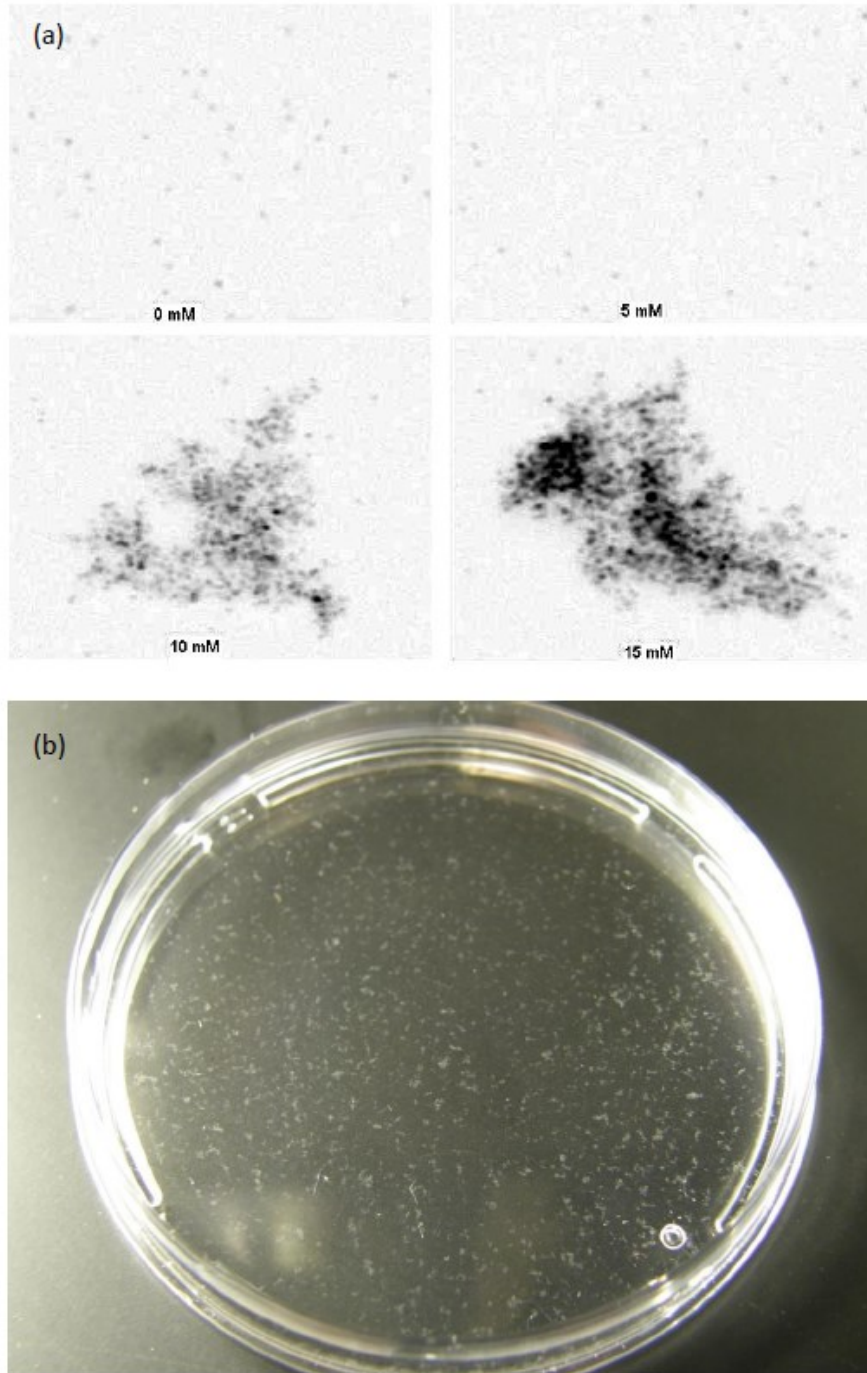


Figure 4.3: Floccs observed by flow-cell imaging during the bioflocculation of 1- μm particles at increasing calcium doses (a) and floccs of 11- μm particles observed by the naked eye at an elevated calcium concentration for better visibility (b).

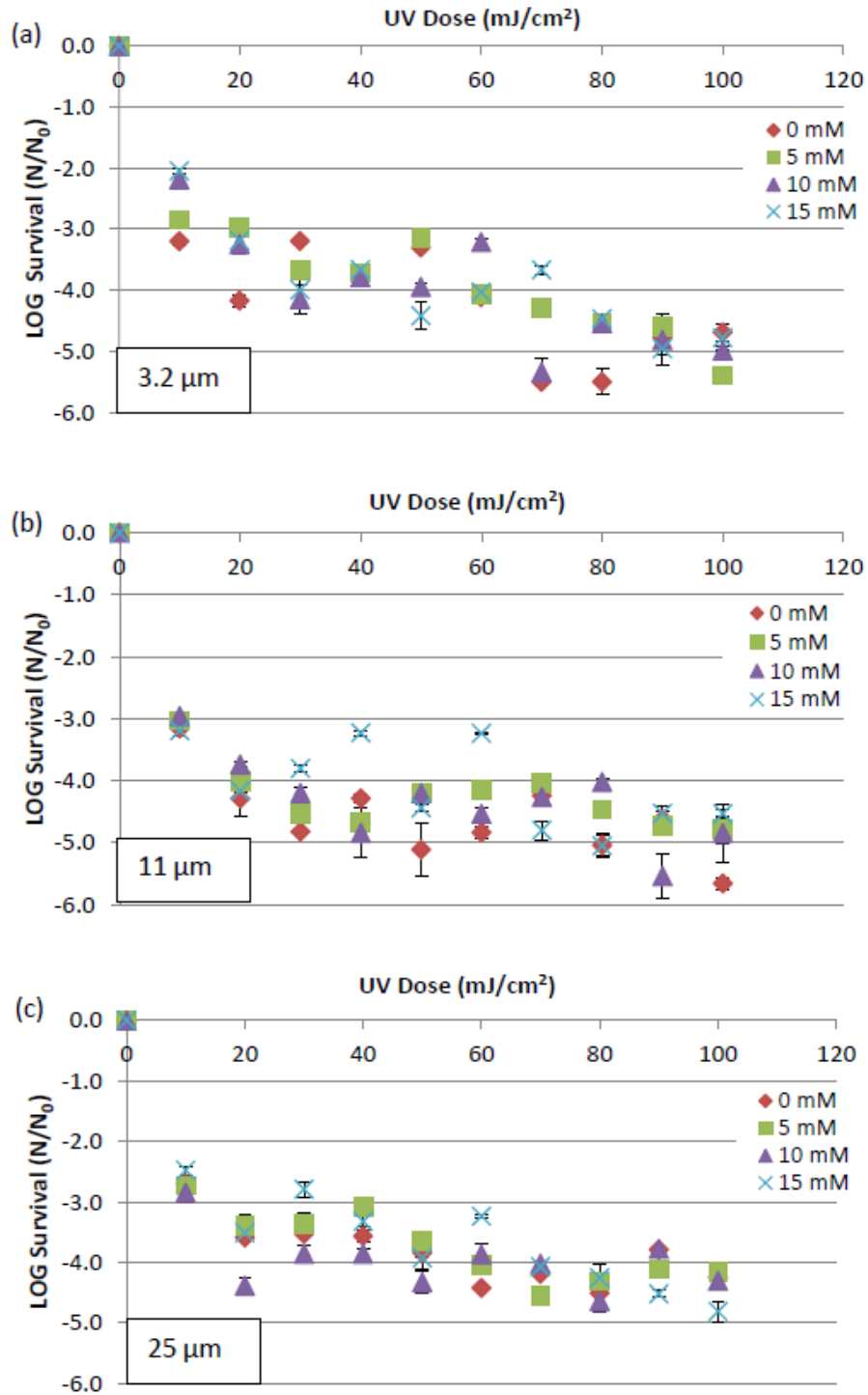


Figure 4.4: *E. Coli* dose-response curves under increasing degrees of flocculation (from 0 mM to 15 mM Ca²⁺) in suspensions of 3.2-μm (a), 11-μm (b), and 25-μm (c) particles.

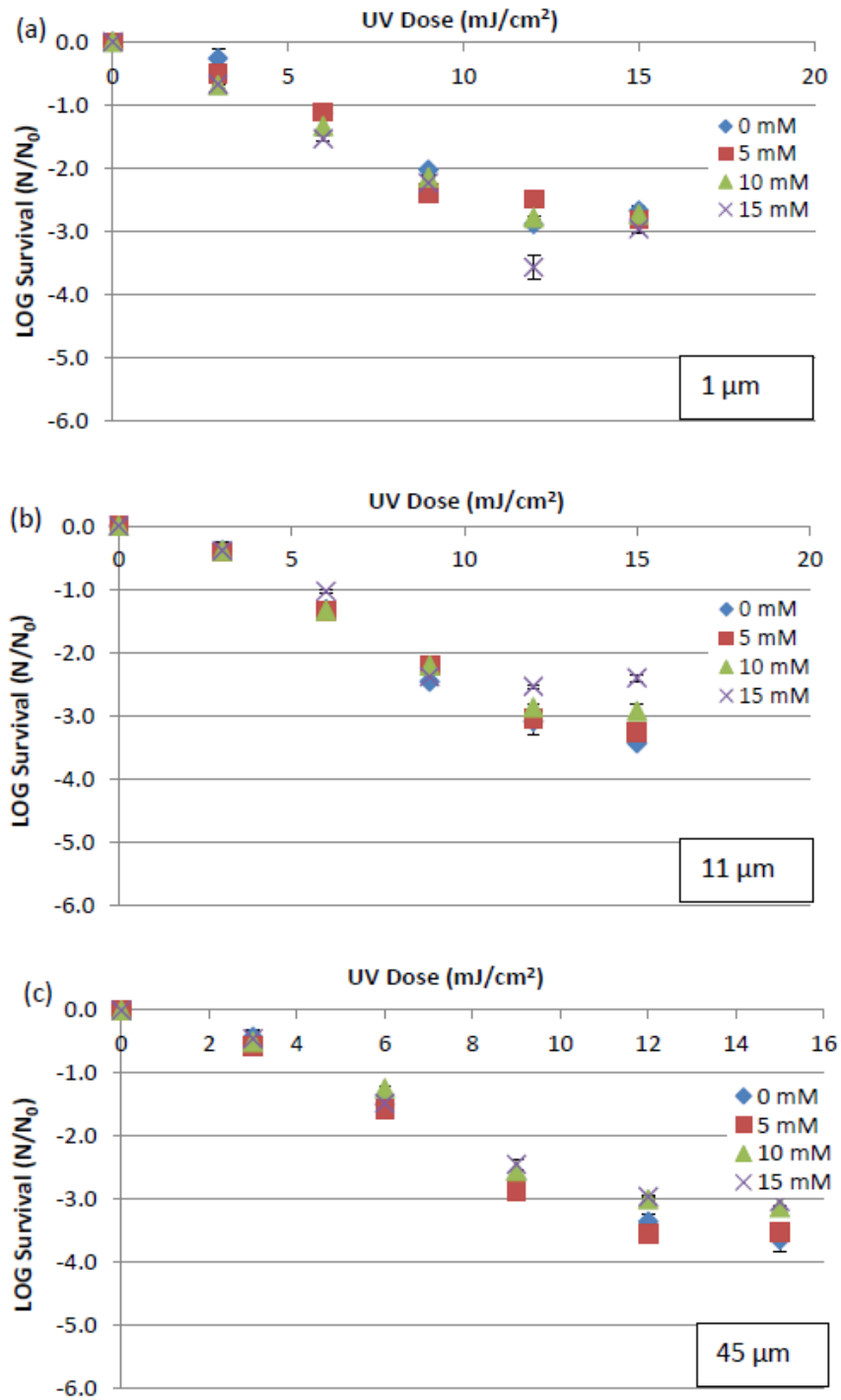


Figure 4.5: *E. Coli* dose-response curves under increasing degrees of flocculation (from 0 mM to 15 mM Ca^{2+}) in suspensions of 1- μm (a), 11- μm (b), and 45- μm (c) particles.

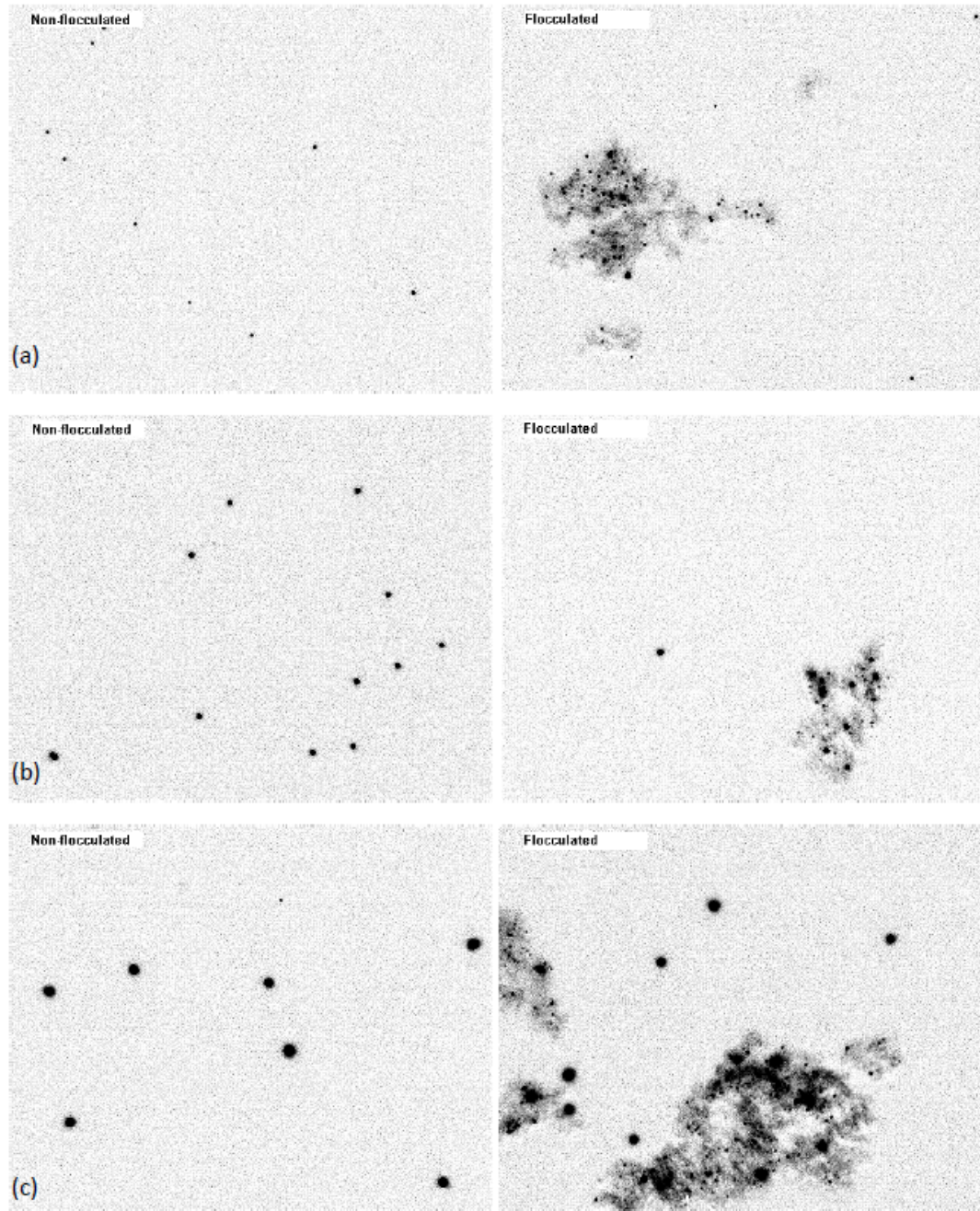


Figure 4.6: Flow-cell images of non-flocculated and flocculated suspensions of 3.2- μm (a), 11- μm (b) and 25- μm (c) particles.

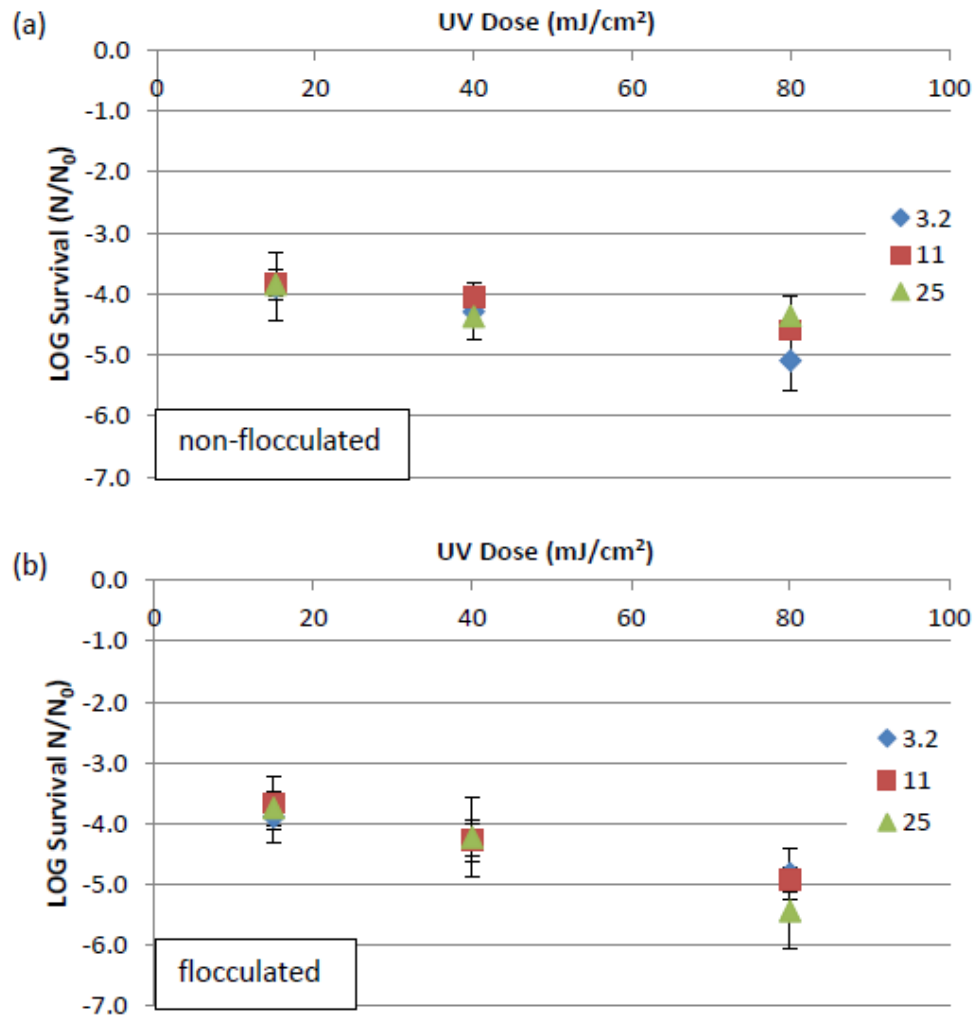


Figure 4.7: *E. coli* dose-response curves in non-flocculated (a) and flocculated (b) suspensions of 3.2, 11, and 25- μm particles.

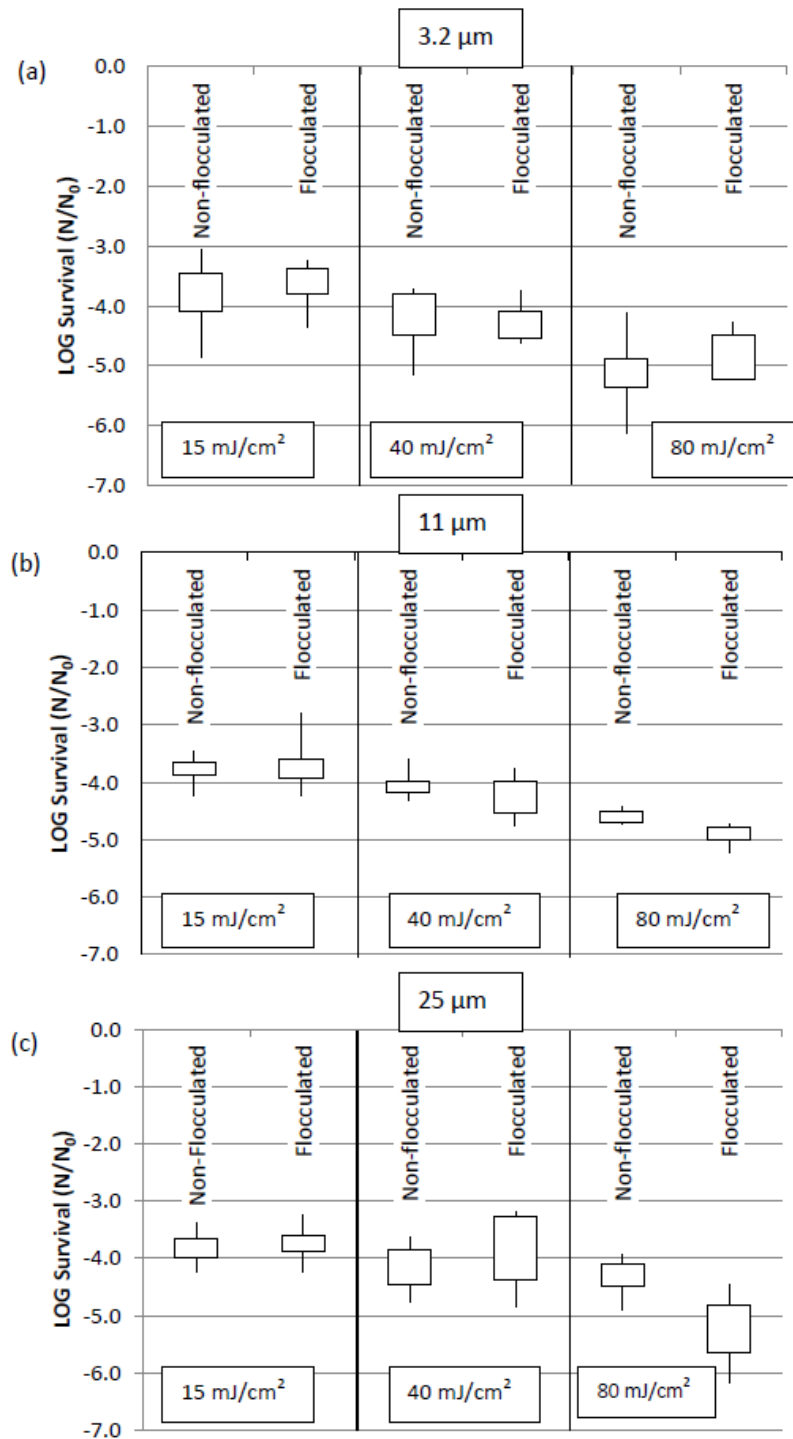


Figure 4.8: Comparison of *E. coli* inactivation levels of non-flocculated and flocculated suspensions of 3.2-µm particles (a), 11-µm particles (b) and 25-µm particles (c) using box-and-whisker diagrams where the box represents the distribution of the inactivation data from the 25th to the 75th percentile value and the whiskers extend to the minimum and maximum inactivation values.

CHAPTER 5

EFFECT OF BIOFLOCCULATION PARAMETERS ON THE SIZE AND STRUCTURE OF FLOCS

5.1. Abstract

Bioflocculation occurs in both engineered and natural systems, and plays an important role in several water treatment processes as well as in pathogen transport and survival. In this study, bioflocculation was simulated in the laboratory for well-controlled experiments. *Escherichia coli* and latex particles of varying sizes (3.2, 10 and 25 μm) were spiked into a buffer solution and were bioflocculated by adding alginate and varying amounts of calcium (0, 5, 10 and 15 mM). The degree of flocculation was determined by the calcium concentration and the floc structure was modified by varying the particle size. The bioflocculation process was monitored with a dynamic particle analyzer and the flocs formed were analyzed with respect to size, shape and porosity parameters. Larger flocs were observed to have a more heterogeneous structure with higher variation in shape and porosity compared to smaller flocs. Circularity and porosity parameters were shown to be strongly correlated with the degree of flocculation. In addition, ultraviolet (UV) irradiation experiments were performed in flocculated and non-flocculated samples and the inactivation data was assessed in the light of floc characteristics determined with the particle counter.

Keywords: Aggregation, Bacteria, Bioflocculation, Floc, Particle, Size, Structure.

5.2. Introduction

Particles in water are either of an organic or inorganic nature. Inorganic particles mainly constitute of iron and alumina oxides, and clays. Organic particles include microorganisms and cellular debris (Wilkinson et al., 1997; Mamane, 2008). Aggregation (flocculation) of particles commonly occurs in engineered systems such as water and wastewater treatment processes as well as in natural aquatic environments (Gregory, 2009; Droppo et al., 1997). Flocculation processes can be enhanced by the addition of inorganic coagulants and synthetic polymers. However, flocculation can also occur naturally by the aggregation of particles and microorganisms in a network of extracellular polymeric substances and divalent cations (Urbain et al., 1993). This type of flocculation is referred to as bioflocculation and has been observed to occur in both engineered and natural systems (Sobeck and Higgins, 2002).

It is very important to monitor the flocculation processes and the resulting flocs formed because they effectively govern the efficiencies of several water and wastewater treatment processes (i.e. filtration, clarification, and disinfection), as well as the way pathogens are transported in engineered and natural water systems. Disinfection efficiency and filtration performance have been linked to parameters such as concentration, size, shape, density and porosity of flocs (Parker and Darby, 1995; Gehr and Nicell, 1996; Emerick et al., 1999, 2000; Jolis et al., 2001; Mamane et al., 2008). These parameters also play an important role in the transport of microorganisms through natural aquatic systems (Droppo, 2001). In addition, when assessing the quality of recreational water bodies and treated water, accurate enumeration of bacteria heavily

depends on the presence of flocs, that is whether or not the bacteria are clumped together and associated with particles. This is problematic because when standard culture techniques such as multiple tube fermentation and membrane filtration are used, clumps of bacteria are counted as single colonies no matter how many bacteria are present in the clumps. Therefore, the bacterial content of the water is underestimated in the presence of flocs (Parker and Darby, 1995).

The monitoring of floc characteristics in water can be achieved by several techniques including particle counters, microscopy imaging and turbidity measurements. Turbidity measurements are commonly used for water quality assessment due to their simplicity but they cannot provide detailed information on particle populations. For instance, when particles' size and refractive index are unknown, it is not possible to determine particle concentration based on turbidity measurements (Gregory, 1998b). In addition, turbidity measurements are noted to have particularly low sensitivity for particles in the size range of a few microns (Gregory, 1998b). Microscopy techniques, on the other hand, provide detailed and accurate information, and are not affected by optical properties of the particles. However, microscopy analyses are labour and time intensive, and sampling size is very limited (Mamane et al., 2008). Furthermore, due to the fragile nature of flocs, microscopy techniques requiring rigorous sample preparation steps are not suitable for examining flocs. Particle counters operate by passing particles and flocs through a zone where a sensor can detect their presence by either electrical or optical methods (Gregory, 2009). A relatively recent technology utilizes a dynamic particle analysis (DPA) technique, which analyzes particle populations in water by directly capturing images of

the particles as the water flows through the instrument's sensing zone. This type of particle counters can simultaneously count and size particles and offer a rapid, real-time and statistically accurate analysis of the water sample (Rabinski and Thomas, 2004).

The goal of this study was to investigate the bioflocculation of particles and determine the effect of initial particle size and degree of flocculation on the size, structure, porosity and morphology of flocs formed. This knowledge would help to improve and optimize treatment processes whose performances are closely related to particle and floc characteristics. To provide an example, the study also illustrated a relationship between the size and structure of flocs and ultraviolet (UV) disinfection performance.

5.3. Materials and Methods

5.3.1. Sample Preparation

Three different sizes of polystyrene latex particles, 3.2 μm , 11 μm and 25 μm , having the same physical and chemical properties were selected to allow full control on particle size and distribution. The particles were obtained from Thermo Scientific (CA, USA). The initial particle number concentration in samples was set as 6,000 (\pm 5%) particles/mL, which was chosen based on typical particle counts measured in surface water and secondary effluent wastewater. The particle stock suspensions were prepared by injecting small amounts of polystyrene latex particle suspensions into a continuously mixed beaker containing particle-free deionized water, which was immediately followed by a particle

concentration check with the particle counter until the desired number concentration of 6,000 ($\pm 5\%$) was achieved.

After the particle suspensions with desired numbers of particles were prepared, magnesium chloride (MgCl_2) and phosphate buffer stock (KH_2PO_4) solutions were added to the samples to provide a stable environment for bacteria. *Escherichia coli* (ATCC[®] 23631[™], Cedarlane Laboratories, ON) was chosen as the testing organism and was spiked in the samples. The bacteria came in the form of a pellet and were revived following the procedures suggested by the main supplier (ATCC). For use in the experiments, a new batch of culture was started from the stock by first incubating the culture overnight at 37 °C to allow for the bacteria to recover from freezing. Then, 1 mL of this culture was added to 100 mL of tryptic soy broth in a flask and incubated at 37 °C for 4-5 h to bring the bacteria to a late exponential growth phase. The bacteria were added in quantities yielding an initial concentration of about 2×10^7 colony forming units per 100 mL (CFU/100 mL) of sample.

5.3.2. Bioflocculation

Bioflocculating agents were chosen based on previous studies on bioflocculation (Sanin and Vesilind, 1996; Örmeci and Vesilind, 2000), but with some modifications. A model bioflocculating system was preferred to allow for well-controlled experiments. Alginate was used as the extracellular polymer, polystyrene latex particles as water/wastewater particles, and calcium as the divalent cation, or bridging agent, to initiate the

bioflocculation process. Degree of flocculation was determined by the alginate and calcium concentrations. Anhydrous calcium chloride salt (CaCl_2) was used to prepare a 1 M calcium stock solution from which desired Ca^{2+} concentrations in the samples were achieved. Alginate solution was prepared by mixing alginic acid (in the form of alginic acid sodium salt derived from brown algae, obtained from Sigma Chemical Company, MO, USA) in deionized water at a concentration of 5 g/L. In order to ensure complete dissolution of alginate in water, the stock solution was thoroughly mixed and let stand for at least 24 hours before it was used.

Bioflocculation was achieved by first adding alginate and then calcium ions (the flocculating agents) into samples already containing bacteria and particles. Alginate concentration was kept fixed at 10 mg/L, while calcium concentration was varied between 0 mM and 15 mM in increments of 5 mM. Therefore, the degree of flocculation and the final floc size were determined by the calcium concentration. It should be noted that flocculation is a time dependent process (i.e., the floc size increases with time) and for this reason each sample was flocculated for the same period of time prior to particle analysis for an accurate comparison. The preliminary experiments indicated that visible flocs started forming within 5 minutes when concentrations of calcium and alginate were 5 mM and 10 mg/L, respectively. Thus, a 5-minute waiting time was applied to all samples prior to particle analysis.

5.3.3. Particle and Floc Analyses

Floc analyses were conducted using the DPA4100 Particle Analysis System (BrightWell Technologies, Ottawa, ON), which utilizes Micro-Flow Imaging™ technology to analyze particle populations in fluids. Since the particle concentrations used fell within the instrument's range, dilution of samples was not necessary. This was critical for accurately analyzing the flocculation process and the flocs formed as flocs tend to have a fragile structure and easily break up upon disturbance. Samples of 10 mL were slowly injected into the sampling syringe of the instrument with wide bore 10 mL pipettes in order to minimize any disturbance to the floc structure. Before each analysis, the illumination field of the flow cell was optimized by passing particle free water through it. This way the background intensity field is determined and objects can be identified against this background. Samples were analyzed at the low magnification setting which corresponds to a size range of 2 – 400 µm. This size range allowed for the exclusion of dispersed bacteria, which in the case of *E. coli* typically have a size of about 1 µm (Schulz and Jørgensen, 2001), while even very large flocs of up to 400 µm could be analyzed without any distortion to the floc structure.

Particle number concentrations and particle size distribution of the samples were assessed. In addition, images of particles and flocs were captured as they were passing through the flow cell for further analysis. On average, 45 images were analyzed corresponding to approximately 750 individual flocs per sample. The software of the instrument provides geometric information based on the image analyses of flocs. The measured parameters were as follows:

Area: Area was measured by using the “area” function of the software and indicates the total number of pixels covering the object.

Maximum Diameter: Maximum diameter indicates the maximum straight line distance between two points on the perimeter of the object. Maximum diameter was measured using the “feret diameter” function of the software.

Equivalent Circular Diameter (ECD): ECD corresponds to the diameter of a circle with an equivalent projected area to that of the object of interest and was measured using the “ECD” function of the software.

Circularity: Circularity is a dimensionless number calculated by dividing the circumference of a circle which has an equivalent area to that of the object by the perimeter of that object. Circularity varies between 0 and 1, where 1 indicates a perfectly spherical object. The closer to 0 the circularity is the farther away the object is from being spherical. Circularity was measured by using the “circularity” function of the software.

Porosity parameter: Porosity parameter is a unitless number derived from the average intensity of an object. The average intensity is calculated by dividing the sum of all pixel intensities in an object by the total number of pixels in the object. Reported intensity varies between 0 and 255, where 255 corresponds to the threshold between the carrier fluid (water) and the objects. Anything with an intensity of less than 255 is identified as an object and anything greater than 255 as the carrier fluid. Porosity was measured using the “intensity” function of the software. Since intensity refers to the intensity of light

reaching the detector end after passing through the sample, higher intensity indicates higher porosity.

5.3.4. UV Disinfection Experiments

The UV collimated beam setup consisted of four low-pressure mercury lamps (Phillips UV-C germicidal lamps, TUV 15W/G15 T8) emitting monochromatic ultraviolet light at 253.7 nm. The collimation of light was achieved by successively placed baffles along the UV light path. UV irradiation experiments were conducted according to the procedures outlined in Bolton and Linden (2003). The 6.5-cm Petri dishes used for the inactivation experiments allowed for a sample solution depth of 0.6 cm when sample volume was 20 mL. The samples were continuously mixed at low speeds with micro stirring rods to avoid vortex formation. The incident UV intensity was measured by a radiometer (International Light, MA, USA, IL 1400) and irradiation times were calculated to provide UV doses of 40 and 80 mJ/cm².

5.4. Results and Discussion

In this study, bioflocculation was achieved in a model system of latex particles (3.2, 11 and 25 µm), *Escherichia coli* bacteria, extracellular polymers (10 mg/L) and varying concentrations of calcium (0, 5, 10 and 15 mM). The extent of flocculation and the final floc size was determined by the calcium concentration. The flocs formed were analyzed to determine number concentration, size distribution, and their structural properties at different concentrations of calcium.

Figure 5.1 shows the particle size distribution plotted as a function of ECD at different calcium concentrations. In each graph, the size distribution of flocs made up of 3.2, 11 or 25 μm particles (Figure 5.1- a, b, and c respectively) are shown with respect to four different flocculation conditions (0, 5, 10 and 15 mM calcium). An initial peak occurs in all of the three plots at the lowest detectable particle size (2 μm) and this peak tends to get higher with increasing calcium concentration. *E. coli* bacteria have a size of about 1 μm which is lower than the detection limit (2 μm) of the instrument. For this reason, the individual bacteria are not counted by the instrument unless they are aggregated. As soon as calcium is spiked, bacteria start to aggregate and are detected by the instrument. Higher concentrations of calcium allow for more bacteria to aggregate and the aggregates can consist of only bacteria or particles and bacteria together. The bacteria-only flocs can be as small as 2 μm since a single bacterium is 1 μm . Considering the high number of bacteria ($2 \times 10^5/\text{mL}$) in the samples, a large number of bacteria-only flocs can form. Therefore, it is reasonable to conclude that the increases observed in particle concentration at around 2 μm originate from the bacterial aggregates.

After the first peak, a second peak is observed in the particle size distribution data in the size range of the selected particle size (Figure 5.1- a, b, and c). In contrast with the first peak, the peaks tend to be higher at lower calcium concentrations. This indicates that at low concentrations of calcium a larger number of the particles did not become part of large flocs. Some bacteria attachment to the particles may have occurred as can be seen

from the variance around the particle size studied. Although the peak is higher at lower calcium concentrations, the variance along the entire size range is larger with higher calcium concentrations. This implies that higher concentrations of calcium yielded a more heterogeneous solution with a diverse population of flocs spread over a wider range of size as compared to lower concentrations of calcium. It should be noted that very large flocs were less in number compared to the rest of the particle-floc population. As the particle analysis is based on counting and thus the number concentration of objects in the water, this aforementioned occurrence can cause misinformation if only the mean number concentration of objects were to be studied rather than the size distribution of the particle-floc population. For the same reason, it was not possible to plot the entire range of size distribution on one graph as the number of large flocs is dwarfed by the numerous small flocs. When the very large floc populations are examined (Table A.1), it can be concluded that a higher calcium concentration leads to a higher number of very large flocs. Here the very large floc is defined with respect to the particle size used in each study, for instance for the 3.2 μm particles large flocs were those larger than 10 μm whereas for the 25 μm particles large flocs were those larger than 32.5 μm . When evaluating the size information, it is important to note that the instrument's detection of objects' size is based on a two dimensional imaging technique, hence a floc made up of three 25 μm particles would not necessarily measure three times as large as the particle (i.e. 75 μm) due to potential overlap of the particles (i.e. depth). As much as the size distribution plots are informative, when studying complex entities like flocs and highly heterogeneous solutions, parameters other than just one dimensional size are needed to properly assess the quality of the water.

One of the main purposes of this study was to analyze images captured during particle counting to gain information on particle characteristics as well as the structure and morphology of flocs. Shape and two dimensional size data (area) as well as some structural information such as density, porosity or transparency would aid researchers, plant operators and engineers greatly in predicting and modeling treatment efficiency of various processes such as clarification, thickening, filtration and disinfection; transportation and fate of pathogens in engineered and natural systems; and potential problems with enumeration of microbial content in the presence of particles and flocs. For instance, Mamane et al. (2008) reported that in addition to size of the flocs, their shape also plays a key role in filtration efficiency and Droppo (2001) concluded that hydrodynamic behavior of flocs, which determines how attached microbes are transported within the water column, depends on their size, shape, porosity, density and composition.

Figure 5.2 – a, b, c and d illustrate the images captured from samples containing 25 μm particles after flocculation with 0, 5, 10 and 15 mM calcium, respectively. The sample that has no calcium clearly shows the discrete particles. Upon addition of 5 mM, particles slowly start flocculating and the degree of flocculation increases further at 10 and 15 mM calcium. Analyses of the captured images using the DPA4100 software can provide additional information on the area, perimeter, diameter, circularity, and porosity of flocs such as those shown in Figures 5.3, 5.4 and 5.5.

Figure 5.3 demonstrates how the maximum diameter, circularity, area, and porosity parameters change with respect to flocculation (increasing calcium concentration) for samples with 3.2, 11 and 25 μm particles. The graphs in Figure 5.3 – a, b, c, d, e, and f were plotted by using mean values representing all the objects in all images captured during the analysis of each sample. Overall, with increasing degree of flocculation, the maximum diameter of the flocs increase, as does their projected area. Flocculation also results in irregularly shaped flocs that are less circular and that have higher porosities. These measurements confirm the visual observations of the captured images from the samples. In general, similar trends in maximum diameter, circularity, area, and porosity were observed for the 3.2 and 11 μm particles, but some variations were observed for the 25 μm particles.

When the mean values were calculated based on all the objects, the plots were skewed because of the small-in-size but high-in-number bacteria-based aggregates at high concentrations of calcium. This can also be observed in the particle size distribution graphs presented in Figure 5.1, where regardless of particle size the highest peak is always around 2 μm . This issue is more pronounced in the case of 25 μm particles as the difference between the size of the particles and the bacteria-based flocs is largest. In order to better evaluate the image analysis parameters, Figure 5.4 was plotted by taking into account the 20 largest flocs in each sample instead of the entire range of particles and flocs. Before discussing these figures, it is important to remember that both rod shaped bacteria and spherical latex particles were in the samples. The bacteria are smaller than the detection limit of the particle counter therefore they cannot be detected when they are

in a dispersed state and can only be counted after they form aggregates with other bacteria or particles. The particles measuring 3.2, 11 or 25 μm can be detected as single entities. Bacteria typically have a refractive index of around 1.4 while latex particles have a refractive index of 1.6 and this affects how much light can be blocked by each (Gregory, 1998a). In this study, porosity was determined based on the intensity measurements as explained in the Materials and Methods section. Since intensity is a measure of how much light passes through an object, it indicates how transparent an object is; and, due to their relative refractive indices, particles would have a lower intensity reading than bacteria. For the particle counter to detect a region as an object against the background, the intensity has to be lower than that of water. For this reason, bacteria and EPS would yield weak signal strengths (high intensity or high porosity) and latex particles would yield high signal strengths (low intensity or low porosity). Another important point is that, in a porous structure where the pores are filled with water, water-filled regions would be registered as background water and not part of the floc itself.

Graphs in Figure 5.4 – a, b, c, d, e and f show very clear trends and strong correlations among the maximum diameter, area, circularity and porosity of flocs for all three particle sizes. When the 20 largest flocs in each sample are examined, it becomes clear that the mean area and diameter of flocs become larger as calcium concentration increases (Figure 5.4 – a, c, and e). This holds for all three particle sizes (3.2, 11, and 25 μm) and indicates that very large flocs did form at 10 and 15 mM calcium although they were fewer in number. Therefore, taking into account only the mean size parameters (area, diameter, perimeter, etc.) of all objects in a sample may conceal the presence and impact

of large flocs. Another implication of this is that mean size analysis based on total number of particles and flocs might be misleading. For instance, analysis of a water sample going through treatment might show a reduced average particle size after treatment while it contains fewer but larger flocs that are concealed by the numerous small particles.

Porosity increased with increasing flocculation for all particle sizes (Figures 5.3 and 5.4). This shows that flocs were not as dense and transmission of light through the flocs was higher after the degree of flocculation was increased. As explained before, bacteria and EPS would transmit light more than the latex particles due to their relatively lower refractive index. Therefore, mean floc transparency would increase as flocs get larger and more bacteria would be incorporated into a voluminous network of EPS. The largest flocs were also observed to become more porous with increasing calcium concentration (Figure 5.4 – b, d, and f). In addition, larger flocs appear to have an increasingly heterogeneous structure in terms of intensity variations, which also implies density and porosity variations. Circularity analyses showed that circularity decreased with flocculation whether all objects or only the 20 largest flocs were included in the mean calculation. (Figures 5.3 and 5.4). Circularity appears to be a promising monitoring parameter as it consistently indicates the presence of large flocs and flocculation in general.

For comparison of flocs composed of different sized particles, image analysis parameters were plotted as a function of particle size at each calcium dose in Figure 5.5 – a, b, c, and d. These plots were based on the 20 largest flocs detected in each sample. The plots show that under the same flocculation conditions, larger particles form larger flocs with lower porosities. This can be clearly seen for all three particle sizes (3.2, 11 and 25 μm) and at different calcium concentrations (0, 5, 10 and 15 mM). When comparisons are made among different flocculation levels, the difference in porosities with respect to particle size is least pronounced at the highest flocculation (15 mM calcium). This implies that density and porosity differences originating from the particle size decrease with growing floc size. Furthermore, although the flocs in 25 μm samples were the least porous, the variation in their porosities was highest. Standard deviation in mean floc porosity for 25 μm particle samples was 49.12 at 15 mM calcium concentration, as compared to 36.81 for 11 μm particle samples and 15.95 for 3.2 μm particle samples. Therefore, the porosities of flocs composed of smaller particles were more uniform in well-flocculated samples whereas the porosities of flocs composed of larger particles were less uniform and showed higher variance.

Figures 5.6 and 5.7 demonstrate how porosity and circularity vary with respect to area. Porosity decreases with increasing area and there is more variation in porosity among large flocs (Figure 5.6 – a, b, and c). Circularity also decreases with growing floc size (Figure 5.7-a, b, and c). Both circularity and porosity figures show that large flocs can be highly variable in structure and composition regardless of what size particles they are

composed of. Therefore, large flocs present a challenge for treatment and removal processes.

The results presented above clearly illustrate the impact of bioflocculation conditions on the final size, structure, porosity and morphology of the flocs formed. This information is important for improving the design and operation of various water and wastewater treatment processes in order to achieve treatment goals. To provide an example, UV disinfection was selected as a sample treatment process to illustrate how UV disinfection performance can be affected by the size and structure of flocs. Relatively high UV doses (40 and 80 mJ/cm²) were chosen to be able to inactivate *E. coli* embedded in flocs. A UV dose of 40 mJ/cm² is typically the minimum requirement for drinking water disinfection plants, whereas recommended design UV doses can go up to 100 mJ/cm² for reclaimed water systems depending on the upstream treatment application.

Results from UV inactivation experiments at 40 and 80 mJ/cm² are presented in Figure 5.8. Figure 5.8a illustrates the inactivation of *E. coli* observed in the presence of discrete (non-flocculated) particles (3.2, 11, and 25 μm) and Figure 5.8b shows the inactivation results in well-flocculated samples of the same particles at 15 mM calcium. As expected, higher inactivation was achieved at a UV dose of 80 mJ/cm² compared to 40 mJ/cm². The error bars in the figure indicate that there is significant variability in inactivation levels among replicates due to the presence of particles and flocs. Some of the free swimming bacteria can potentially survive 40 mJ/cm² but are likely completely inactivated at 80

mJ/cm². Therefore, inactivation of aggregated or embedded bacteria can be better observed at 80 mJ/cm². When the mean log inactivation was examined at 80 mJ/cm² for the flocculated samples (Figure 5.8-b), regardless of the particle size, inactivation levels were the same. On the other hand, when there was no flocculation (Figure 5.8-a), inactivation levels did differ with respect to particle size at 80 mJ/cm² and larger particles protected *E. coli* from UV light better in the following order: 25 µm > 11 µm > 3.2 µm. The variation in porosity was observed to be highest for flocs composed of 25 µm particles (Figure 5.6-c), and similarly variation in log inactivation was also highest for the 25 µm particles (Figure 5.8 a and b). Although the overall size distribution of flocs varied with respect to particle size (Figure 5.1), the porosity and shape of these flocs were highly variable for 3.2, 11 and 25 µm particles (Figures 5.6 and 5.7). Therefore, how much embedded bacteria are protected from UV light is a function of multiple parameters, and cannot be predicted by particle or floc size only.

The results of this study illustrate the impact of bioflocculation on the final size, structure, and morphology of flocs and how changes in these properties may affect treatment processes. This information is currently lacking in the literature and it is important for improving the design and operation of various water and wastewater treatment processes in order to achieve treatment goals. Simple turbidity or particle count measurements are most commonly used for characterization of water samples; however, they cannot provide information on the structure and morphology of flocs which play an important role in determining the performance of various treatment processes including clarification, thickening, filtration and disinfection. The instrument used in this study

allowed for capturing and analyzing images of particles and flocs passing through a flow-cell and permitted a thorough analysis of their size, shape, structure, porosity, and morphology.

5.5. Conclusions

In this study, a model system was used to simulate bioflocculation of bacteria and particles under controlled conditions. The results showed that increasing the degree of bioflocculation resulted in an increase in the size (area and diameter) of flocs. Bioflocculation also resulted in irregularly shaped flocs that are less circular and more porous. Transmission of light through the flocs was higher after flocculation. Larger flocs had a more heterogeneous structure with higher variation in shape and porosity compared to smaller flocs. Circularity and porosity parameters were shown to be strongly correlated with the degree of flocculation. Under the same flocculation conditions, larger particles formed larger flocs that were less porous. Flocs formed by larger particles also had a more heterogeneous structure compared to flocs formed by smaller particles. Overall, large flocs were found to be highly variable in structure and composition regardless of the size of particles they were made of. UV disinfection experiments showed that particle size data alone cannot explain how much *E. coli* are protected from UV light in the presence of particles and flocs. A complete understanding of this phenomenon requires knowledge of floc size, shape, structure, and porosity.

5.6. References

- Droppo, I. G., Leppard, G. G., Flannigan, D. T. and Liss, S. N. (1997). The freshwater floc: a functional relationship of water and organic and inorganic floc constituents affecting suspended sediment properties. *Water Air and Soil pollution*, 99 (1-4), 43-53.
- Droppo, I. G. (2001). Rethinking what constitutes suspended sediments. *Hydrological Processes*, 15 (9), 1551-1564.
- Emerick, R. W., Loge, F. J., Thompson, D. and Darby, J. L. (1999). Factors influencing ultraviolet disinfection performance part II: association of coliform bacteria with wastewater particles. *Water Environment Research*, 71(6), 1178-1187.
- Emerick, W. R., Loge, F. J., Ginn, T. and Darby, J. L. (2000). Modeling the inactivation of particle-associated coliform bacteria. *Water Environment Research*, 72(4), 432-438.
- Gehr, R. and Nicell, J. (1996). Pilot studies and assessment of downstream effects of UV and ozone disinfection of a physicochemical wastewater. *Water Qual. Res. J. Can.*, 31 (2), 263-281.
- Gregory, J. (1998a). Turbidity and Beyond. *Filtration & Separation*, 35 (1), 63-67.
- Gregory, J. (1998b). The role of floc density in solid-liquid separation. *Filtration & Separation*, 35 (4), 367-371.
- Gregory, J. (2009). Monitoring particle aggregation processes. *Advances in colloid and interface science*, 147-148, 109-123.

Jolis, D., Lam, C. and Pitt, P. (2001). Particle effects on ultraviolet disinfection of coliform bacteria in recycled water. *Water Environment Research*, 73 (2), 233-236.

Mamane, H. (2008). Impact of particles on UV disinfection of water and wastewater effluents: a review. *Reviews in Chemical Engineering*, 24 (2-3), 67-157.

Mamane, H., Kohn, C. and Adin, A. (2008). Characterizing shape of effluent particles by image analysis. *Separation Science and Technology*, 43, 1737-1753.

Örmeci, B. and Vesilind, A. P. (2000). Development of an improved synthetic sludge: a possible surrogate for studying activated sludge dewatering characteristics. *Water Research*, 34 (4), 1069-1078.

Parker, J. A. and Darby, J. L. (1995). Particle-associated coliform in secondary effluents: shielding from ultraviolet light disinfection. *Water Environment Research*, 67 (7), 1065-1075.

Rabinski, G. and Thomas, D. (2004). Dynamic digital image analysis: emerging technology for particle characterization. *Water Science and Technology*, 50 (12), 19-26.

Sanin, D. F. and Vesilind, A. P. (1996). Synthetic sludge: a physical/chemical model in understanding bioflocculation. *Water Environment Research*, 68 (5), 927-933.

Schulz, N. H. and Jørgensen, B. B. (2001). Big Bacteria. *Annual Review of Microbiology*, 55, 105-137.

Sobeck, D. C. and Higgins, M. J. (2002). Examination of three theories for mechanisms of cation-induced bioflocculation. *Water Research*, 36 (3), 527-538.

Urbain, V., Block, J. C. and Manem, J. (1993). Bioflocculation in activated sludge: an analytic approach. *Water Research*, 27 (5), 829-838.

Wilkinson, K. J., Negre, J. C. and Buffle, J. (1997). Coagulation of colloidal material in surface waters: the role of natural organic matter. *Journal of Contaminant Hydrology*, 26, 229-243.

5.7. Figures and Tables

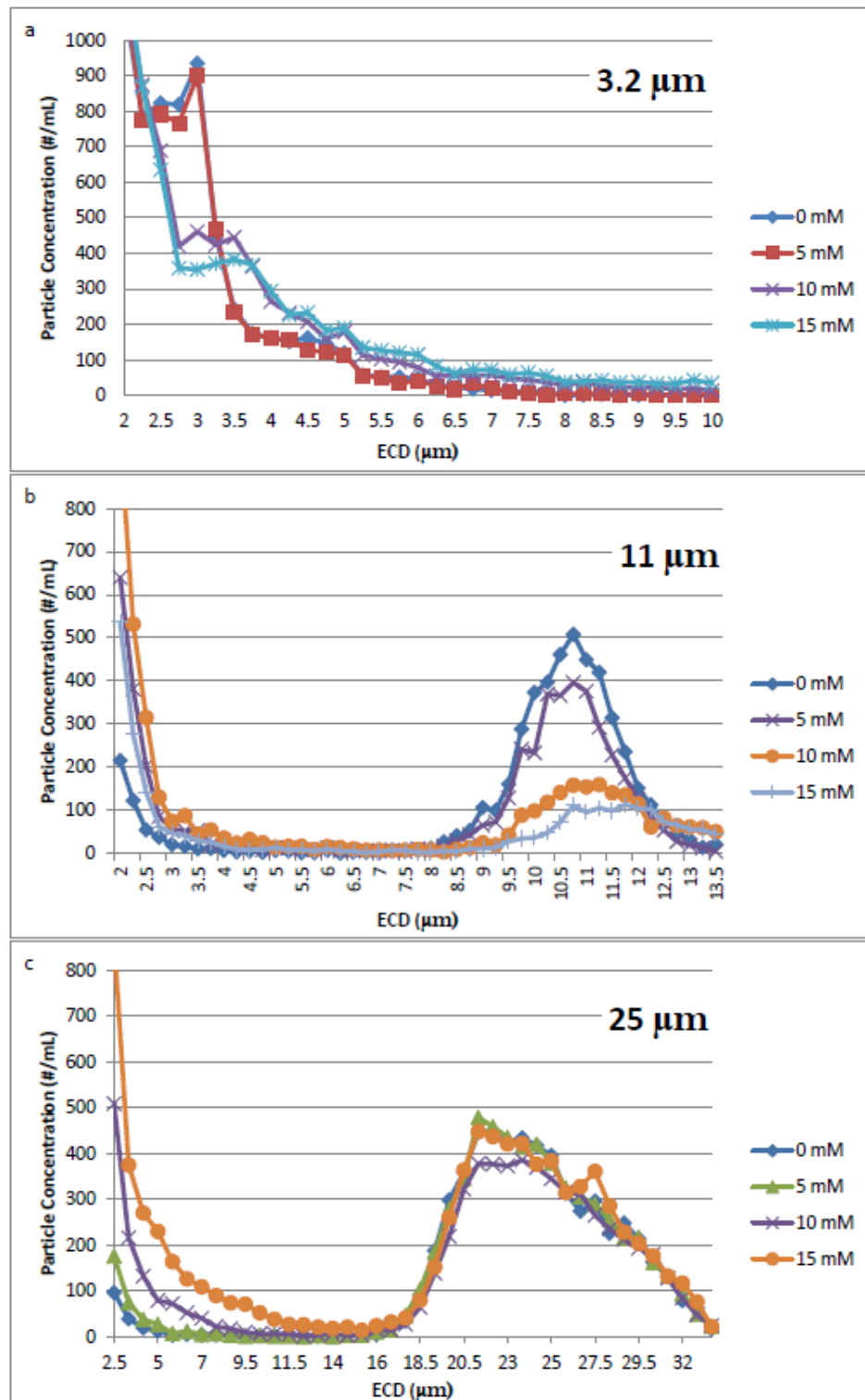


Figure 5.1: Particle size distributions at a given particle size, 3.2 μm (a), 11 μm (b) and 25 μm (c), and at calcium concentrations of 0, 5, 10 and 15 mM.

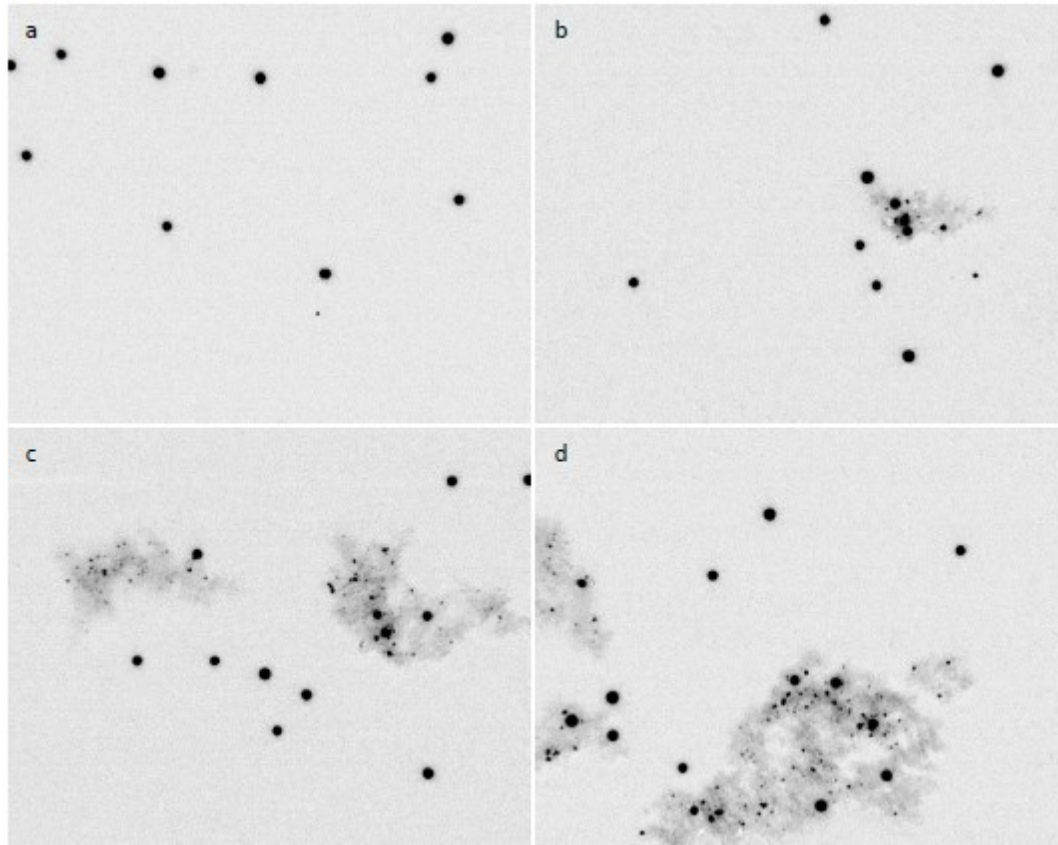


Figure 5.2: Floccs observed by flow-cell imaging during the bioflocculation of 25- μm particles at calcium concentrations of 0 mM (a), 5 mM (b), 10 mM (c), 15 mM (d).

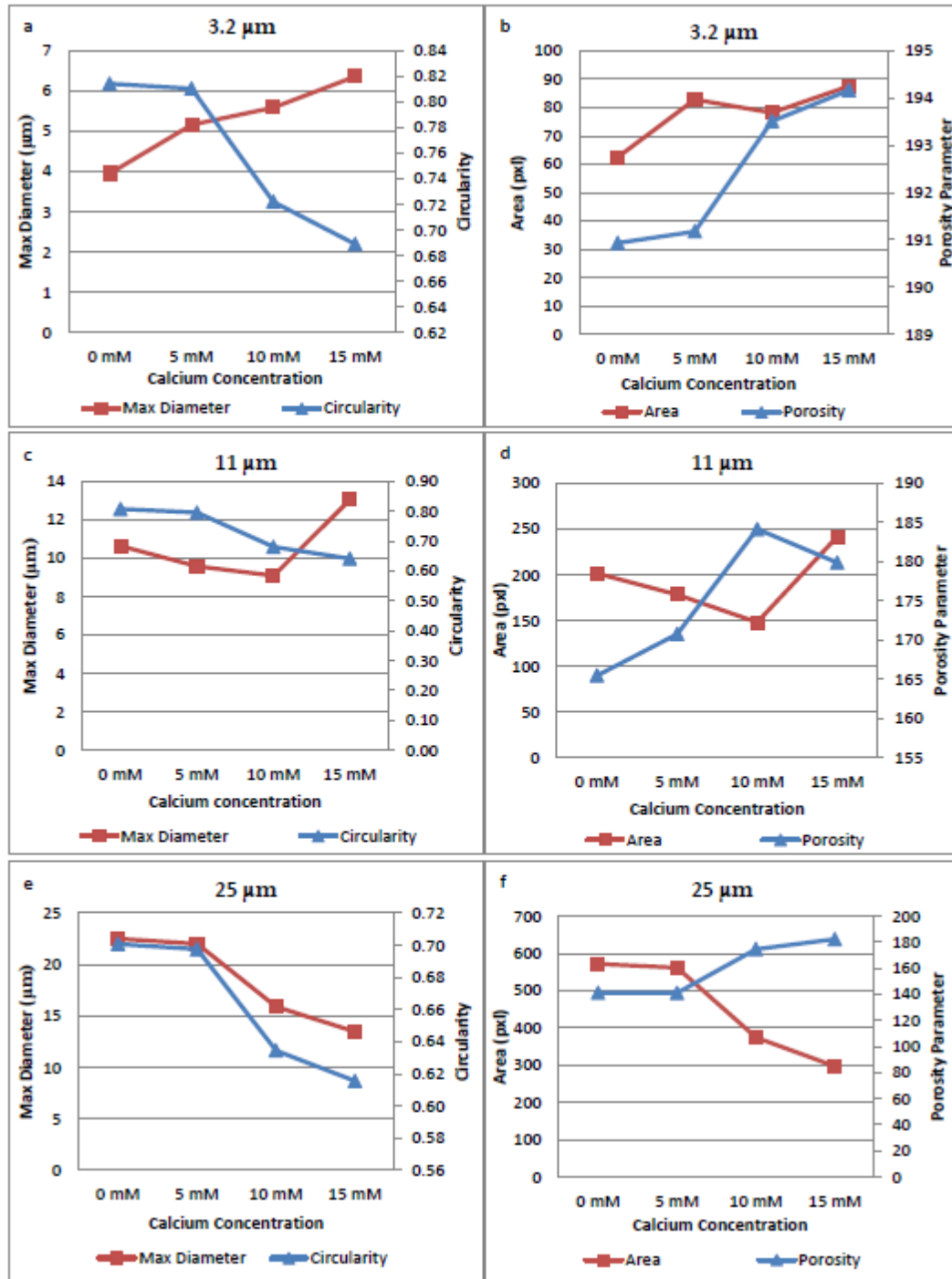


Figure 5.3: Analyses of flocs formed at calcium concentrations of 0, 5, 10 and 15 mM with respect to maximum diameter, circularity, area and porosity when particles used were 3.2 μm (a, b), 11 μm (c, d) and 25 μm (e, f).

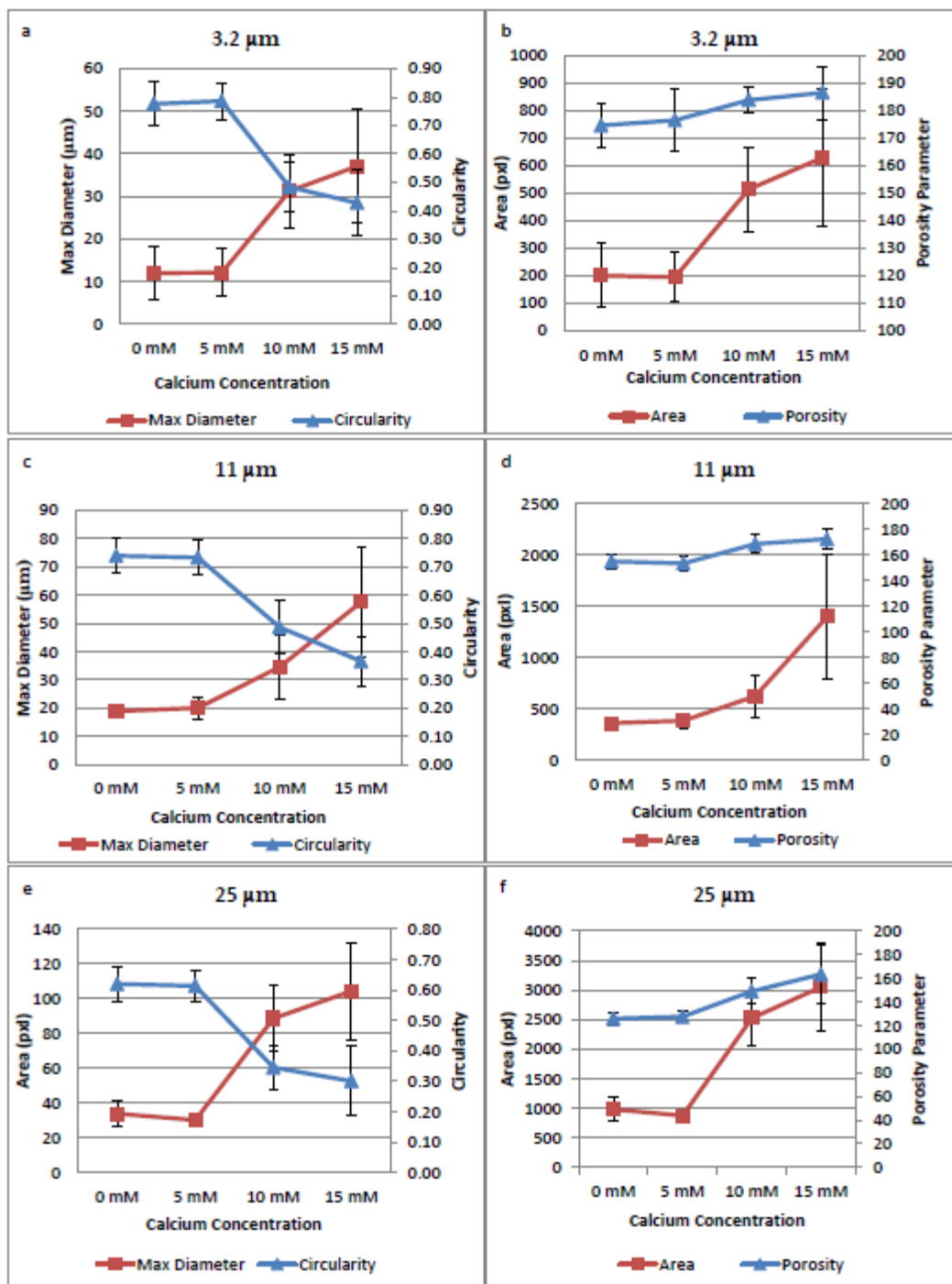


Figure 5.4: Analyses of the twenty largest (by area) flocs formed at calcium concentrations of 0, 5, 10 and 15 mM with respect to maximum diameter, circularity, area and porosity when particles used were 3.2 μm (a, b), 11 μm (c, d) and 25 μm (e, f).

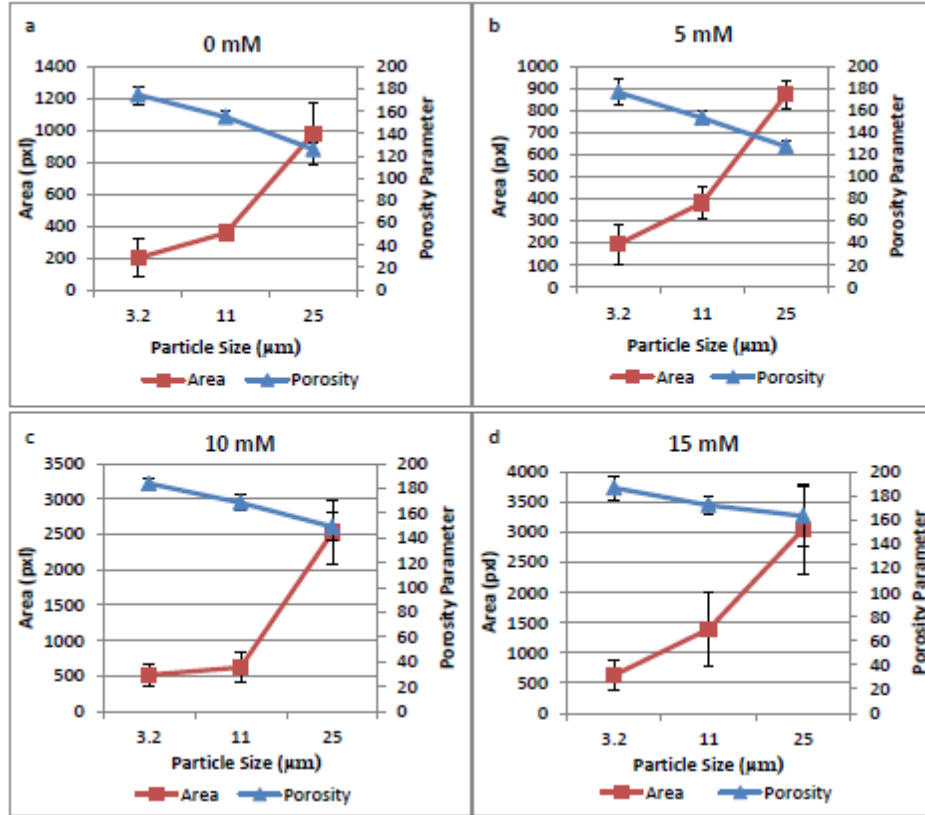


Figure 5.5: Comparison of particle sizes used for making flocs with respect to floc porosity and area at calcium concentrations of 0 mM (a), 5 mM (b), 10 mM (c) and 15 mM (d).

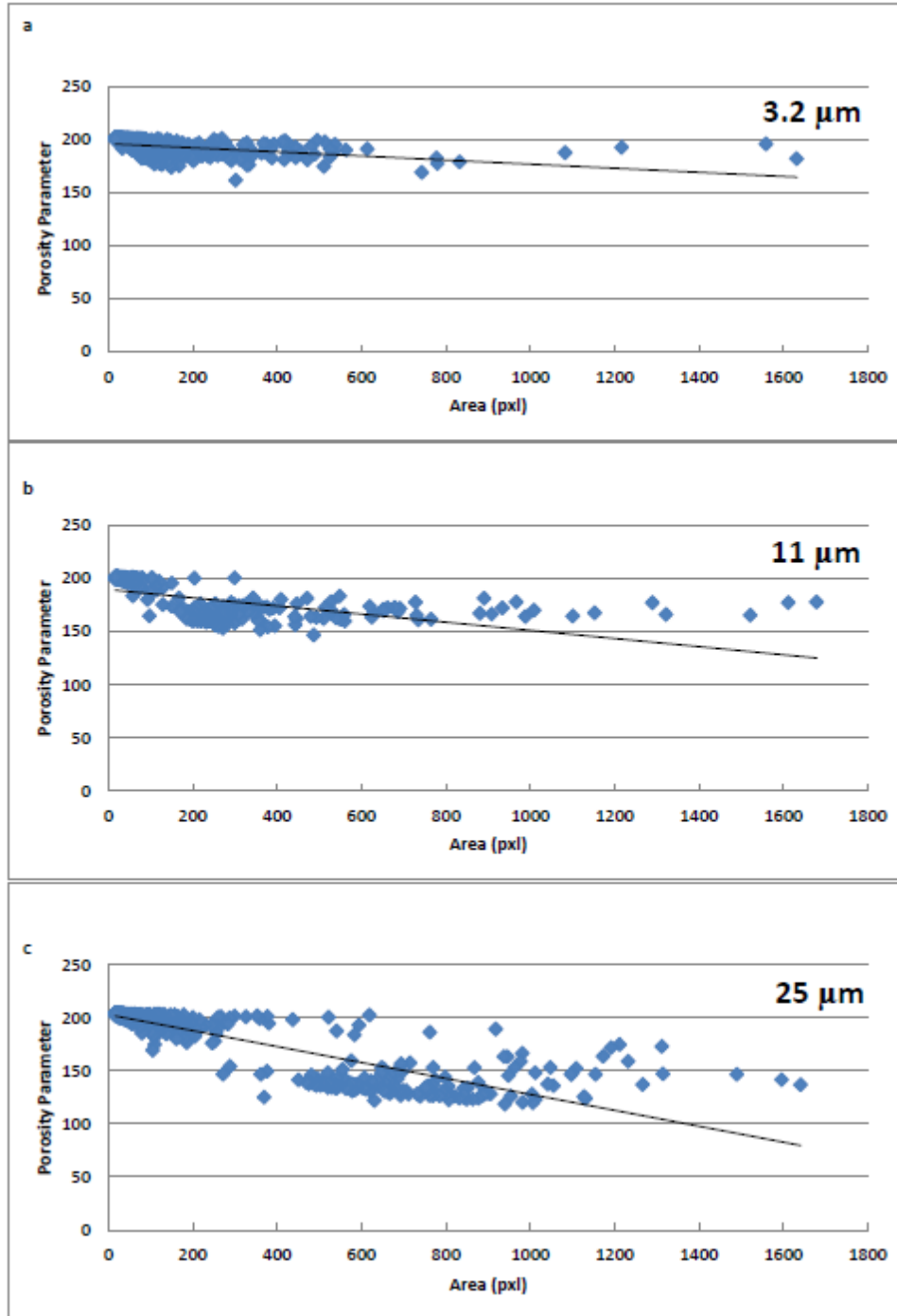


Figure 5.6: Floc porosity versus area when samples were flocculated by adding 15 mM of calcium and $3.2 \mu\text{m}$ (a), $11 \mu\text{m}$ (b) and $25 \mu\text{m}$ (c) particles.

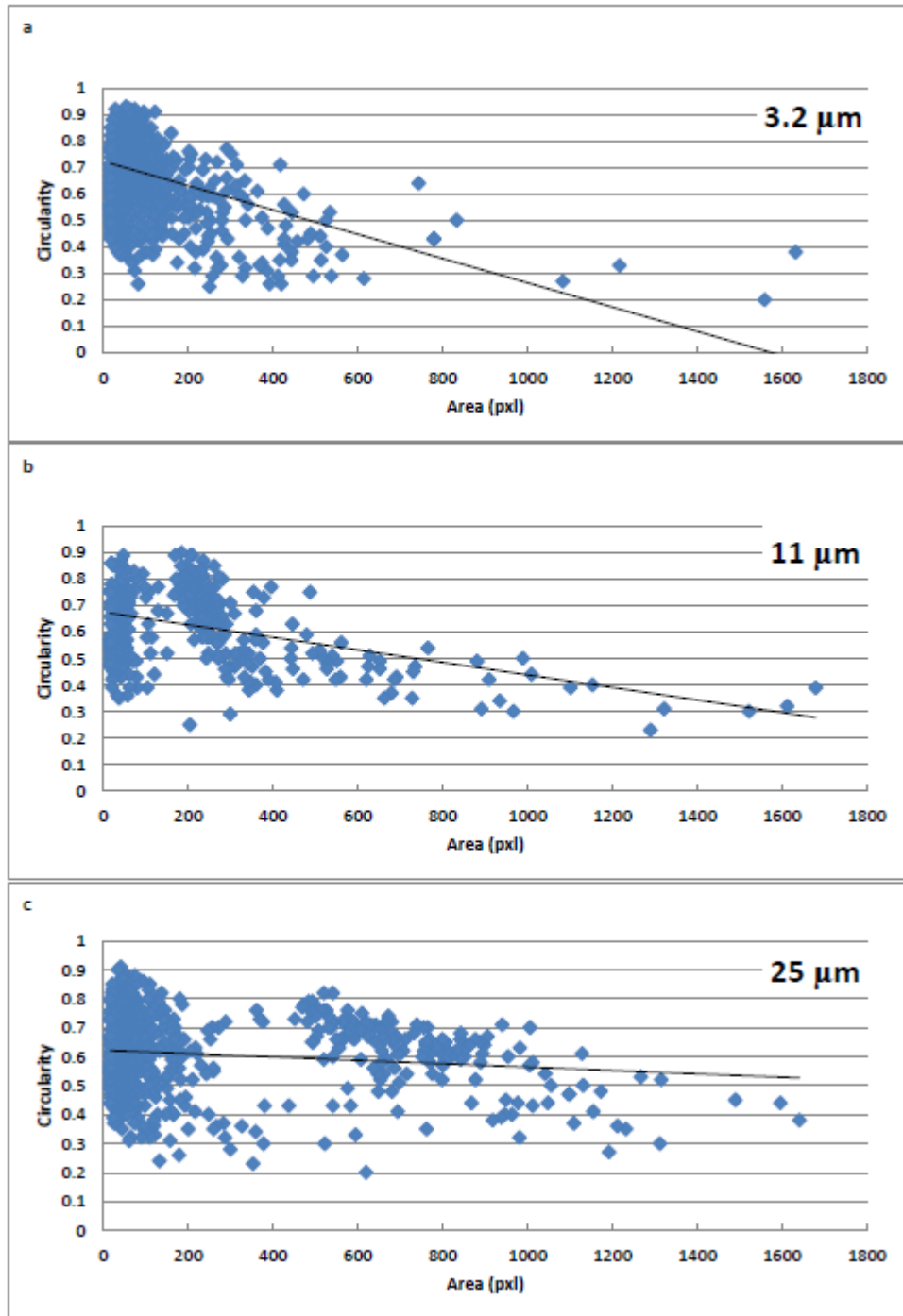


Figure 5.7: Floc circularity versus area when samples were flocculated by adding 15 mM of calcium and 3.2 μm (a), 11 μm (b) and 25 μm (c) particles.

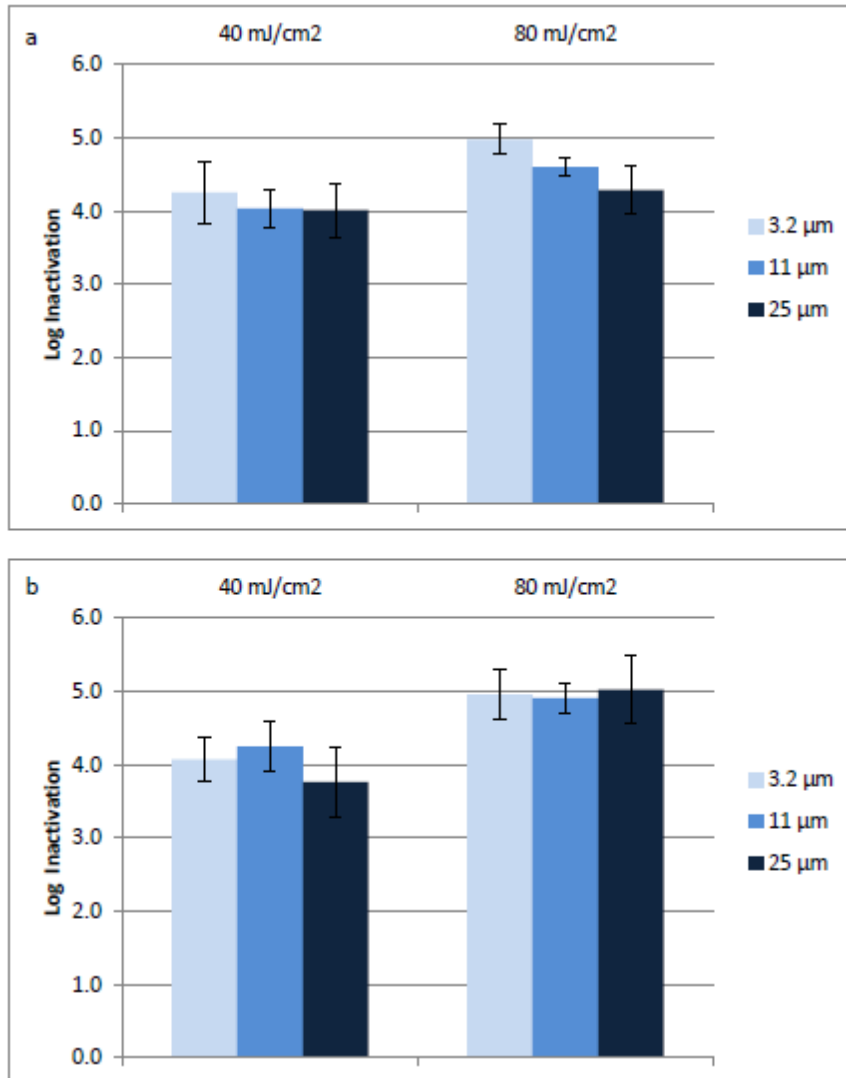


Figure 5.8: Log inactivation of *E. coli* when only particles were added (a), samples were flocculated by adding 15 mM of calcium (b).

CHAPTER 6

UV-INDUCED SELF-AGGREGATION OF *E. COLI* AFTER LOW AND MEDIUM PRESSURE ULTRAVIOLET IRRADIATION

6.1. Abstract

Presence of aggregated bacteria has been shown to decrease the efficacy of ultraviolet (UV) disinfection. Bacteria may naturally be present in aggregates in water; however, there is also some evidence that UV irradiation may promote aggregation of bacteria among themselves. This study aims to provide an in-depth understanding of the effect of UV light in inducing self-aggregation of *Escherichia coli* bacteria by using microscopy and particle counter analysis techniques in a stable and well-controlled synthetic system. The bacteria were observed and quantified before and after UV irradiation by employing size and concentration parameters. Four doses of low-pressure (LP) UV irradiation, 20, 40, 60 and 80 mJ/cm², and two doses of medium-pressure (MP) UV irradiation, 40 and 80 mJ/cm², were tested. At all LP UV doses tested, a significant increase in particle size was observed following UV exposure, indicating UV-induced self-aggregation. However, the magnitude of UV dose did not seem to have an impact. In the MP UV experiments, only a dose of 80 mJ/cm² had an impact on the formation of aggregates upon UV exposure. This prompted the question of whether the two components of the UV dose, light intensity and exposure time, would independently affect the process of self-aggregation. Experiments were conducted with the LP system at lowered light intensity and elongated exposure times. The results indicated that light intensity might be playing an important role in initiating the self-aggregation process.

Keywords: Aggregation, Bacteria, Size Distribution, Ultraviolet Disinfection, Tailing.

6.2. Introduction

In theory, the disinfection of microorganisms by ultraviolet (UV) irradiation is expected to result in a log-linear survival curve following the Chick-Watson kinetic model, where the logarithm of surviving microbial population decreases linearly with respect to increasing UV dose (Farnood, 2004). However, in water and wastewater disinfection, often a survival curve characterized by the shoulder effect at low UV doses and tailing at high UV doses is encountered (Severin et al., 1983; Qualls et al., 1983; Mamane-Gravetz and Linden, 2005). Tailing refers to the presence of a residual surviving population of microorganisms even at very high UV doses, and is therefore a public health concern. One of the possible explanations for the tailing phenomenon is the presence of aggregates. Aggregation of cells with other cells may be induced by the UV treatment (CERF, 1977; Blatchley et al., 2001, Mamane-Gravetz and Linden, 2005) or microbes may be associated with particulate matter (Parker and Darby, 1995; Gehr and Nicell, 1996; Loge et al., 1996, 1999, 2001; Emerick et al., 1999, 2000; Jolis et al., 2001; Madge and Jensen, 2006; Morgan-Sagastume, 2008).

Microorganisms that form aggregates are better protected from environmental stresses such as solar UV radiation (Callieri et al., 2011). It was suggested that external stress factors might lead to the activation of certain genes that help the organism's adaptation to the changing conditions by altering surface characteristics of the organism and increasing

EPS (extracellular polymeric substances) production (Rainey et al., 1993). Both of these processes can initiate aggregation. Warne et al. (1990) identified a particular gene in *E. coli*, designated *mor*, which is employed in changing some of the surface properties of the organism and hence in controlling the self-aggregation process.

Previous research has pointed out the importance of an aggregation process, possibly triggered by the UV irradiation, in protecting *E. coli* (Blatchley et al., 2001), fecal coliforms (Gilboa and Friedler, 2008) and spores (Mamane-Gravetz and Linden, 2005) from the UV light and reducing the overall UV disinfection efficacy. It is important to note that even in the absence of particulate matter in the water matrix to be disinfected, aggregation of cells among themselves may lead to formation of sufficiently large and dense flocs to cause tailing, and thus hinder the disinfection performance. For instance, Mamane and Linden (2006) reported that spore-spore aggregates were in fact equally effective at protecting the spores from UV inactivation as were the spore-clay aggregates.

Blatchley et al. (2001) examined the bacteria using epifluorescence microscopy before and after UV treatment for a dose range of 15-100 mJ/cm² (doses where tailing was observed) and detected large aggregates of bacteria only in the irradiated samples. No follow up studies were carried out in the literature to confirm these initial findings and investigate the phenomenon further. For disinfection applications, it is important to understand whether UV irradiation causes aggregation of bacteria and if it is significant enough to impact disinfection performance. The aggregation process may depend on the

UV dose, exposure time, or light intensity as well as the wavelength range of UV irradiation.

The goal of this research was to investigate the extent of UV-induced aggregation of *E. coli* by using microscopy and particle counter analysis techniques. The effects of UV dose applied, exposure time to UV light and the difference between low-pressure (LP) and medium-pressure (MP) UV irradiation in terms of initiating aggregation were studied. The degree to which UV-induced aggregation occurs was quantified by analyzing particle size distributions and number concentrations before and after irradiation.

6.3. Materials and Methods

6.3.1. Sample Preparation

Water samples were collected from the Rideau River (Ottawa, ON) and immediately filtered through Millipore filter paper with a pore size of 0.45 μm . The filtration was repeated twice and the final product was used to establish the base solution for the experiments. The filtration step aimed to remove the suspended matter and indigenous bacteria from the river water while leaving the minerals behind, which provided a balanced medium for the spiked *E. coli* to survive. Earlier tests were conducted in the phosphate buffered saline (PBS) medium instead of the filtered river water. However, some precipitation occurred over time in the PBS, which did not happen in the filtered river water. The filtered river water was analyzed through a particle counter (DPA4100)

in order to determine the background particle size distribution and stored in a sealed container for future use.

E. coli (ATCC[®] 23631[™]) was chosen as the testing organism. The bacteria were revived from a frozen stock by overnight incubation at 37 °C. The following day a new batch of *E. coli* was started in a fresh broth solution by inoculation with the overnight grown stock (in a ratio of 1:100) and this new batch was incubated for 4 hours at 37 °C. This ensured that the bacteria reached a growth phase between late log and stationary.

Experiments were conducted in glass petri dishes of 6.5 cm in diameter. For each experiment 25 mL of filtered river water was seeded with 250 µL of *E. coli* suspension yielding a concentration of 10⁹ colony forming units per 100 mL. The samples were then sealed with parafilm and mixed for 1 h before being analyzed by microscopy and particle counting.

6.3.2. UV Irradiation Setups

LP and MP UV setups were used for the UV irradiation experiments. In the LP UV system doses of 20, 40, 60 and 80 mJ/cm² were tested while in the MP UV system doses of 40 and 80 mJ/cm² were tested. The intensity of UV light reaching the surface of the samples was detected with a radiometer (International Light, MA, USA, IL 1400). The intensity was measured immediately before the irradiation for each exposure and varied

between 0.273 and 0.319 mW/cm² for LP lamps, and between 5.41 and 6.16 mW/cm² for MP lamps. The exposure times required to achieve the desired doses were determined according to the intensity readings. Procedures outlined by Bolton and Linden (2003) were followed for the calculation of the delivered UV dose. This involved correcting the measured UV light intensity by determining and applying the petri factor, reflection factor, divergence factor, and water factor for the LP setup. While LP UV lamps generate nearly monochromatic light at 254 nm, MP UV lamps generate light at a range of wavelengths (200-400 nm). Since not all light emitted from an MP UV lamp is equally germicidal and the sensitivity of the detector varies with respect to wavelength, two additional correction factors were needed for the MP setup. Therefore, in addition to the four correction factors applied to the LP UV dose calculation, sensor factor and germicidal factor were also applied to the MP UV dose calculation (Bolton and Linden, 2003). Samples were continuously mixed during irradiation and analyzed immediately afterwards.

In the LP UV setup, the collimation of the light was achieved by placing a series of baffles with varying openings along the light path. Therefore, the intensity of UV light reaching the samples could be modified by rearranging these baffles. For instance, it was possible to reduce it from an average of 0.297 mW/cm² to 0.060 mW/cm². This allowed for the study of the effect of exposure time and light intensity on UV-induced self-aggregation for the same UV dose. In the MP UV setup, the collimation of the light was achieved with a collimation tube and adjustments to the intensity of light reaching the sample were not possible.

6.3.3. Microscopy and Particle Count Analyses

After being mixed for 1 h, the samples were analyzed by microscopy and particle counting before UV exposure. Then the samples were exposed to UV irradiation at different doses in the LP and MP setups and were analyzed immediately after UV exposure.

For microscopy analyses, 0.15 mL were drawn from the samples and placed into microscope dishes. The samples were observed under an inverted microscope (Nikon Eclipse Ti) by using the phase contrast technique. Inverted microscopes provide an important advantage by allowing direct visualization of bacteria and their aggregates in a solution. The samples can be analyzed in their intact form and without any preparation steps such as sample fixation, staining, rinsing or dehydration. Aggregates of bacteria tend to be fragile and can easily break apart due to handling (Droppo et al., 1997). For microscopy analyses 5 samples were analyzed for each experimental replicate.

The particle counter analyses were conducted with a dynamic-particle-analysis particle counter (BrightWell Technologies, Ottawa, ON, DPA4100) which utilizes the flow cell imaging technology, where the sample is imaged continuously while flowing through a flow cell. It is possible to analyze particle size distributions and number concentrations as well as some shape parameters with this instrument. For particle count analysis, a volume of 5 mL was analyzed from each sample for volume based analyses and 10 mL for time-

resolved analyses. During the analyses, the samples were gently mixed to prevent settling. The UV exposure experiments were replicated 3 times.

6.4. Results and Discussion

6.4.1. Effect of LP UV irradiation

In Figure 6.1, microscopy images of the water sample before and after LP UV irradiation are shown for doses of 40 and 60 mJ/cm² to provide a visual illustration of aggregates. Parallel to what has been observed by Blatchley et al. (2001) most cells existed as cell pairs or discrete cells before the samples were exposed to UV light, while after the UV irradiation some large aggregates consisting of many bacteria and measuring larger than 10 µm were observed in the samples.

The quantitative analyses of UV-induced aggregation were performed by analyzing samples before and after UV irradiation at different doses with a DPA 4100 particle counter. The particle counter employed in this study measures number concentration, where a large aggregate would be counted as only one entity among many other small entities even when it actually consists of many bacteria. Hence, larger particles are usually underrepresented when number concentration is used. In order to better analyze the change in size distribution, particles were grouped into the following size categories: $\leq 2 \mu\text{m}$, $> 2 \mu\text{m}$, $>3 \mu\text{m}$, $> 4 \mu\text{m}$, $> 5 \mu\text{m}$ and $> 10\mu\text{m}$. Before discussing the data, it is important to note that the minimum detection limit for the particle counter was 2 µm. Hence, the particles that fell in the $\leq 2 \mu\text{m}$ size bin were those that were just short of 2

μm . Considering that the bacteria used in this study (*E. coli*) typically measure about $1 \times 2 \mu\text{m}$ (Schulz and Jørgensen, 2001), most bacteria would be counted in the $\leq 2 \mu\text{m}$ size bin before UV irradiation, as they exist either as discrete cells or in cell pairs. Therefore, it would be reasonable to assume that an increase in the proportion of particles in larger size bins would be indicative of aggregate formation.

Figures 6.2 through 6.5 show particle size distributions in different size bins before and after LP UV irradiation at doses of 20, 40, 60 and 80 mJ/cm^2 , respectively. Following UV irradiation, there was a shift in size distributions towards a larger particle size on average in all of the UV doses examined. The proportion of particles falling in the first size bin ($\leq 2 \mu\text{m}$) decreased after UV irradiation as compared to before UV at all doses and replicates with the exception of 80 mJ/cm^2 . At 80 mJ/cm^2 , the fraction of particles with a size of $\leq 2 \mu\text{m}$ increased and the fraction of particles in the $> 2 \mu\text{m}$ size bin decreased after exposure to UV irradiation particularly in replicate 3 (Figure 6.5-a, -b). The abnormality in this replicate shifted the overall average particle size distribution as well (Figure 6.6-d) and was contrary to what was observed at other doses. Villarino et al. (2000) observed that some cells became elongated as a result of UV treatment. Considering that the lower size detection limit for the particle counter was $2 \mu\text{m}$, some cells that were below detection before irradiation could possibly be detected after irradiation at 80 mJ/cm^2 due to UV-induced cell elongation. Such an elongation of the cells can increase the per cent of particles in the $\leq 2 \mu\text{m}$ size range. Therefore, while aggregates were formed after UV irradiation, as indicated by the increases in the proportion of particles larger than 3, 4, 5 and $10 \mu\text{m}$ (Figure 6.5-c, -d, -e and -f), the shift

in the $\leq 2 \mu\text{m}$ bin was towards a higher particle count (Figure 6.5-a). The proportion of particles falling in the larger particle size bins (>2 , >3 , >4 , >5 and $>10 \mu\text{m}$), increased after UV irradiation at all UV doses tested. However, the shift in size was variable among the replicates at a given UV dose as well as among the UV doses. For instance, at 20 mJ/cm^2 large increases were observed in the >3 , >4 , >5 and $>10 \mu\text{m}$ size bins for replicate 2, while for replicate 3 the majority of increase occurred in the >2 and $>3 \mu\text{m}$ size bins with almost no change in the >4 , >5 and $>10 \mu\text{m}$ bins (Figure 6.2). This variance is possibly due to fact that aggregation tends to be a heterogeneous process where aggregates formed may vary greatly in size and shape. It should be noted that there is also variance among the replicates even before UV irradiance, which highlights the importance of running before-after experiments on the same sample and analyzing the change. This is also why the replicates were shown separately in Figures 6.2 through 6.5 as the variance among the replicates inflates the standard deviation from the mean when the overall averages are plotted.

Figure 6.6 shows how the size distributions of all replicates combined differ before and after UV irradiation at 20, 40, 60, and 80 mJ/cm^2 . In this figure, a clear shift in size can be observed between before and after UV exposure curves for all UV doses. The highest statistical significance was observed at a dose of 20 mJ/cm^2 with a p value of 0.03. The after UV exposure size was always larger than the before UV exposure size for the same sample; however, due to the variation among the samples themselves the overall variation ballooned. One of the possible reasons for this is that around $2 \mu\text{m}$ (which is the lower detection limit for the instrument) the accuracy is relatively low and the analysis of even

the same sample results in some variance. Increasing the dose did not seem to have an effect on the size distributions except at a dose of 80 mJ/cm², at which point potential UV-induced cell elongation may have altered the results by increasing the number of detected particles in the ≤ 2 μm size bin after the irradiation. However, a two-factor ANOVA of the mean size data from all doses indicated a significant increase due to UV exposure ($p = 0.044$) with no significant effect of UV dose ($p = 0.958$) and no interaction between exposure and dose ($p = 0.933$).

6.4.2. Effect of MP UV irradiation

In Figures 6.7 and 6.8, the size distributions of particles before and after exposure to MP UV irradiation are shown in the same fashion as LP experiments. Unlike LP UV irradiation, MP UV irradiation did not clearly yield to a decrease in the proportion of particles ≤ 2. In the larger particle size bins, the change was more prominent at 80 mJ/cm². At this dose, there was an increase in the percentage of large particles following UV exposure and the increase was consistent among the replicates ($p = 0.049$ for particles > 3μm and $p = 0.019$ for particles >5 μm, Figure 6.8-c and -e). A key difference between LP and MP UV lamps is that LP lamps generate monochromatic light at 254 nm, while MP lamps generate polychromatic light between 200 and 400 nm. For this reason, their effects on inducing bacterial aggregation might differ. In addition, MP lamps generate UV light at a much higher intensity, in the range of 5.6 mW/cm² as opposed to about 0.3 mW/cm² for LP, which results in much shorter exposure times for the same dose compared to LP UV lamps. It is possible that a certain amount of time is needed for UV-induced aggregates to form and the MP exposure times may be too short to initiate

this aggregation. In Figure 6.9, particle size distributions of all replicates before and after exposure to an MP UV dose of 40 and 80 mJ/cm² are shown. At both of the tested doses the change in overall distribution of particles among size bins was relatively small as compared to LP results. However, when particles larger than 3 μm were examined, 80 mJ/cm² yielded statistically significant results with the larger particles constituting a greater proportion of the particle population following UV exposure as compared to before UV exposure. When the mean sizes were compared, there was a very slight decrease at 40 mJ/cm² and some increase at 80 mJ/cm². Both of these changes were statistically insignificant although the increase at 80 mJ/cm² ($p = 0.07$) was much more pronounced than the decrease at 40 mJ/cm² ($p = 0.63$).

6.4.3. Effect of UV light intensity and exposure time

Due to the different results observed in MP and LP experiments, it was necessary to investigate the effect of light intensity and exposure time on the aggregation of bacteria. In these experiments, the light intensity was decreased and the exposure time was increased without changing the UV dose applied, which was possible with the LP collimated beam setup. The baffles along the light path were rearranged to lower the intensity of UV light reaching the sample, which increased the exposure time required to achieve the same UV dose. For a dose of 40 mJ/cm², a nearly 6-fold increase in exposure time, from 3 min 32 s to 17 min and 34 s, was attained by lowering the intensity from a range of 0.273-0.305 mW/cm² down to 0.060-0.065 mW/cm². As can be seen in Figure 6.10, there was a slight increase in the proportion of larger particles, in size bins >5 μm and >10 μm. The mean size also increased to some degree after UV exposure. However,

the change in mean size was not statistically significant ($p = 0.16$). Figure 6.11 shows a comparison of the overall size distributions for a dose of 40 mJ/cm^2 between high intensity-short exposure time (a) and low-intensity-long-exposure-time (b) experiments. There was less difference between before and after irradiation distributions in the low intensity-long exposure time case. Considering that the effective UV dose achieved in either case is essentially the same, it is possible that a threshold light intensity might be required to initiate UV-induced aggregation among bacteria.

6.4.4. Time resolved analysis of aggregates

Another way to analyze samples with the DPA4100 particle counter is to run a time resolved analysis. Rather than analyzing a predetermined amount of volume, the time resolved analysis method measures data parameters at each screen shot of the sample going through the flow cell and plots the accumulated data points against time. Based on the maximum amount of sample that can be injected into the sample syringe apparatus of the particle counter, a 40 min run was performed for samples before and after LP UV exposure at doses of 40 and 80 mJ/cm^2 . One advantage of this method is that it generates a scatter plot where it is possible to examine the trend of change in particle concentration and mean particle size over time. In Figure 6.12, the plots are provided for 40 mJ/cm^2 experiments. Figures 6.12-a and 12-b compare the particle concentration variation over time before and after the sample was exposed to the UV light. Before UV exposure, the particle concentration varied between 1500 particles/mL and 3500 particles/mL with the mean concentration remaining close to 2500 particles/mL over the 40 minutes of testing. After UV exposure, the mean concentration was more than halved and most of the data

points were between 1500 and 500 particles/mL. Upon examination of the mean size data, Figures 6.12-c and 6.12-d, an increase in the mean size of particles was observed after UV light exposure. This was concurrent with the decrease observed in the concentration of particles following UV exposure. As large aggregates of bacteria form, the mean size of the particle population increases; however, the particle concentration decreases as many particles become part of one larger entity and are counted as one particle. While before UV exposure the mean size data points were concentrated just below 3 μm with some variation due to the presence of larger particles, after UV exposure mean size data points were much more scattered and included many particles with a size of above 4 μm .

In Figure 6.13, time resolved analysis data before and after the samples were exposed to a UV dose of 80 mJ/cm^2 is shown. Similar to the results of the 40 mJ/cm^2 experiments, when the particle concentration data were plotted, no clear decreasing or increasing trend over time emerged (Figure 6.13-a and b). However, once again the mean concentration was more than halved (from 1700 to 500 particles/mL) after UV irradiation. As was the case in the 40 mJ/cm^2 samples, the decrease in concentration after UV exposure was parallel to the increase in the variation of mean size data in the 80 mJ/cm^2 (Figure 6.13-c and d). Although it was not possible to draw a conclusion on whether the mean size significantly changed over time before or after UV exposure, it was clear that after UV exposure the variance in mean size was larger. The aggregates formed after UV exposure consisted of many entities having a size larger than 4 μm and a high number of aggregates

measured between 3 and 4 μm in size. Before UV exposure on the other hand, the samples mostly consisted of aggregates less than 3 μm in size.

In addition to the mean size and particle concentration data, images that were captured as the samples were passing through the flow cell were analyzed to compare the diameter and area of the aggregates, and the intensity of light penetrating the aggregates before and after UV irradiation. Twenty images were analyzed per each sample. The results are summarized in Table 6.1. At either dose, both the diameter and area of the aggregates increased while the intensity decreased. The increases in diameter and area, and the decrease in intensity were all greater at 80 mJ/cm^2 than at 40 mJ/cm^2 . The area parameter here is measured directly and is equal to the total number of pixels that an aggregate covers in the image. Thus, it is not derived from the diameter data. The increase in area was greater than the increase in diameter at both UV doses. This is to be expected as area is a two dimensional measure of size. Although volume of aggregates cannot be directly measured by the particle counter, it is possible to estimate the change in the third dimension, depth, by analyzing the intensity data. Intensity refers to the amount of light that penetrates through an aggregate and therefore is correlated to the density and porosity of the aggregate. When bacteria form aggregates an increase in depth would yield to a longer penetration path for the light and hence reduce the intensity. As can be seen in Table 6.1, the mean intensity of aggregates decreased after UV exposure at both doses. This conforms to the increases observed in area and diameter as the aggregates become larger in all three dimensions.

6.4.5. Implications for UV disinfection applications

UV irradiation appears to promote aggregation of bacteria. Although this is not likely to have a significant effect on the overall disinfection performance, it might pose problems for achieving complete inactivation at high UV doses. Self-aggregation of bacteria could potentially lead to tailing and impact the UV doses required for complete inactivation of bacteria. When the disinfection process reaches the tailing region, it may not be feasible to achieve further inactivation by increasing the UV dose. In addition, the two most commonly used methods for enumeration of fecal coliform in water, membrane filtration and multiple tube fermentation, work best for quantifying dispersed bacteria.

6.5. Conclusions

Although statistical significance was low in some cases, the overall data indicated an increase in the size of aggregates after the samples were irradiated with UV light. As the study samples contained only bacteria suspended in filtered river water, the increase in size can be explained by aggregation of bacteria upon exposure to UV irradiation. This UV-induced self-aggregation of bacteria can be observed visually through microscopy or monitored quantitatively through particle counter analysis. However, due to the small size of bacteria and the size detection limit of the particle counter, the increase in the mean size of particle populations was small and not statistically significant in all experiments. It appears that a comparison of the distributions of the particle concentration and the mean size data before and after UV irradiation is more consistently indicative of self-aggregation than a lump parameter such as mean size of the entire particle population. Grouping particles into different size bins to avoid the overshadowing of

large aggregates by small particles also helps to clarify the size distributions analyses. In LP experiments, UV dose did not seem to be an important factor in determining the degree of induced aggregation. However, in MP experiments there was a significant difference between a dose of 40 mJ/cm² and 80 mJ/cm². Although the same doses were delivered to the samples by the MP and the LP lamps, exposure times were very short in the MP setup, 8 s for 40 mJ/cm² and 16 s for 80 mJ/cm², due to the high intensity of UV light generated. On the other hand, in the LP setup exposure times were relatively much longer, within the order of 2 to 7 min depending on the dose. Longer exposure-time-lower-intensity experiments carried out with the LP setup resulted in slightly smaller levels of aggregation. Therefore, it is possible that light intensity plays an important role in initiating the UV-induced self-aggregation process.

6.6. References

- Blatchley, E. R., Dumontier, N., Halaby, T. N., Levi, Y. and Laine, J. M. (2001). Bacterial responses to ultraviolet irradiation. *Water Science and Technology*, 43(10), 179-186.
- Bolton, J. R. and Linden, K. G. (2003). Standardization of methods for fluence (UV dose) determination in bench-scale UV experiments. *Journal of Environmental Engineering*, 129(3), 209-215.
- Callieri, C., Lami, A. and Bertoni, R. (2011). Microcolony formation by single-cell *Synechococcus* strains as a fast response to UV radiation. *Applied and Environmental Microbiology*, 77(21), 7533-7540.

- Cerf, O. (1977). Tailing of survival curves of bacterial spores. *Journal of Applied Microbiology*, 42, 1-19.
- Droppo, I. G., Leppard, G. G., Flannigan, D. T. and Liss, S. N. (1997). The freshwater floc: a functional relationship of water and organic and inorganic floc constituents affecting suspended sediment properties. *Water Air and Soil pollution*, 99 (1-4), 43-53.
- Emerick, R. W., Loge, F. J., Thompson, D. and Darby, J. L. (1999). Factors influencing ultraviolet disinfection performance part II: association of coliform bacteria with wastewater particles. *Water Environment Research*, 71(6), 1178-1187.
- Emerick, W. R., Loge, F. J., Ginn, T. and Darby, J. L. (2000). Modeling the inactivation of particle-associated coliform bacteria. *Water Environment Research*, 72(4), 432-438.
- Farnood, R. (2004). Investigation of factors affecting the ultraviolet disinfection of biological aggregates. PARTEC 2004, Nuremberg, Germany.
- Gehr, R. and Nicell, J. (1996). Pilot studies and assessment of downstream effects of UV and ozone disinfection of a physicochemical wastewater. *Water Qual. Res. J. Can.*, 31 (2), 263-281.
- Gilboa, Y. and Friedler, E. (2008). UV disinfection of RBC-treated light greywater effluent: Kinetics, survival and regrowth of selected microorganisms. *Water Research*, 42, 1043-1050.
- Jolis, D., Lam, C. and Pitt, P. (2001). Particle effects on ultraviolet disinfection of coliform bacteria in recycled water. *Water Environment Research*, 73 (2), 233-236.

Loge, F. J., Darby, J. L. and Tchobanoglous, G. (1996). UV disinfection of wastewater: a probabilistic approach to design. *Journal of Environmental Engineering*, 122(12), 1078-1084.

Loge, F. J., Emerick, R. W., Thompson, E. D., Nelson, D. C. and Darby, J. L. (1999). Factors influencing ultraviolet disinfection performance part I: light penetration to wastewater particles. *Water Environment Research*, 71(3), 377-381.

Loge, F. J., Bourgeois, K., Emerick, R. W. and Darby, J. L. (2001). Variations in wastewater quality influencing UV disinfection performance: relative impact on filtration. *Journal of Environmental Engineering*, 127 (9), 832-837.

Madge, B. A. and Jensen, J. N. (2006). Ultraviolet disinfection of fecal coliform in municipal wastewater: effects of particle size. *Water Environment Research*, 78, 294-304.

Mamane-Gravetz, H. and Linden, K. G. (2005). Relationship between physicochemical properties, aggregation and u.v. inactivation of isolated spores in water. *Journal of Applied Microbiology*, 98, 351-363.

Mamane, H. and Linden, K. G. (2006). Impact of particle aggregated microbes on UV disinfection. I: Evaluation of spore-clay aggregates and suspended spores. *Journal of Environmental Engineering*, 132(6), 596-606.

Morgan-Sagastume, F., Larsen P., Nielsen, J. L. and Nielsen P. H. (2008). Characterization of the loosely attached fraction of activated sludge bacteria. *Water Research*, 42, 843-854.

- Parker, J. A. and Darby, J. L. (1995). Particle-associated coliform in secondary effluents: shielding from ultraviolet light disinfection. *Water Environment Research*, 67(7), 1065-1075.
- Qualls, R. G., Flynn, M. P. and Johnson, J. D. (1983). The role of suspended particles in ultraviolet disinfection. *Journal of Water pollution Control federation*, 55(10), 1280-1285.
- Rainey, P. B., Moxon, E. R., Thompson, I. P. (1993). Intracloonal polymorphism in bacteria. *Advances in Microbial Ecology*, 13, 263-300.
- Schulz, N. H. and Jørgensen, B. B. (2001). Big Bacteria. *Annual Review of Microbiology*, 55, 105-137.
- Severin, B. F., Suidan, M. T. and Engelbrecht, R. S. (1983). Kinetic modeling of UV disinfection of water. *Water Research*, 17(11), 1669-1678.
- Villarino, A., Bouvet, O. M. M., Regnault, B., Martin-Delautre, S., and Grimont, P. A. D. (2000). Exploring the frontier between life and death in *Escherichia coli*: evaluation of different viability markers in live and heat- or UV-killed cells. *Research in Microbiology*, 151, 755-768.
- Warne, S. R., Varley, J. M., Boulnois, G. J. and Norton, M. G. (1990). Identification and characterization of a gene that controls colony morphology and auto-aggregation in *Escherichia coli* K12. *Journal of General Microbiology*, 136, 455-462.

6.7. Figures and Tables

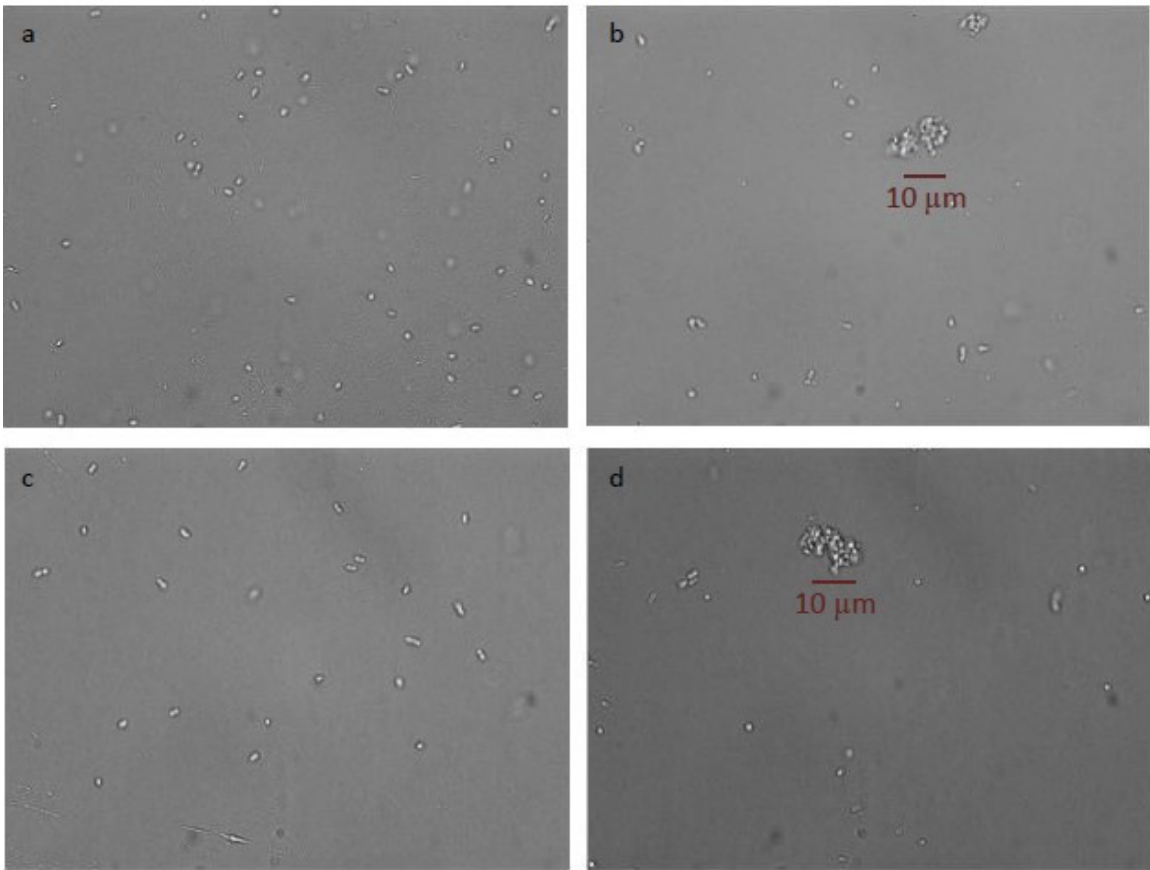


Figure 6.1: Effect of UV irradiation on aggregate formation. Low-pressure 40 mJ/cm^2 before (a) and after (b) UV irradiation. Low-pressure 60 mJ/cm^2 before (c) and after (d) UV irradiation.

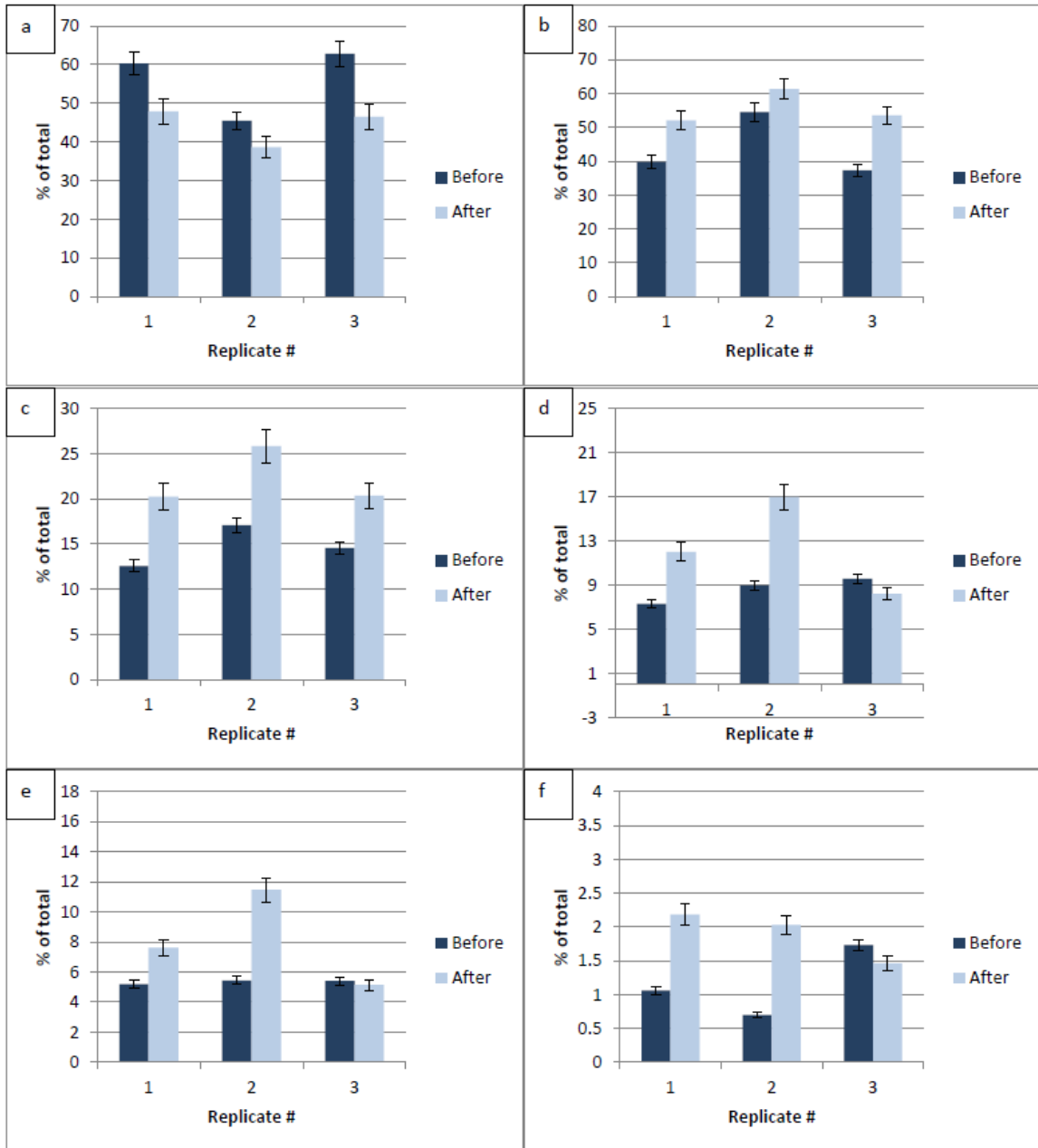


Figure 6.2: Effect of UV irradiation on size distribution. Low-pressure 20 mJ/cm^2 , % of particles which are $\leq 2 \mu\text{m}$ (a), $> 2 \mu\text{m}$ (b), $> 3 \mu\text{m}$ (c), $> 4 \mu\text{m}$ (d), $> 5 \mu\text{m}$ (e), $> 10 \mu\text{m}$ (f).

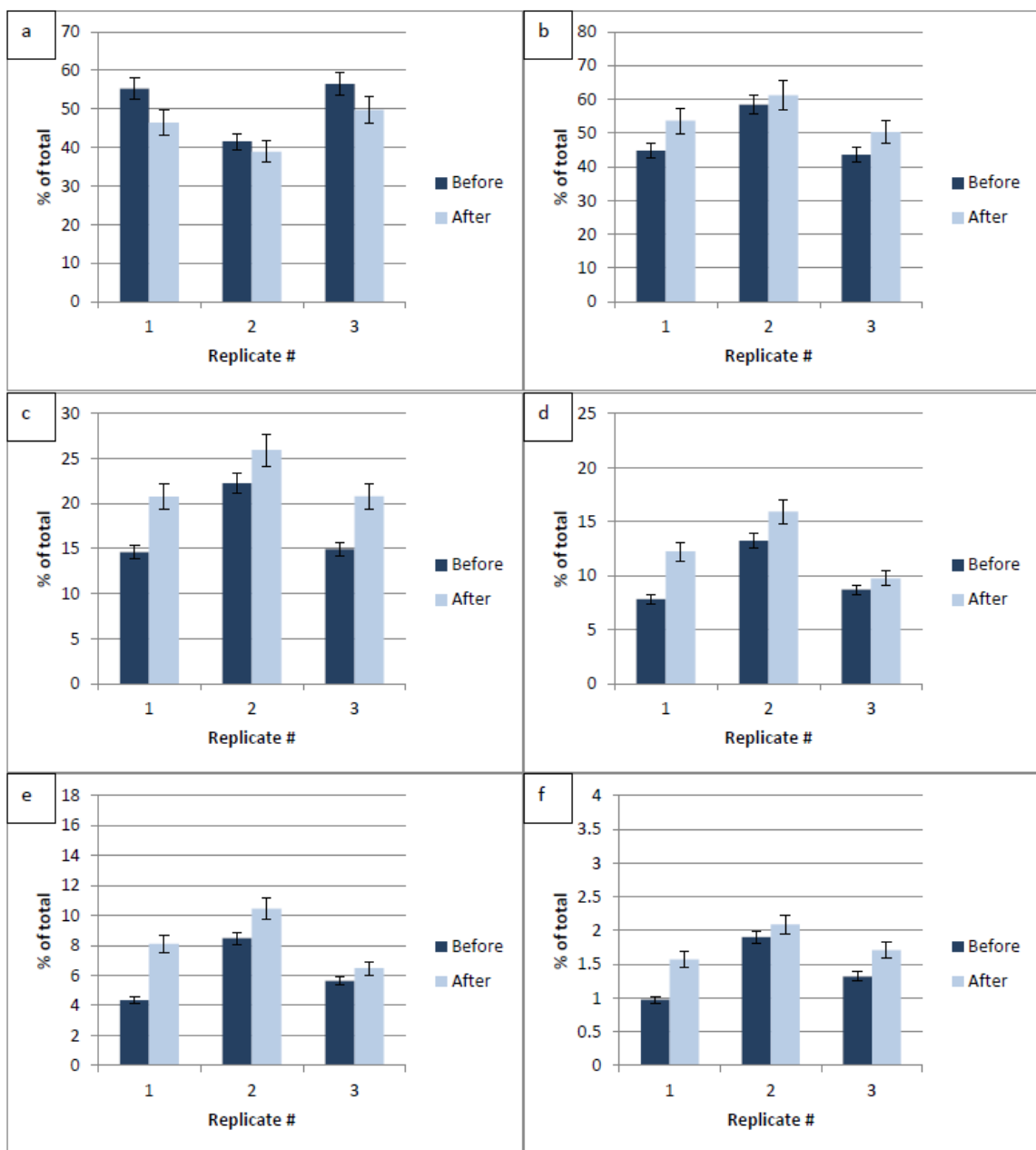


Figure 6.3: Effect of UV irradiation on size distribution. Low-pressure 40 mJ/cm², % of particles which are $\leq 2 \mu\text{m}$ (a), $> 2 \mu\text{m}$ (b), $> 3 \mu\text{m}$ (c), $> 4 \mu\text{m}$ (d), $> 5 \mu\text{m}$ (e), $> 10 \mu\text{m}$ (f).

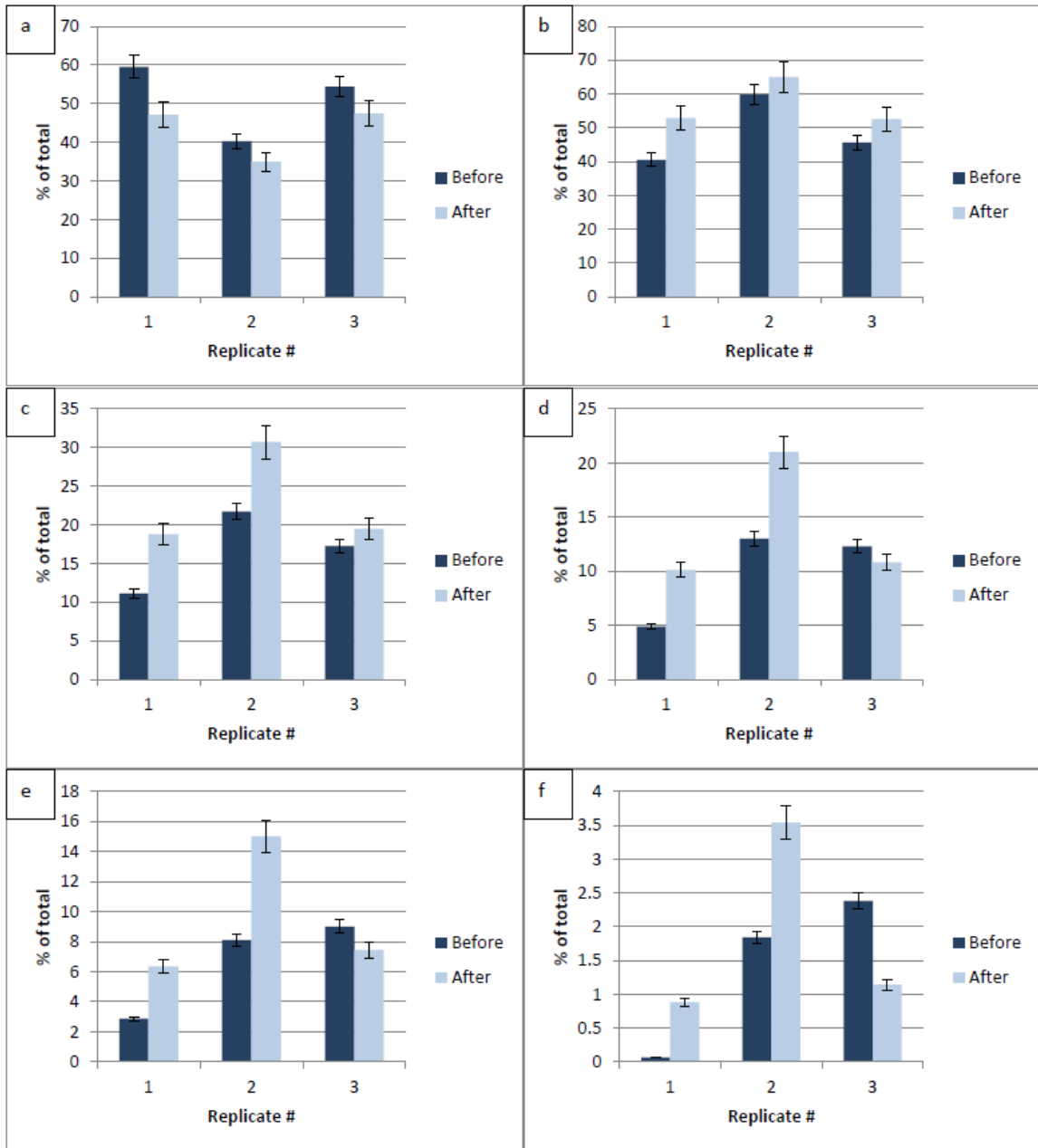


Figure 6.4: Effect of UV irradiation on size distribution. Low-pressure 60 mJ/cm^2 , % of particles which are $\leq 2 \mu\text{m}$ (a), $> 2 \mu\text{m}$ (b), $> 3 \mu\text{m}$ (c), $> 4 \mu\text{m}$ (d), $> 5 \mu\text{m}$ (e), $> 10 \mu\text{m}$ (f).

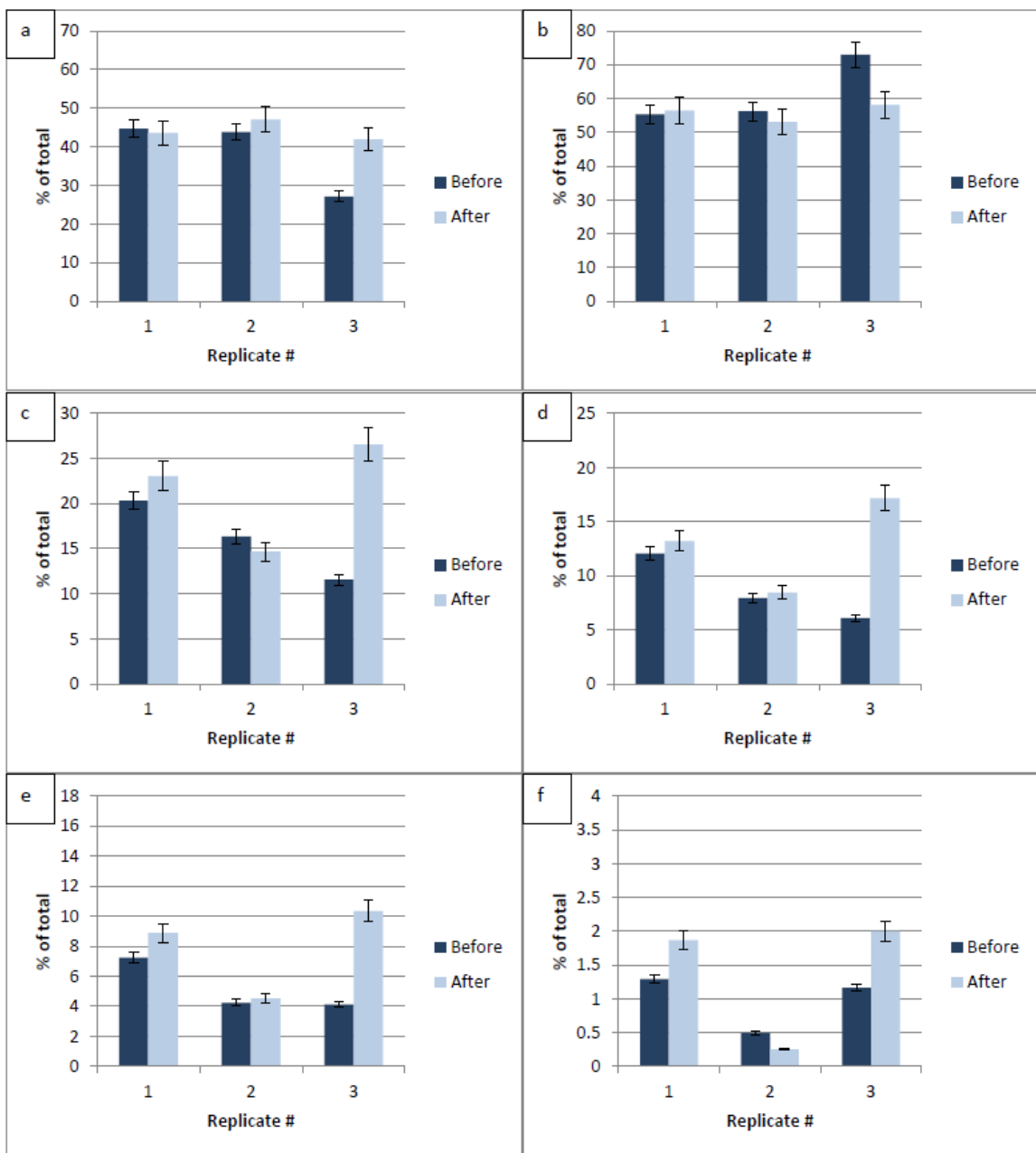


Figure 6.5: Effect of UV irradiation on size distribution. Low-pressure 80 mJ/cm^2 , % of particles which are $\leq 2 \mu\text{m}$ (a), $> 2 \mu\text{m}$ (b), $> 3 \mu\text{m}$ (c), $> 4 \mu\text{m}$ (d), $> 5 \mu\text{m}$ (e), $> 10 \mu\text{m}$ (f).

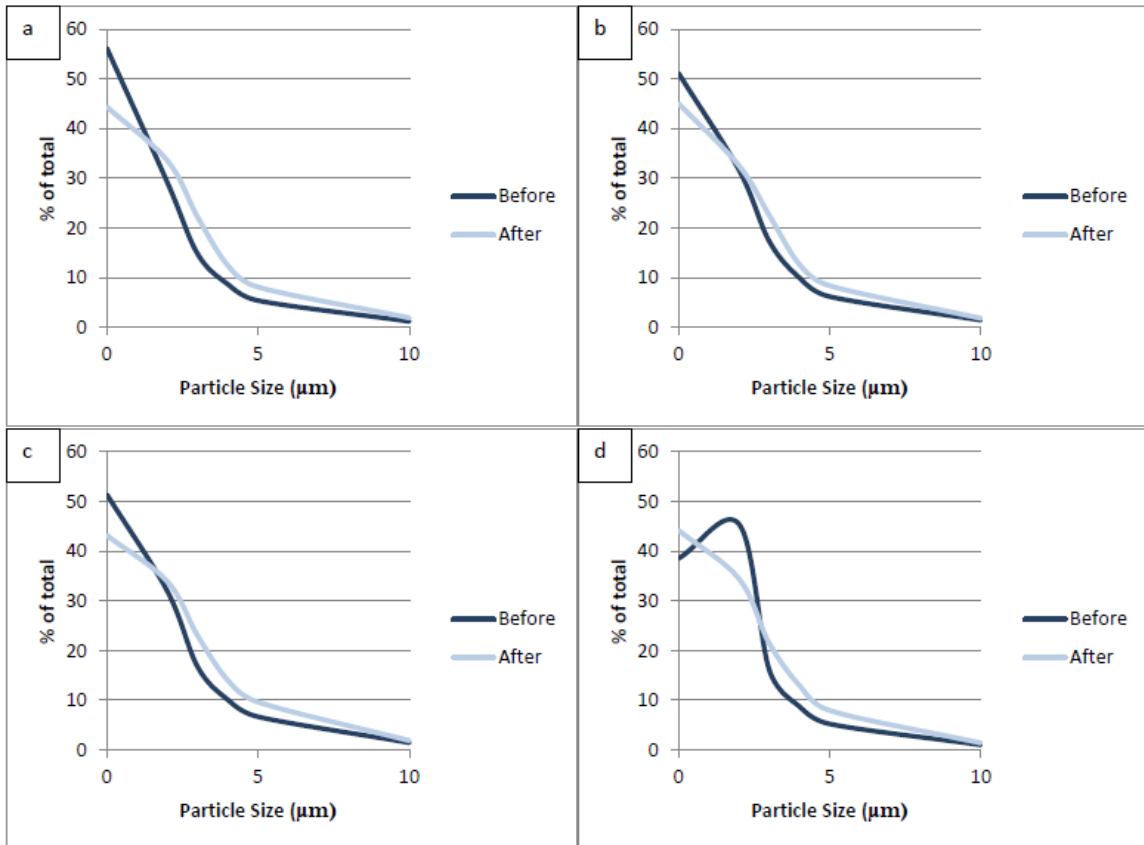


Figure 6.6: Size distribution before and after UV irradiation, low-pressure lamps, doses of 20 (a), 40 (b), 60 (c), and 80 (d) mJ/cm².

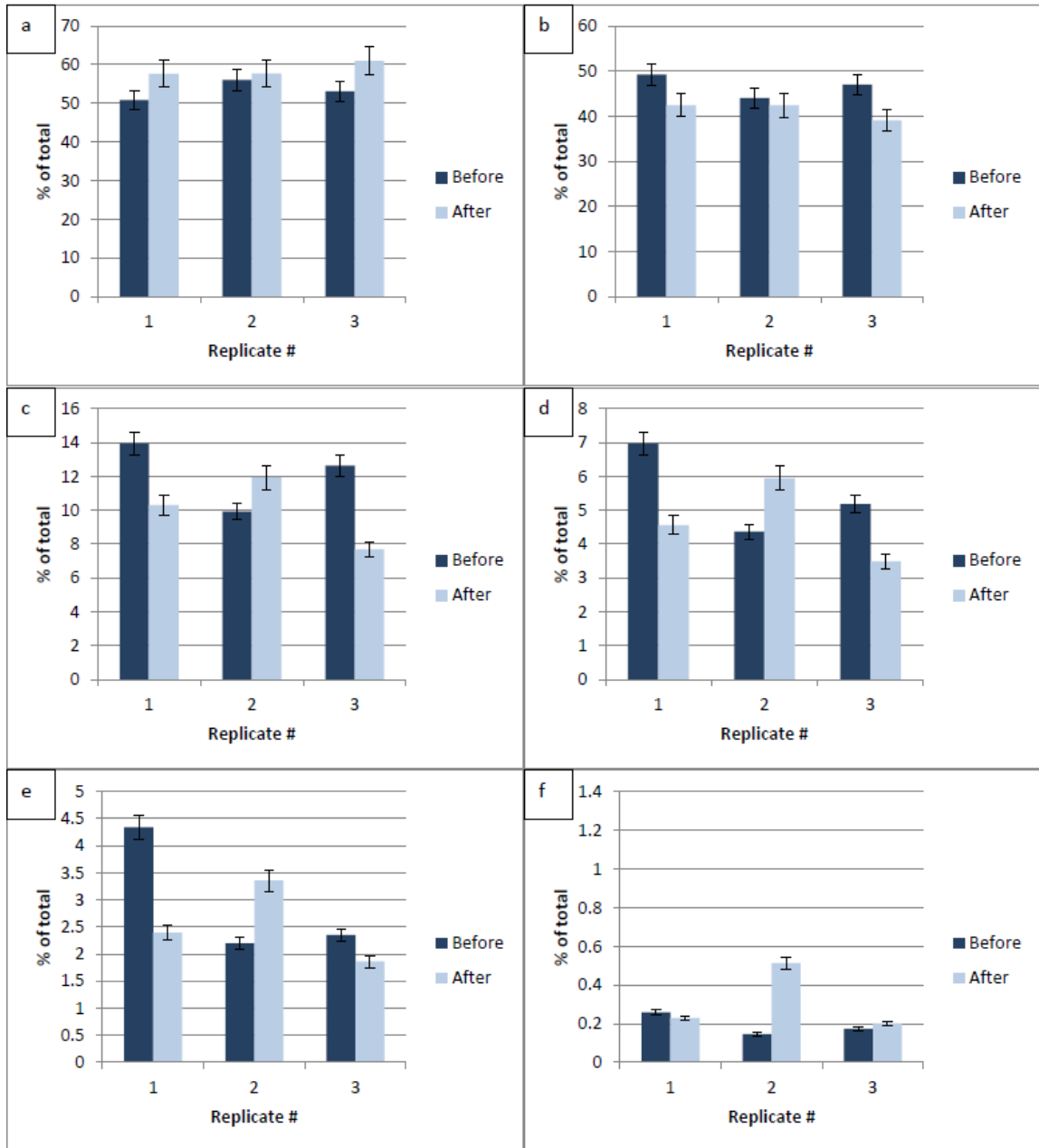


Figure 6.7: Effect of UV irradiation on size distribution. Medium-pressure 40 mJ/cm², % of particles which are $\leq 2 \mu\text{m}$ (a), $> 2 \mu\text{m}$ (b), $> 3 \mu\text{m}$ (c), $> 4 \mu\text{m}$ (d), $> 5 \mu\text{m}$ (e), $> 10 \mu\text{m}$ (f).

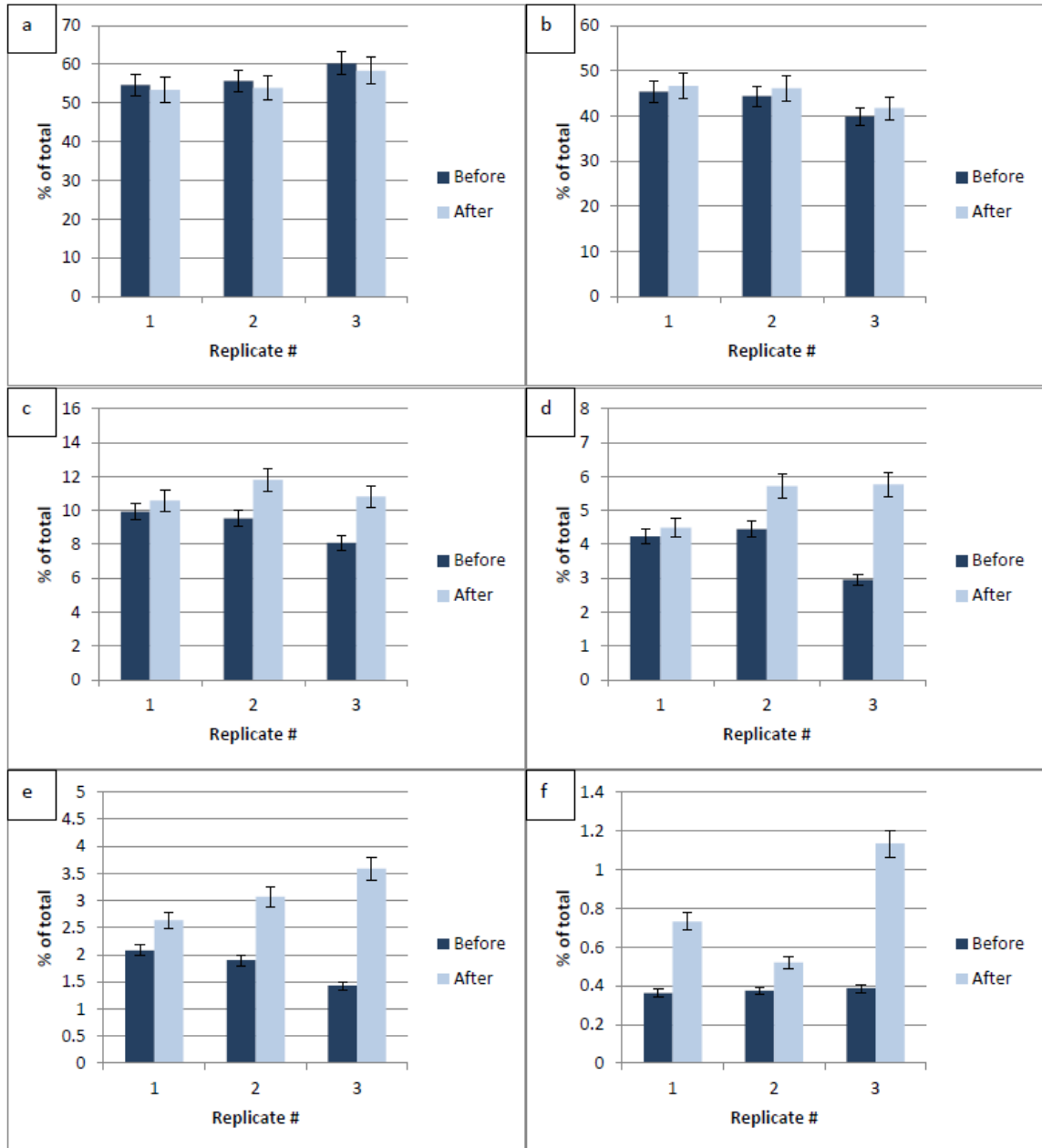


Figure 6.8: Effect of UV irradiation on size distribution. Medium-pressure 80 mJ/cm², % of particles which are $\leq 2 \mu\text{m}$ (a), $> 2 \mu\text{m}$ (b), $> 3 \mu\text{m}$ (c), $> 4 \mu\text{m}$ (d), $> 5 \mu\text{m}$ (e), $> 10 \mu\text{m}$ (f).

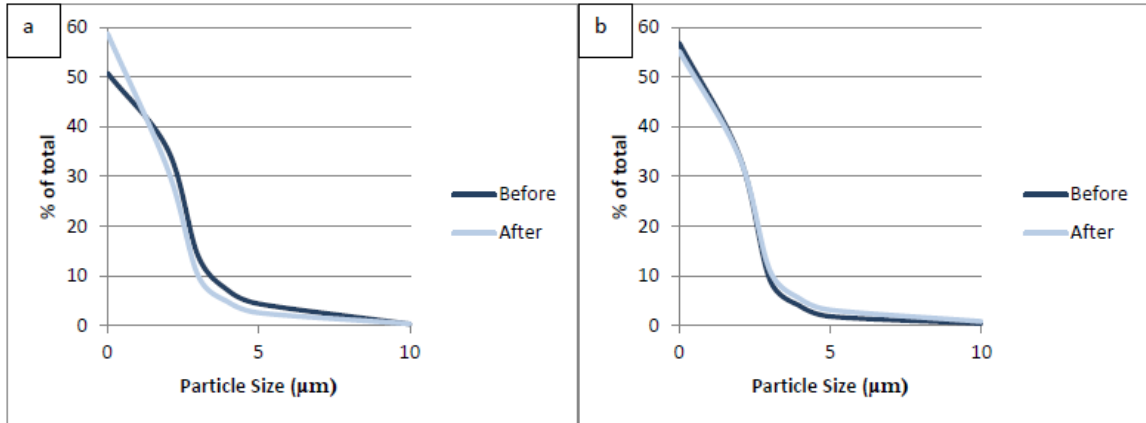


Figure 6.9: Size distribution before and after UV irradiation, medium-pressure lamps, doses of 40 (a), and 80 (b) mJ/cm².

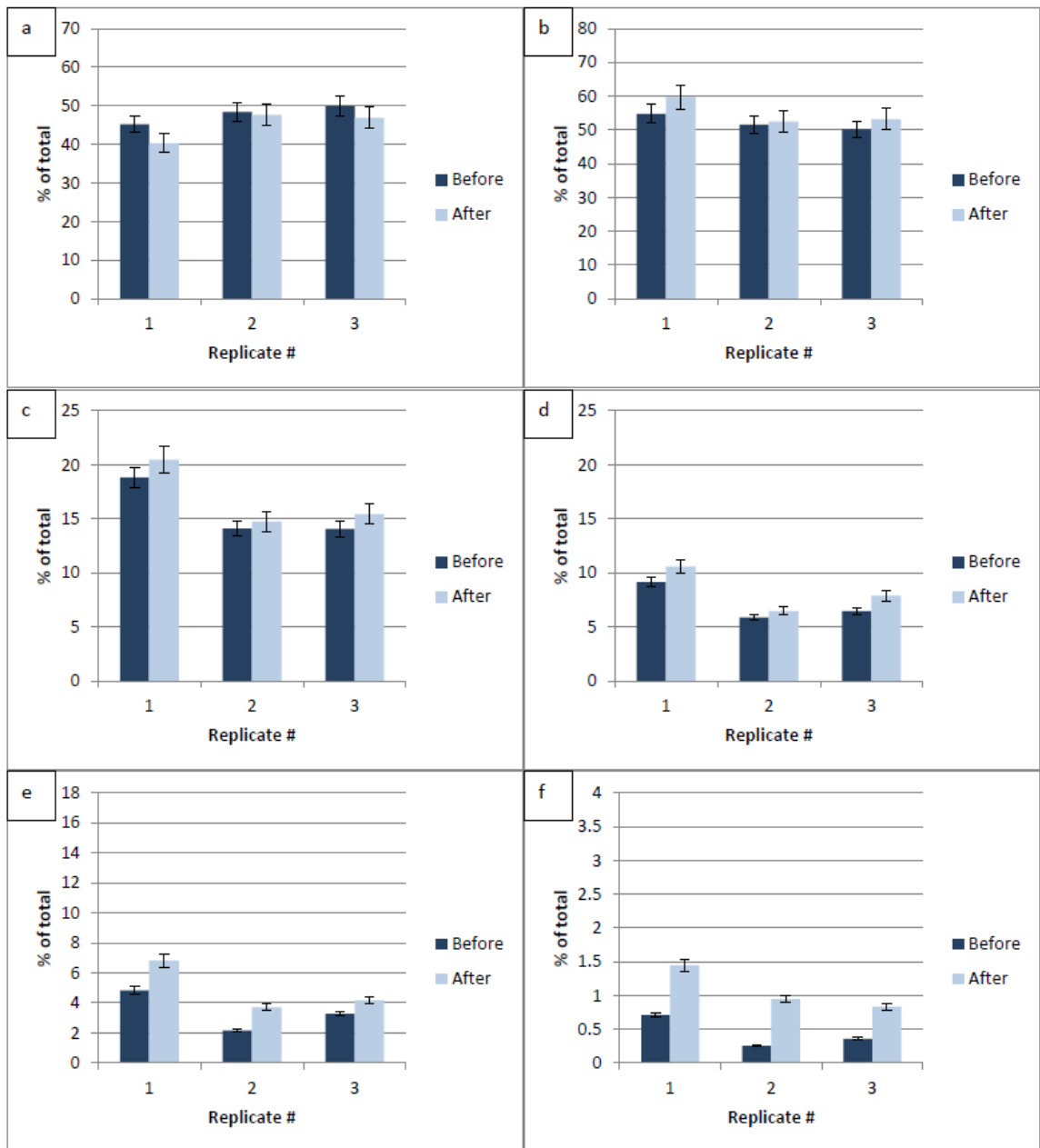


Figure 6.10: Effect of UV irradiation on size distribution. Low-pressure 40 mJ/cm^2 , low intensity and long exposure time experiments, % of particles which are $\leq 2 \mu\text{m}$ (a), $> 2 \mu\text{m}$ (b), $> 3 \mu\text{m}$ (c), $> 4 \mu\text{m}$ (d), $> 5 \mu\text{m}$ (e), $> 10 \mu\text{m}$ (f).

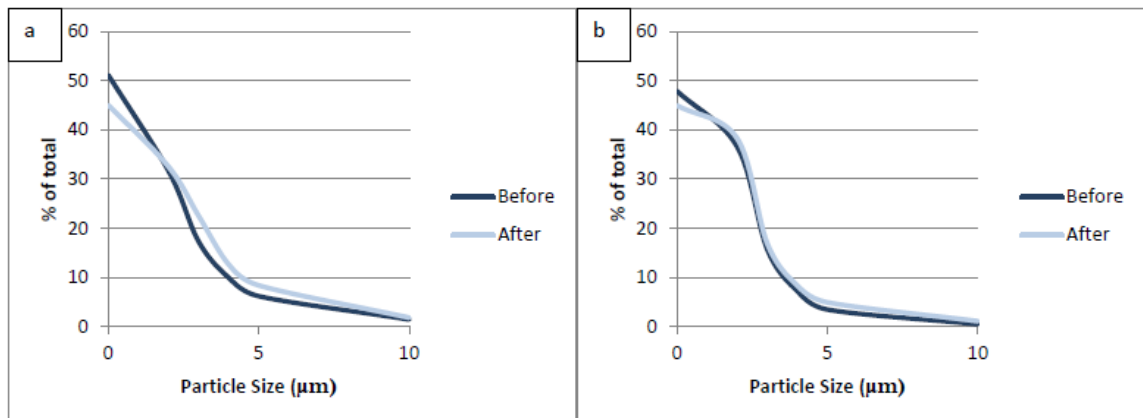


Figure 6.11: Size distribution before and after UV irradiation, low-pressure lamps, dose of 40 mJ/cm^2 , short exposure time (a) versus long exposure time (b).

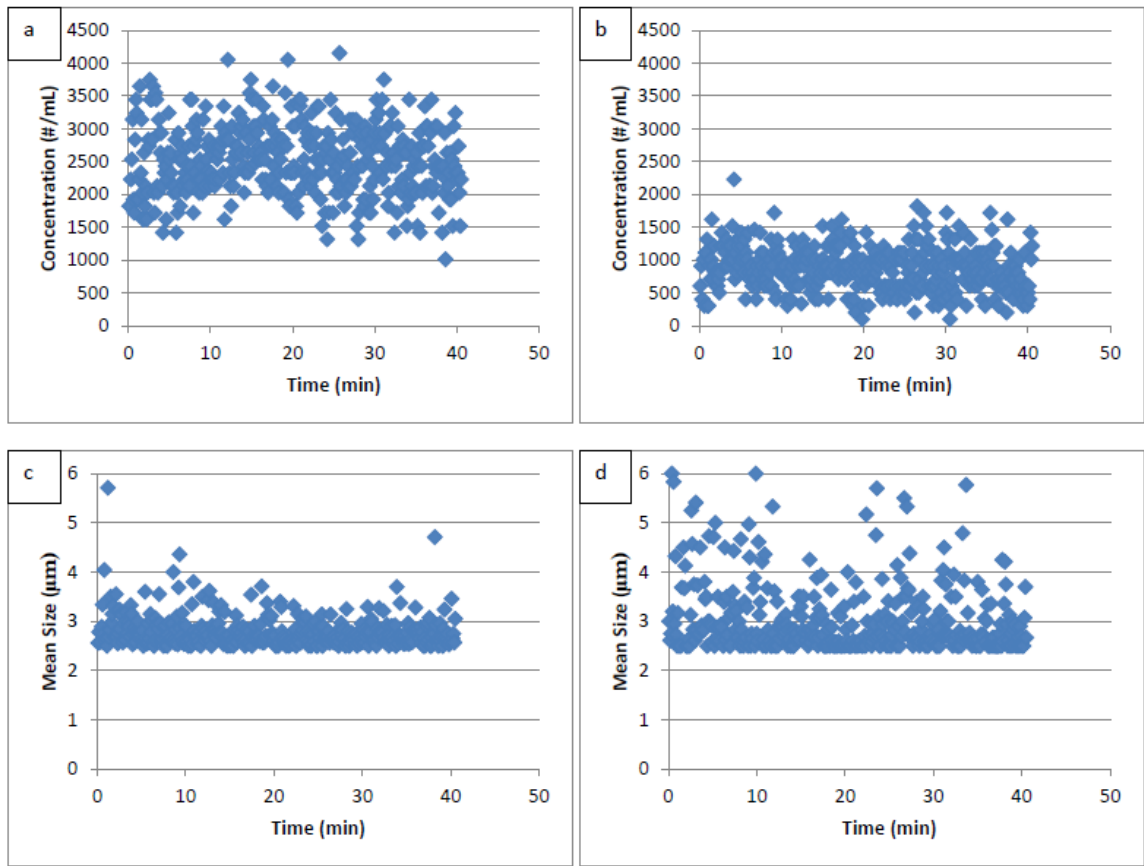


Figure 6.12: Time Resolved Sampling. Low-pressure 40 mJ/cm². Number concentration of particles before (a) and after (b) exposure to UV light. Mean size of the particle population before (c) and after (d) exposure to UV light.

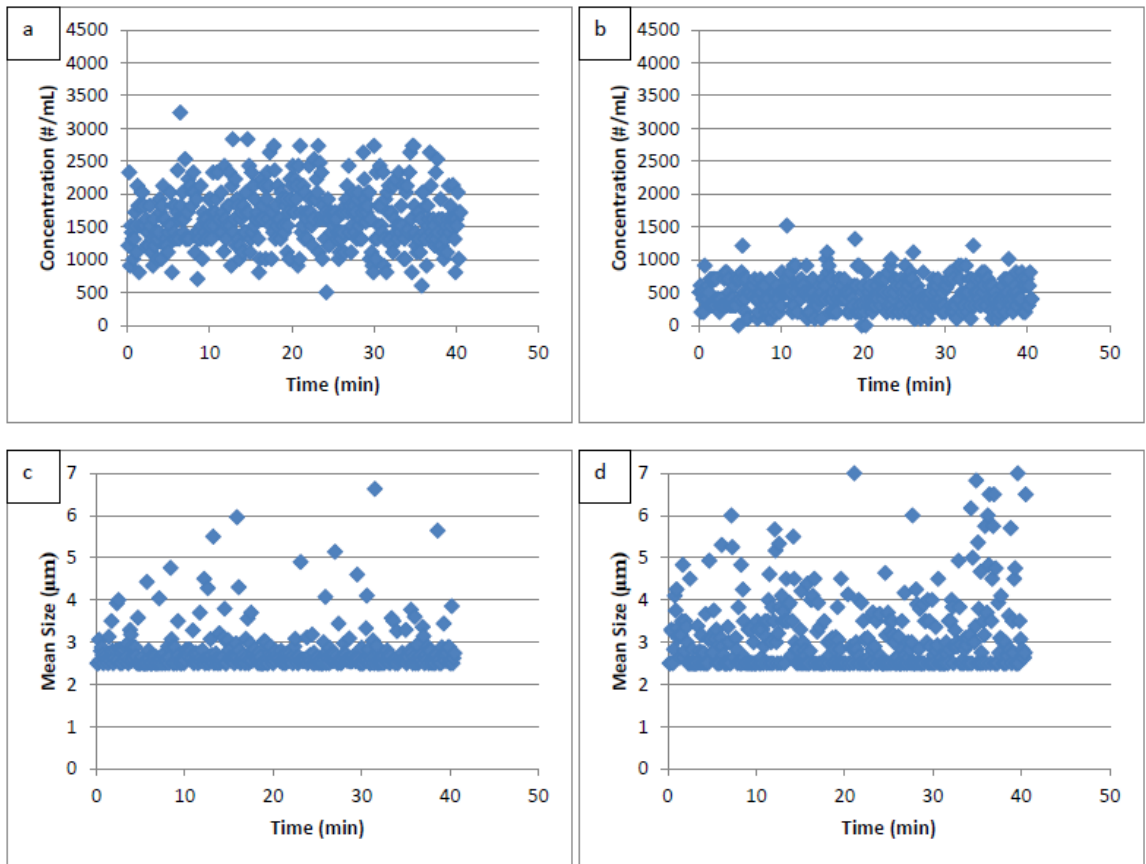


Figure 6.13: Time Resolved Sampling. Low-pressure 80 mJ/cm². Number concentration of particles before (a) and after (b) exposure to UV light. Mean size of the particle population before (c) and after (d) exposure to UV light.

Table 6.1: Percent change from before UV irradiation to after UV irradiation.

UV Dose (mJ/cm ²)	Diameter	Area	Intensity
40	+49.1%	+57.7%	-5.13%
80	+56.3%	+68.0%	-5.81%

CHAPTER 7

REGROWTH POTENTIAL OF BACTERIA AFTER ULTRAVIOLET DISINFECTION IN ABSENCE OF LIGHT AND DARK REPAIR

7.1. Abstract

The objective of this study was to investigate the regrowth potential of *E. coli* and indigenous wastewater bacteria after ultraviolet (UV) disinfection in absence of light and dark repair and under different nutrient conditions. Light repair was prevented by keeping the samples in the dark following UV exposure (15 and 40 mJ/cm²). Dark repair was controlled for by varying the initial and surviving bacteria concentrations, and achieving complete inactivation and no growth in control samples. Net growth and die-off in samples were determined 6, 18, 24, 30 and 48 hours after UV disinfection. The results of this study showed that percent regrowth of *E. coli* and indigenous wastewater bacteria were higher after UV disinfection at 40 mJ/cm² than at 15 mJ/cm², and the regrowth was also sustained for a longer time. Even in the absence of any nutrients, significant regrowth of *E. coli* was observed in phosphate-buffered saline (PBS) indicating that lysis of UV-damaged cells may provide a source of nutrients for the surviving bacteria. In spite of the availability of nutrients in wastewater, the presence of inhibiting and toxic substances appeared to slow down the regrowth of *E. coli*. Indigenous coliform bacteria in wastewater could achieve much higher regrowth compared to laboratory cultured *E. coli* even after a UV dose of 40 mJ/cm².

Keywords: Bacteria, Dark Repair, Light Repair, Regrowth, Ultraviolet (UV) Disinfection, Water, Wastewater.

7.2. Introduction

Ultraviolet (UV) disinfection has become a well-accepted alternative to chlorine for water and wastewater disinfection. One of the primary limitations of UV disinfection arises from the absence of a residual disinfecting dose. For this reason, in systems where disinfected water is stored before its use, regrowth of organisms might significantly alter the microbial quality of the treated water. Since regrowth of microorganisms mainly depends on the availability of nutrients, this aforementioned issue would be especially problematic in treatment of wastewater or graywater. In addition, UV irradiation itself might promote microbial growth by increasing the availability of nutrients to microorganisms via the breakdown of large carbon molecules into smaller ones (Shaw et al., 2000; Van der Maas et al., 2010).

UV inactivated cells will eventually lyse, release their intracellular material, and become a food source to other microorganisms. Similarly, nutrients are released from algae and cyanobacteria cells through lysis in natural aquatic systems (Krog et al., 1986) and these nutrients can make up an important portion of the carbon and energy source for the heterotrophic bacteria (Hansen et al., 1986). Further, UV-inactivated cells might regain viability via repair mechanisms if the UV damage is not substantial (Malley et al., 2004). The reactivation potential of microorganisms has been studied widely in the literature and there is strong evidence that significant levels of reactivation occur for most organisms of concern after water and wastewater disinfection (Harris et al., 1987; Zimmer and Slawson, 2002; Kalisvaart, 2004). However, majority of previous research did not correct

for regrowth of bacteria during reactivation experiments and simply treated the total increase in bacteria counts as reactivation.

Reactivation is the ability of an organism to repair itself by means of light repair (photoreactivation) or dark repair, and regain the ability to reproduce after UV-induced damage. Regrowth, on the other hand, refers to the reproduction of healthy organisms that survive the disinfection process without any significant damage. While reactivation has been shown to heavily depend on light exposure (Sinha and Hader, 2002), regrowth is governed by the availability of nutrients and the viability status of bacteria.

After UV disinfection, water samples are likely to have UV-damaged or non-damaged cells which may both contribute to an increase in the microbial density in a relatively short period of time. In order to accurately study the magnitude and impact of regrowth, the increase in microbial density caused by reactivation of bacteria should be distinguished from the increase caused by regrowth. The main goal of this research was to investigate the regrowth potential of *E. coli* and indigenous wastewater bacteria after UV disinfection in absence of light and dark repair and under different nutrient conditions.

We examined regrowth after low-pressure UV irradiation at two different UV doses and in four different water matrices with varying amounts of nutrients. In all experiments,

photoreactivation was controlled for by keeping the samples in the dark following UV exposure. Increases in bacteria counts attributable to dark repair was determined by varying the initial and surviving bacteria concentrations, and achieving complete inactivation and no growth in control samples. *E. coli* and indigenous wastewater bacteria counts were monitored for growth and die-off for 48 hours after UV disinfection.

7.3. Materials and Methods

7.3.1. Experimental design

Four different water matrices were used to study the regrowth behaviour of bacteria: 1) *E. coli* spiked in PBS (phosphate-buffered saline), 2) *E. coli* spiked in nutrient-enriched PBS, 3) *E. coli* spiked in autoclaved secondary wastewater and 4) secondary wastewater with indigenous microorganisms. These water matrices provided a range of growth conditions for laboratory cultured and indigenous bacteria. Light repair was prevented by keeping the samples in the dark. The initial concentration of bacteria was varied to control for dark repair while examining regrowth. Samples were exposed to UV doses of 15 and 40 mJ/cm². After exposure to UV light, samples were kept at room temperature, in the dark, and were continuously stirred. Bacteria densities were checked immediately after UV irradiation (t=0) as well as 6, 18, 24, 30 and 48 hours afterwards.

7.3.2. Culture preparation

Escherichia coli (ATCC[®] 23631[™]) was chosen as the testing organism and was obtained from Cedarlane Laboratories (Hornby, ON). The bacteria came in the form of a freeze-

dried pellet and were revived following the procedures suggested by the main supplier (ATCC). In brief, the procedures involved rehydrating the pellet in 0.5 mL of TYG broth (ATCC Medium #603) and transferring this aliquot into a tube containing 6 mL of TYG medium which then was incubated at 37 °C for 24 hours. This culture formed the primary stock of *E. coli* for the experiments and was stored in a deep-freezer at -20 °C or below. For each experiment set, a batch was started from this stock by first incubating the culture overnight at 37 °C to allow for the bacteria to recover from freezing. Then, 1 mL of this culture was added to 100 mL of tryptic soy broth in a flask and incubated at 37 °C for 4-5 h to bring the bacteria to a late-log/stationary phase. Different growth phases were found to result in different levels of *E. coli* resistance to UV light (Malley et al., 2004). Thus, cultures were always brought to stationary phase prior to their use in the inactivation experiments. The main advantage of using a stationary phase culture is the stability of the microbial population, which does not change over the experiment period.

Once the stationary phase was reached, cells were harvested from the broth by centrifugation at 14,480 g for 15 min. The purpose of this step was to wash the broth off of the cells and eliminate introduction of nutrients from the broth into the sample. After centrifugation, the supernatant was removed and the remaining pellet was re-suspended in PBS by vortex mixing. The cells were washed by repeating the following procedure twice: first the suspension was centrifuged again, second the supernatant was removed, and finally the pellet was re-suspended in a fresh PBS medium. This yielded a bacterial concentration of approximately 10^9 colony forming units per mL (CFU/mL) in the final suspension.

7.3.3. Water matrices

Experiments were carried out in four different water matrices, which provided a range of growth conditions for pure *E. coli* culture and indigenous wastewater bacteria (Figure 7.1). The PBS medium lacked any nutrients whereas nutrient-enriched PBS contained an ample amount of food source for bacteria, and allowed to compare the regrowth of *E. coli* in presence and absence of nutrients. The wastewater samples were also used to study the regrowth behaviour of laboratory cultured bacteria and indigenous wastewater coliforms. More information on the preparation of the water matrices is provided below.

7.3.3.1. E. coli (ATCC[®] 23631[™]) spiked in PBS: The PBS medium was prepared by adding magnesium chloride (MgCl₂) and phosphate buffer stock (KH₂PO₄) to deionized water according to the guidelines provided in Standard Methods (APHA, 2005). Thus, the PBS medium did not contain any carbon or nitrogen sources and the PBS experiments were critical for determining how much bacteria can regrow in the absence of nutrients and whether cell lysis after UV exposure can be a significant nutrient source for surviving bacteria.

7.3.3.2. E. coli (ATCC[®] 23631[™]) spiked in nutrient-enriched PBS: The experiments were designed to study the regrowth behaviour of *E. coli* in a nutrient-rich environment. The nutrient-enriched PBS was prepared by adding tryptic soy broth to PBS at a ratio of 1/100. This also made it possible to observe whether nutrients have a promoting effect on dark repair.

7.3.3.3. *E. coli* (ATCC[®] 23631[™]) spiked in autoclaved wastewater: The purpose of these experiments was to repeat the above experiments in secondary effluent wastewater. In order to be able to modify the initial concentration of bacteria and run controlled experiments, wastewater was first autoclaved to eliminate all indigenous microorganisms. After autoclaving, the laboratory culture of *E. coli* (ATCC[®] 23631[™]) was spiked into the autoclaved wastewater to give the desired initial bacteria density.

7.3.3.4. *Secondary wastewater with indigenous microorganisms*: These experiments provided a basis for comparison for the growth behavior of laboratory cultured and indigenous wastewater bacteria. The wastewater samples were obtained from the effluent of a secondary clarifier before disinfection and the experiments were conducted on the same day the samples were acquired. Initial concentration of the total indigenous coliform bacteria in the wastewater was determined to be 3×10^5 CFU per 100 mL.

7.3.4. Control for light and dark repair

One of the main goals of this study was to distinguish regrowth from reactivation. The main challenge in doing so is that regrowth and reactivation occur simultaneously. There are two reactivation mechanisms: light and dark repair. As light repair requires light exposure, it was prevented simply by keeping samples in the dark after UV irradiation. However, dark repair has been observed to occur regardless of light's presence or absence (Sinha and Hader, 2002). Increases in bacteria counts attributable to dark repair was determined by varying the initial and surviving bacteria concentrations, and

achieving complete inactivation and no growth in control samples over the next 48 hours. For every water matrix and UV dose studied, there were three starting concentrations: 10^5 , 10^7 and 10^9 CFU per 100 mL (these will be referred to as 5-log, 7-log and 9-log for simplicity). This, in turn, resulted in different numbers of surviving bacteria for the same UV dose. As injured cells first need to repair UV damage before being able to reproduce, a sample in which there are no surviving bacteria after UV irradiation and no increase during an incubation time can serve as a baseline for repair, hence also as a control that shows the bacteria are not capable of dark repair under the test conditions. Then, in samples where some bacteria do survive the UV disinfection, all of the increase in the bacteria concentration during the post-UV hours can be attributed to regrowth under the same test conditions.

A variation in the number of surviving bacteria could also be achieved by changing the UV dose. However, UV dose was reported to affect the reactivation of bacteria (Lindenauer and Darby 1994; Hu et al., 2005; Bohrerova and Linden, 2007) since higher UV doses would lead to more UV damage on cells. Higher UV doses were also reported to decrease the dark repair potential of *E. coli* (Guo et al., 2011). Therefore, it was critical to keep the UV dose same and change the initial bacteria concentrations to achieve varying numbers of surviving bacteria to serve as a control for dark repair.

7.3.5. UV reactor setup and dose calculations

The UV reactor used was a collimated beam setup that consisted of four low-pressure mercury lamps (Phillips UV-C germicidal lamps, Ottawa, ON) emitting monochromatic ultraviolet light at 253.7 nm. The collimation of light was achieved by successively placing baffles along the UV light path. UV irradiation experiments were conducted according to the procedures outlined in Bolton and Linden (2003), which included correction factors for the calculation of the true UV dose by accounting for the reflection and absorption of the UV light by the sample solution, unequal distribution of UV light over the surface of the sample, and divergence of the UV light before reaching the sample surface. The 6.5-cm Petri dishes used for the inactivation experiments allowed for a sample solution depth of less than 2 cm (categorized as shallow) when the sample volume was 60 mL or less. The samples were continuously mixed, at low speeds with micro stirring rods to avoid vortex formation. The incident UV intensity was measured by a radiometer (International Light, MA, USA) immediately before each sample was exposed to UV light in order to account for the small fluctuation in the light intensity reaching the samples.

UV doses of 15 and 40 mJ/cm² were used in the study. UV dose values from 5 to 15 mJ/cm² are considered sufficient to inactivate *Cryptosporidium parvum* and *Giardia lamblia*. A UV dose of 40 mJ/cm² is the minimum requirement for drinking water disinfection plants in Austria and Germany (ÖNORM, 2001; DVGW, 2006). Higher doses were not considered as they would result in very few bacteria surviving the disinfection.

7.3.6. Enumeration

Membrane filtration was used to enumerate bacteria according to Protocol 9222 B given in the Standard Methods (APHA, 2005). M-Endo Agar LES medium (Becton, Dickinson & Company, MD, USA) was used as the selective growth medium. After filtration, the samples were incubated for 24 (\pm 3) hours at 37°C before colony counting. The reported values are the averages of three sampling (or plating) replicates.

7.4. Results and Discussion

Figure 7.2 shows the numbers of surviving *E. coli* in PBS after UV exposures of 15 mJ/cm² or 40 mJ/cm². Three different initial bacteria concentrations (5-, 7-, and 9-log) were used and the bacteria counts were monitored for 48 hours after UV exposure. Photoreactivation (light repair) was prevented by keeping the samples in the dark. The 5-log sample served as a control for dark repair since complete inactivation was achieved at both 15 mJ/cm² and 40 mJ/cm², and there was no growth during the 48 hours following the UV irradiation. This indicates that there was no dark repair occurring at 15 mJ/cm² and 40 mJ/cm² under the specific conditions used for this experiment. If there was dark repair, an increase in the bacteria counts in the post-UV hours would have been observed after total inactivation was achieved for the 5-log sample. Since the 7- and 9-log samples were also exposed to the same UV doses (15 mJ/cm² and 40 mJ/cm²) under the same experimental conditions, there was no dark repair occurring in these samples either. As a result, any increase in the bacteria concentrations during the 48 hours could be attributed to regrowth.

For the 7- and 9-log samples, complete inactivation was not achieved at 15 mJ/cm² or 40 mJ/cm² and some of the bacteria survived the UV disinfection. In addition, the total bacteria counts first increased and then started decreasing over the next 48 hours. It is important to note that these were PBS samples and hence there was no external source of nutrients to fuel the growth of bacteria. However, the intracellular material released by the lysis of UV inactivated cells may have provided a limited food source for the surviving bacteria. No increase in *E. coli* counts were observed in PBS samples that were not exposed to UV dose.

Figure 7.3 is complementary to Figure 7.2 and shows the percent change in the concentration of surviving bacteria to better represent the magnitude of regrowth and die off with respect to UV dose. The calculation of percent change was carried out as follows:

$$\text{percent change} = 100 \times \frac{N_t - N_0}{N_0}$$

where N_0 is the number of organisms surviving UV disinfection as measured immediately after the exposure ($t = 0$ h), and N_t is the number of organisms detected at time t ($t = 6, 18, 24, 30,$ and 48 h).

The 5-log data was excluded from Figure 7.3 as there was no growth over 48 hours. At 15 mJ/cm² UV dose, the highest percent regrowth was observed after 6 hours and was 3% for the 7-log and 9% for the 9-log sample. Beyond 6 hours, bacteria quickly started dying

due to lack of nutrients and by 18 hours a 22% decrease in the bacteria concentration was observed for the 9-log sample. In general, the percent increases and decreases observed in the bacteria counts in the 9-log samples were rapid compared to the 7-log samples due to the higher number of bacteria that survived the disinfection. At the higher UV dose of 40 mJ/cm², the highest percent regrowth was observed after 24 hours for the 7-log sample and after 6 hours for the 9-log sample (35% and 40% respectively). Because the 7-log sample had a lower concentration of bacteria to start with, there was less competition and more nutrients available to support their growth longer. At 40 mJ/cm², not only the percent of regrowth was higher but also it was maintained for a longer duration when compared to 15 mJ/cm² (30 hours as opposed to 6 hours). The results are particularly interesting in showing that a higher degree of regrowth occurred in PBS when the UV dose was higher, which may imply that the higher UV dose resulted in higher cell lysis that provided a larger food source for a smaller group of surviving bacteria. The opposite is true for the repair processes where higher UV doses cause more DNA damage to bacteria and thus decrease the extent of repair (Lindenauer and Darby, 1994; Hu et al., 2005). In fact, repair may cease altogether beyond a certain dose (Kashimada et al., 1996).

The next step was to study the effect of nutrients on the extent of dark repair and regrowth. In these experiments (Figure 7.4), a nutrient-rich medium was added to PBS to provide a food source for bacteria. Then, samples containing 5-, 7-, and 9-log *E. coli* were exposed to a UV dose of 15 mJ/cm², and regrowth was monitored for 48 hours. Once again, complete inactivation was achieved for the 5-log sample and there was no

increase in the bacteria concentration afterwards. This showed that the injured bacteria were not able to repair themselves in the presence of nutrients either. In contrast, a rapid and sustained increase in regrowth was observed which was due to the plenty of nutrients available for the bacteria population. The bacteria counts exceeded 10^8 CFU/100 mL for both the 7- and 9-log samples after 48 hours.

The above experiments were carried out in PBS and it was necessary to study the regrowth and repair behaviour of *E. coli* in wastewater under similar conditions for comparison. For these experiments, wastewater was first autoclaved and spiked with *E. coli* to prepare samples with initial *E. coli* concentrations of 5-, 7-, and 9-log. Autoclaving killed the competing microorganisms in wastewater but the nutrients were still available to seeded bacteria. The samples were then exposed to 15 mJ/cm² or 40 mJ/cm² UV dose and regrowth and dark repair was monitored for 48 hours. Figures 7.5 and 6.6 show the number and percent change of surviving bacteria over time. Complete inactivation was again achieved for the 5-log sample at both 15 and 40 mJ/cm², and no increase in the bacteria concentrations were observed afterwards (Figure 7.5). This indicated that dark repair did not occur under the test conditions and the increases observed in the 7- and 9-log samples over the 48 hours were due to regrowth of bacteria. Lack of dark repair for the *E. coli* K-12 strain was reported by other studies as well (Kashimada et al., 1996; Sommer et al., 2000; Oguma et al. 2001). Surprisingly, in spite of the availability of nutrients in wastewater, the regrowth of *E. coli* was slower in wastewater compared to PBS. This could be caused by the presence of inhibiting or toxic substances in wastewater. An initial regrowth was observed in the first 6 hours after

inactivation at 15 and 40 mJ/cm² but afterwards the bacteria quickly started dying off. Similar to the results obtained from PBS, the percent regrowth was higher when the UV dose was higher and the bacteria were able to survive for a longer time (Figure 7.6). For example, the 9-log sample showed a 25% increase after 15 mJ/cm² and a 256% increase after 40 mJ/cm² in the first 6 hours. Percent decrease from the initial counts was 84% for 15 mJ/cm² and 49% for 40 mJ/cm² after 48 hours. The 7-log samples did not follow a clear pattern as the vast majority of bacteria died within 18 hours following UV exposure.

In the final phase, secondary wastewater effluent containing indigenous bacteria was used in the experiments and changes in total coliform counts were monitored for 48 hours after UV irradiation at 15 and 40 mJ/cm². The initial concentration of total coliform in the wastewater was 3x10⁵ CFU/100 mL and no bacteria were spiked in samples. Total inactivation was not achieved at either 15 or 40 mJ/cm² (Figure 7.7), therefore if there was dark repair occurring, it could not be distinguished from regrowth. However, all or most of the observed increase was likely due to regrowth in the light of the information obtained from previous experiments. Overall, the growth patterns showed an initial increase followed by a decrease and the highest bacteria counts were observed after 24 hours as opposed to 6 hours for PBS. There was again a larger percent increase in the bacteria counts after irradiation at 40 mJ/cm² than at 15 mJ/cm² (Figure 7.8) as was the case in the previous experiments (Figure 7.3 and Figure 7.6). In addition, despite the time delay in the growth of bacteria, the percent increase was much higher compared to the PBS and autoclaved wastewater experiments. It should be noted that wastewater contains a large number and variety of microorganisms in addition to the coliform bacteria and the

reported numbers are only for the coliform bacteria. It is possible that more intracellular material originating from lysed cells may have supported the growth of coliforms after UV irradiation. In addition, UV irradiation itself might have promoted microbial growth by increasing the availability of nutrients to microorganisms via the breakdown of large carbon molecules into smaller ones (Shaw et al., 2000; Ijpelaar et al., 2001; Liu et al., 2002; van der Maas et al., 2010).

In this study, the observed regrowth was less significant than the reported levels of photoreactivation in the literature. While the reported numbers for maximum photoreactivation vary from 2.1 log (Oguma et al., 2001) to 3.56 log (Sommer et al., 2000) for *E. coli*, the highest levels of regrowth detected in this study were only 0.14 log in PBS, 0.55 log in autoclaved wastewater and 1.74 log in intact wastewater. A full recovery was observed in the nutrient enriched PBS samples; however, the study conditions in those experiments were unrealistic, as a near ideal amount and composition of nutrients were provided. Nonetheless, regrowth still significantly altered the biological quality of the water even in the absence of external sources of nutrients. Thus, regrowth might pose problems for meeting stringent water quality standards, particularly when the effect of UV dose is considered.

Regrowth was also a relatively slower process than reactivation. While reactivation has been reported to reach a maximum in about 2 to 3 hours (Sommer et al., 2000; Zimmer

and Slawson, 2002), the time at which maximum regrowth was observed varied between 6 and 24 hours depending on the water matrix and the initial concentration of bacteria.

The results of the PBS experiments suggest that some amount of nutrients may have been released from the inactivated cells, as there was no other source of nutrients in the PBS matrix. Most studies have shown that low-pressure UV radiation at low doses has negligible effects on the formation of assimilable organic carbon (AOC), which is the biologically more available organic carbon (Shaw et al., 2000; Ijpelaar et al., 2001; Liu et al., 2002). However, in those studies the focus was on the breakup of larger carbon molecules into smaller biodegradable ones. In the PBS experiments of this study, these substances were absent to begin with, which suggests that AOC might have formed via lysis of cells inactivated by UV light. The higher levels of regrowth observed at the higher UV dose supports this hypothesis. As higher UV doses result in more bacteria being inactivated, more nutrient release from lysing cells would be expected. This would then translate into more regrowth.

Overall, the results of this study show that regrowth of bacteria can significantly alter the microbial quality of water even in the absence of external sources of nutrients. In the absence of light and dark repair, regrowth of pure-culture and indigenous wastewater bacteria was higher after exposure to higher UV doses compared to lower UV doses, which indicate that UV-caused cell lysis may promote the growth of surviving bacteria. The study is unique in that it studied the effect of regrowth alone by controlling for both

light and dark repair. The results also show that indigenous bacteria can regrow at a much higher rate compared to pure culture strains. These findings are particularly important for water reuse applications (e.g. wastewater, graywater) where the storage times can be longer and the water might be prone to biological instability due to regrowth of microorganisms (Friedler et al., 2011).

7.5. Conclusions

Regrowth of *E. coli* and indigenous wastewater bacteria after UV disinfection (15 and 40 mJ/cm²) was studied in absence of light and dark repair and under different nutrient conditions. The results of this study indicate that:

- Regrowth of *E. coli* and indigenous wastewater bacteria were higher after UV disinfection at 40 mJ/cm² than at 15 mJ/cm², and the regrowth was also sustained for a longer time under higher UV doses.
- Even in the absence of any nutrients, significant regrowth of *E. coli* was observed in PBS after UV disinfection indicating that lysis of UV-damaged cells may provide a food source for the surviving bacteria.
- Addition of nutrients did not boost dark repair of *E. coli* under the conditions tested but greatly increased its regrowth.
- In spite of the availability of nutrients, regrowth of *E. coli* in wastewater was slower and they died off quicker compared to PBS, which could be caused by the presence of inhibiting and toxic substances in wastewater.

- Regrowth of indigenous coliform bacteria in wastewater was much higher (approximately 50 times at 15 mJ/cm² and 200 times at 40 mJ/cm²) than the regrowth of laboratory cultured *E. coli* in wastewater.
- Regrowth of bacteria can be significant even after exposure to a UV dose of 40 mJ/cm² and particularly in nutrient-rich waters.

7.6. References

American Public Health Association (APHA), American Water Works Association and Water Pollution Control Federation, 2005. Standard Methods for the Examination of Water and Wastewater. APHA/AWWA, Washington DC.

Bohrerova, Z., Linden, K. G., 2007. Standardizing photoreactivation: Comparison of DNA photorepair rate in *Escherichia coli* using four different fluorescent lamps. *Water Research*, 41 (12), 2832-2832.

Bolton, J. R., Linden, K. G., 2003. Standardization of methods for fluence (UV dose) determination in bench-scale UV experiments. *Journal of Environmental Engineering* 129 (3), 209-215.

DVGW, 2006. UV Disinfection Devices for Drinking Water Supply Requirements and Testing. DVGW W294-1, -2, and -3. German Gas and Water Management Union (DVGW), Bonn, Germany.

Friedler, E., Yardeni, A., Gilboa, Y., Alfiya, Y., 2011. Disinfection of greywater effluent and regrowth potential of selected bacteria. *Water Science and Technology* 63 (5), 931-940).

Guo, M-T, G., Huang, J-J., Hu, H-Y., H., Liu, W-J., 2011. Growth and repair potential of three species of bacteria in reclaimed wastewater after UV disinfection. *Biomedical and Environmental Sciences*, 24 (4), 400-407.

Hansen, L., Krog, G. F., Søndergaard M., 1986. Decomposition of lake phytoplankton. 1. Dynamics of short-term decomposition. *Oikos* 46, 37-44.

Harris, G. D., Adams, V. D., Sorensen, D. L., Curtis, M. S., 1987. Ultraviolet inactivation of selected bacteria and viruses with photoreactivation of the bacteria. *Water Research* 21 (6), 687-692.

Hu, J. Y., Chu, X. N., Quek, P. H., Feng, Y. Y., Tan X. L., 2005. Repair and regrowth of *Escherichia coli* after low- and medium-pressure ultraviolet disinfection. *Water Science and Technology: Water Supply* 5 (5), 101-108.

Ijpelaar, G. F., Beerendonk, E. F., 2001. Formation of by-products by UV disinfection – comparison of various UV beamers on laboratory scale. Kiwa report BTO 2001.193. (c) (in Dutch).

Kalisvaart, B. F., 2004. Re-use of wastewater: preventing the recovery of pathogens by using medium-pressure UV lamp technology. *Water Science and Technology* 50 (6), 337-344.

Kashimada, K., Kamiko, N., Yamamoto, K., Ohgaki, S., 1996. Assessment of photoreactivation following ultraviolet light disinfection. *Water Science and Technology* 33, 261-269.

Krog, G. F., Hansen, L., Sondergaard, M., 1986. Decomposition of lake phytoplankton. 2. Composition and lability of lysis products. *Oikos* 46, 45-50.

Lindenauer, K. G., Darby, J. L., 1994. Ultraviolet disinfection of wastewater: effect of dose on subsequent photoreactivation. *Water Research* 28 (4), 805-817.

- Liu, W., Andrews, S. A., Bolton, J. R., Linden, K. G., Sharpless, C., Stefan, M., 2002. Comparison of disinfection byproduct (DBP) formation from different UV technologies at bench scale. *Water Science and Technology: Water Supply* 2 (5-6), 515-521.
- Malley, J. P., Ballester, N. A., Margolin, A. B., Linden, K. G., Mofidi, A., Bolton, J. R., Crozes G., Cushing B., Mackey, E., Laine J. M., Janex M. L., 2004. Inactivation of Pathogens with Innovative UV Technologies. American Water Works Association Research Foundation, USA.
- Oguma, K., Katayama, H., Mitani, H., Morita, S., Hirata, T., Oghaki S., 2001. Determination of pyrimidine dimers in *Escherichia coli* and *Cryptosporidium parvum* during UV light inactivation, photoreactivation, and dark repair. *Applied and Environmental Microbiology* 67(10), 4630-4637.
- ÖNORM, 2001. Plants for the Disinfection of Water Using Ultraviolet Radiation Requirements and Testing Part 1: Low Pressure Mercury Lamp Plants. ÖNORM M 5873-1. Österreichisches Normungsinstitut, Vienna, Austria.
- Shaw, J. P., Malley, J. P., Willoughby, S. A., 2000. Effects of UV irradiation on organic matter. *Journal of American Water Works Association* 92 (4), 157-167.
- Sinha, R. P., Hader, D. P., 2002. UV-induced DNA damage and repair: a review. *Photochemical and Photobiological Sciences* 1 (4), 225-236.
- Sommer, R., Lhotsky, M., Haider, T., Cabaj, A., 2000. UV inactivation, liquid-holding recovery and photoreactivation of *Escherichia coli* O157 and other pathogenic *Escherichia coli* strains in water. *Journal of Food Protection* 63 (8), 1015-1020.

Van der Maas, P., Van der Woerd D., Wübbels, G., Van der Kooij, D. (2010) Impact of low pressure UV on the regrowth potential of drinking water. Proceedings of the IWA World Water Congress, Montreal, Canada.

Zimmer, J. L., Slawson, R. M., 2002. Potential repair of *Escherichia coli* DNA following exposure to UV radiation from both medium and low pressure UV sources in drinking water treatment. Applied Environmental Microbiology 68 (7), 3293-3299.

7.7. Figures and Tables

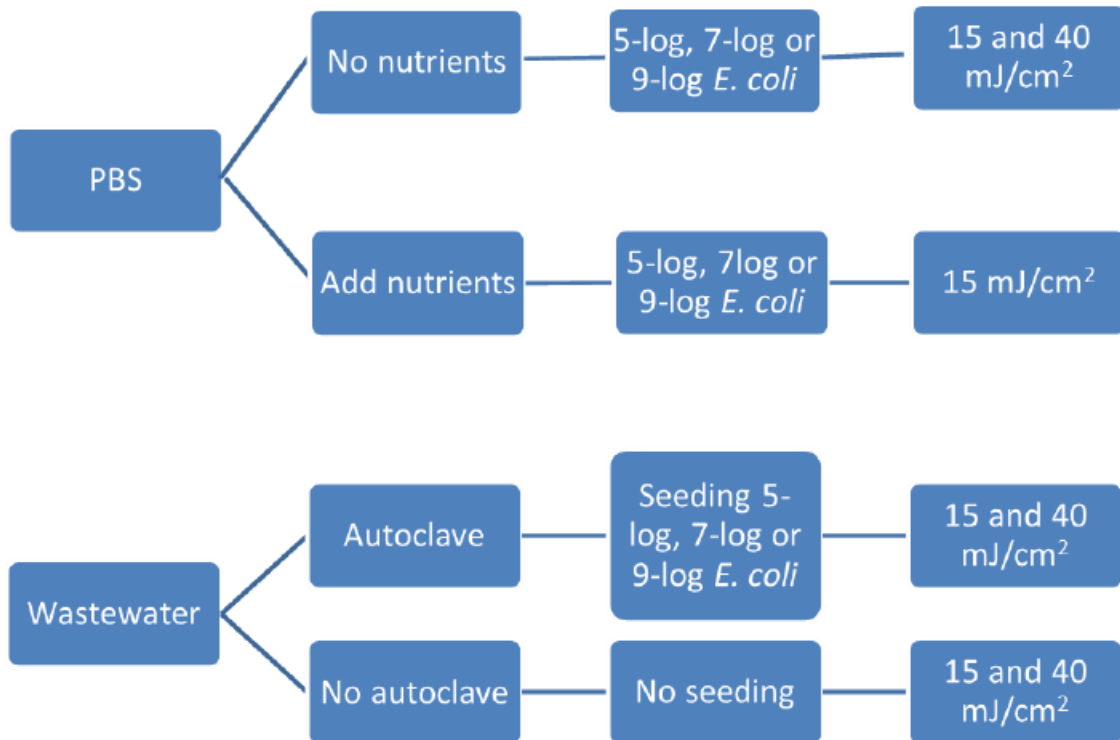


Figure 7.1: Experimental design.

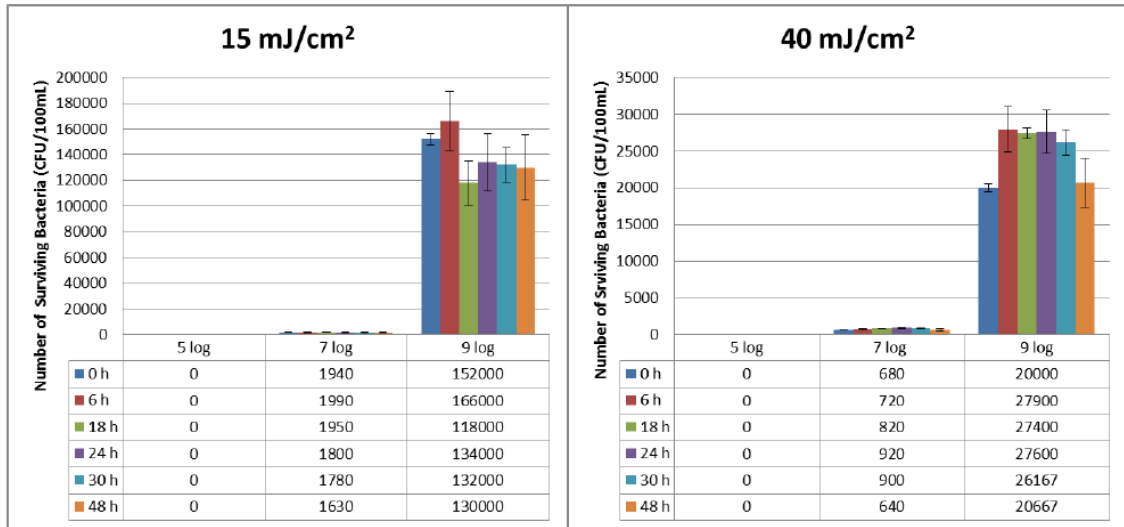


Figure 7.2: Number of surviving *E. coli* in PBS over 48 hours after exposure to 15 and 40 mJ/cm² when initial *E. coli* concentration was 5-, 7- or 9-log.

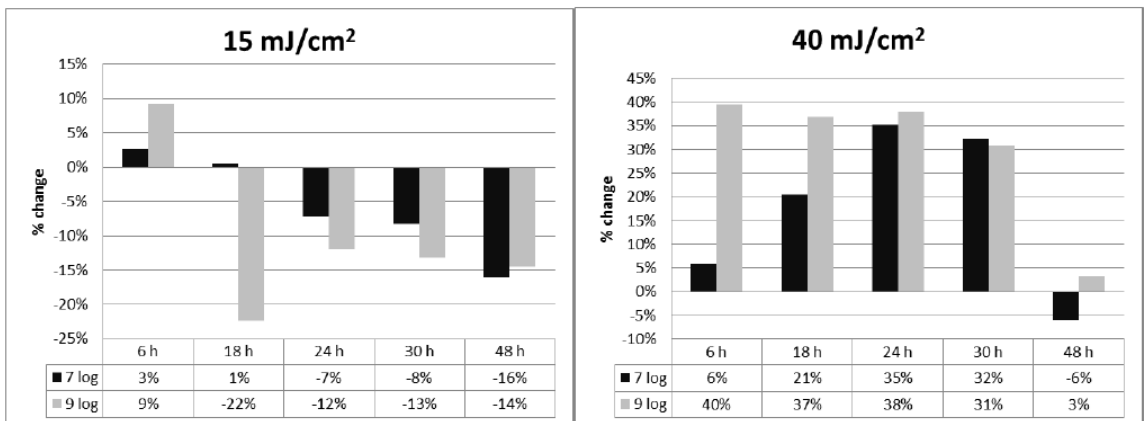


Figure 7.3: Percent change in *E. coli* concentration in PBS for the 7- and 9-log samples after exposure to 15 and 40 mJ/cm².

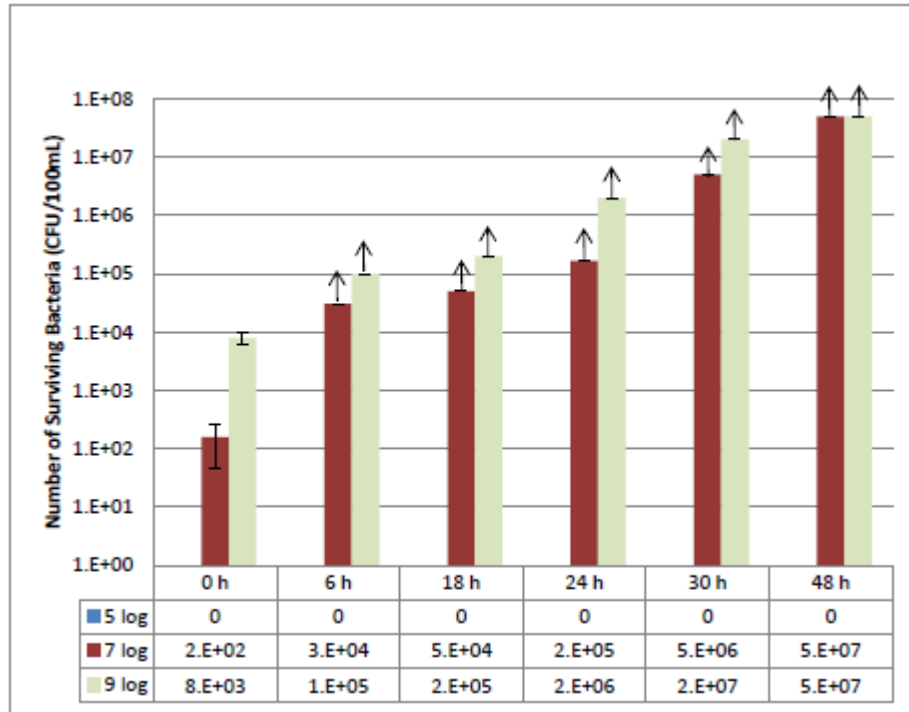


Figure 7.4: Number of surviving *E. coli* in nutrient enriched PBS over 48 hours after exposure to 15 mJ/cm² when initial *E. coli* concentration was 5-, 7- or 9-log. Arrows show that the actual *E. coli* concentrations were higher than the measured values.

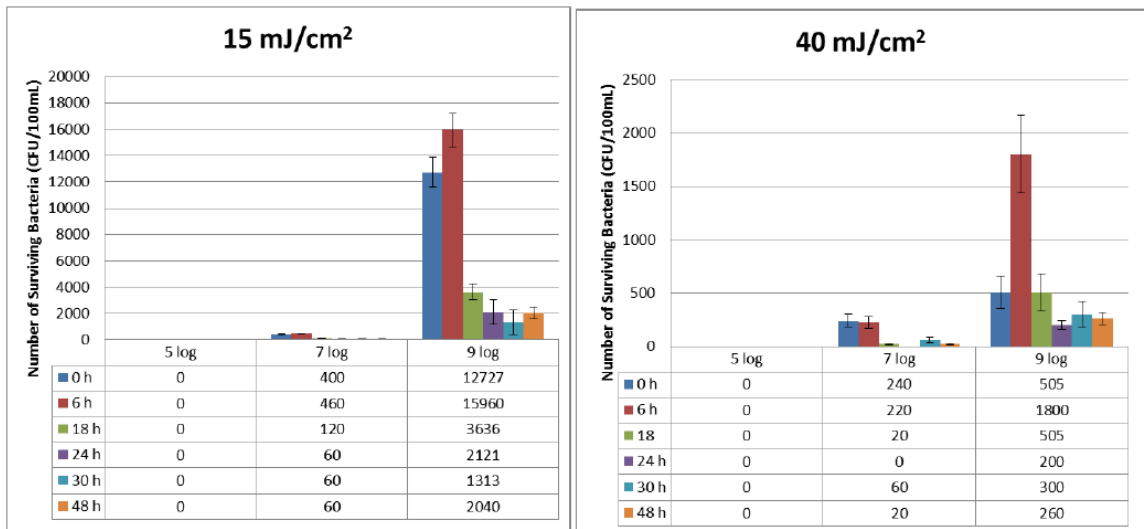


Figure 7.5: Number of surviving *E. coli* in autoclaved secondary wastewater over 48 hours after exposure to 15 and 40 mJ/cm² when initial *E. coli* concentration was 5-, 7- or 9-log.

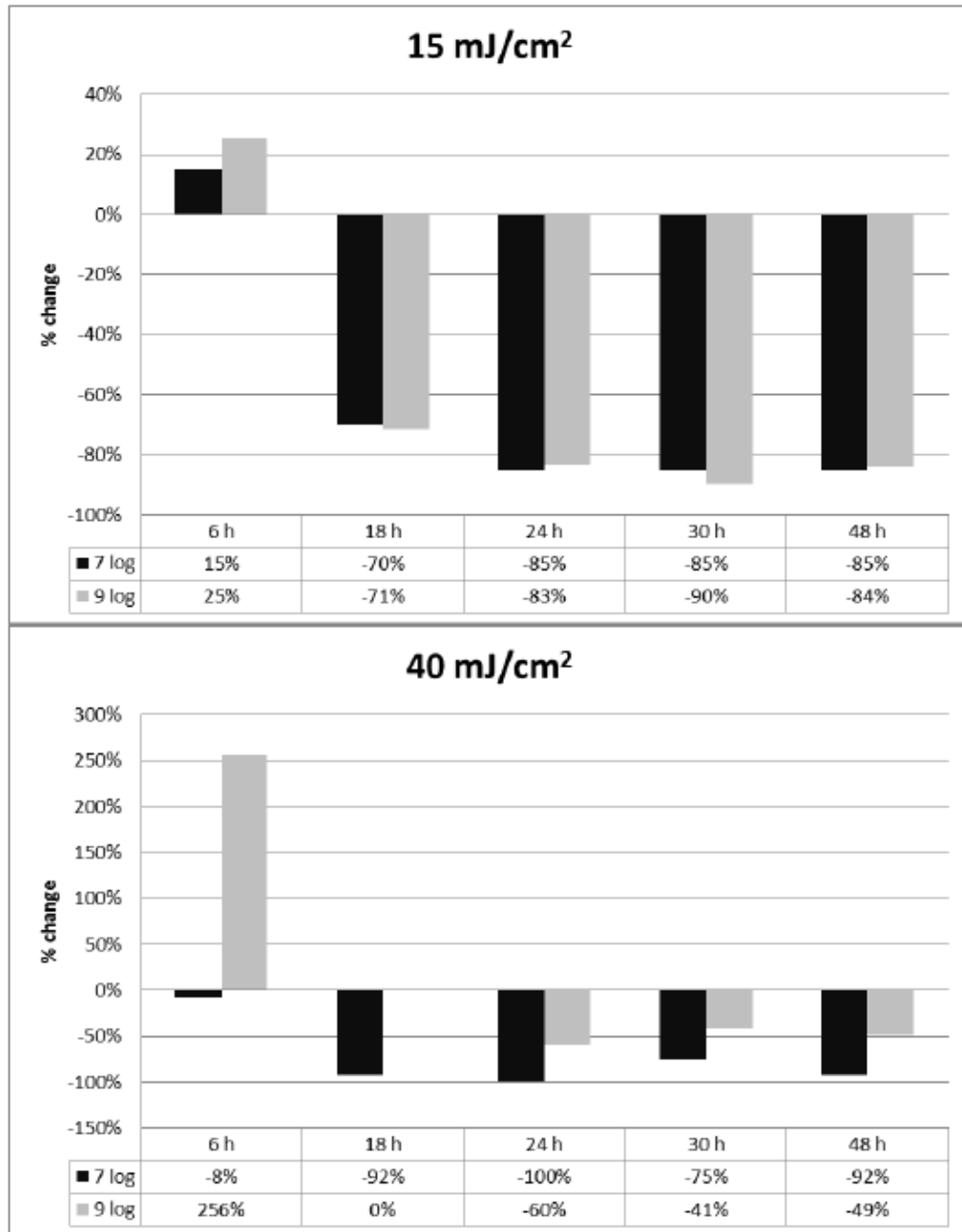


Figure 7.6: Percent change in *E. coli* concentration in autoclaved wastewater for the 7- and 9-log samples after exposure to 15 and 40 mJ/cm².

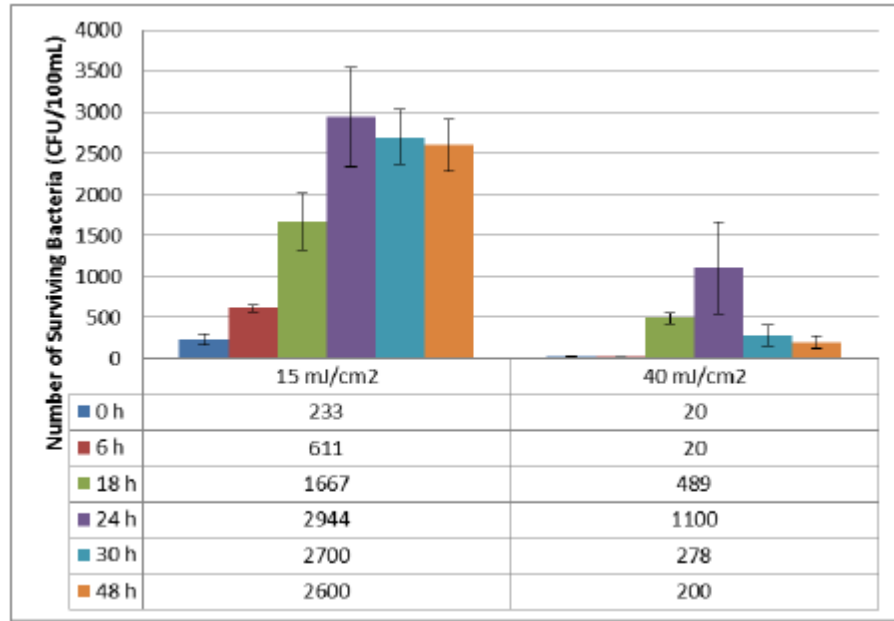


Figure 7.7: Number of surviving total coliform in wastewater over 48 hours after exposure to 15 and 40 mJ/cm².

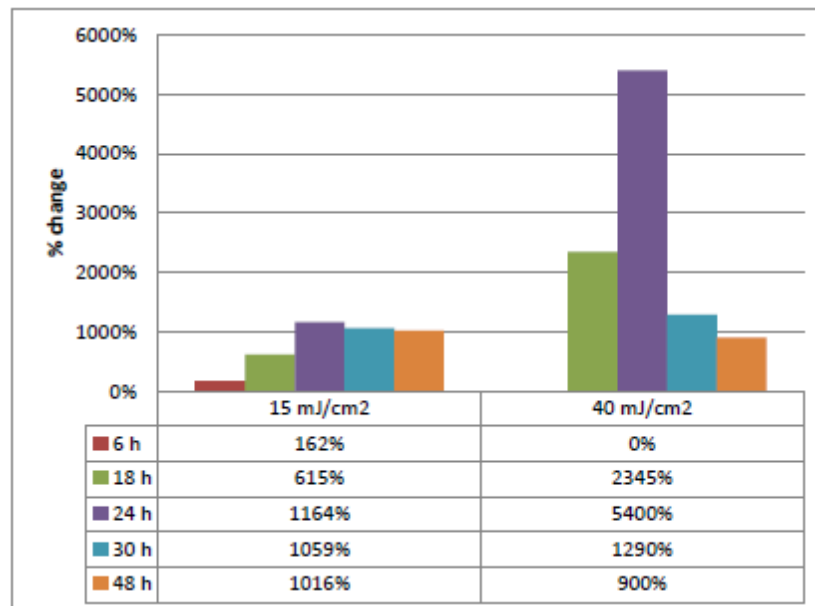


Figure 7.8: Percent change in total coliform concentration in wastewater over 48 hours after exposure to 15 and 40 mJ/cm².

CHAPTER 8

CONCLUSIONS AND SUGGESTIONS FOR FUTURE RESEARCH

Several conclusions and promising future research directions emerged from this work. Detailed conclusions are presented in each chapter. The most important ones are summarized below.

The first theme addressed in this research was that the effect of flocculation and flocs on UV disinfection is a complex matter. For instance, at UV doses lower than 9 mJ/cm², neither particle size nor degree of flocculation had a significant effect on the inactivation of *E. coli* primarily because the inactivation process was dominated by dispersed bacteria, and embedded bacteria did not determine the ultimate level of inactivation. At high UV doses, and for larger particles and well-flocculated samples a statistically significant effect of particles and bioflocculation on UV disinfection of *E. coli* could be observed. In addition, the size of particles and flocs was not the only factor playing an important role in determining the overall efficacy of UV disinfection. Several other factors related to microbe, particle, and solution characteristics such as shape, structure and porosity of the flocs, need to be understood as well. In this thesis, some of the complexity of the situation was overcome by using a synthetic floc system where bioflocculation was simulated in the laboratory, but closely mimicked the actual natural process. This allowed for a complete control over particle size and shape, and yielded high reproducibility. Even so, bioflocculation resulted in irregularly shaped flocs that are not very circular and quite porous. Furthermore, larger flocs had a more heterogeneous structure with higher

variation in shape and porosity compared to smaller flocs. Circularity and porosity parameters were observed to be strongly correlated with the degree of flocculation. UV disinfection experiments showed that the magnitude of variance in floc size, structure and porosity were closely reflected in the inactivation data where a 1-log difference among the replicates could be seen for highly flocculated samples.

The second theme highlighted was that even in the absence of already existing flocs and flocculating agents, the UV-induced self-aggregation of bacteria might lead to formation of relatively large flocs and hinder UV irradiation efficacy. In this study, *E. coli* were observed to self-aggregate upon exposure to low-pressure UV light in all of the doses tested. UV dose did not seem to be an important factor in determining the degree of induced aggregation. However, when the bacteria were irradiated with medium-pressure UV light, there was a significant difference between a dose of 40 mJ/cm² and 80 mJ/cm². Low-pressure and medium-pressure UV lights significantly differ from one another in terms of the wavelength of UV light generated, light intensity and the exposure times needed for an equivalent dose. Any of these parameters might have an important role in determining how much bacteria self-aggregate. The longer exposure time and lower UV light intensity experiments resulted in lower levels of aggregation, which further supports the role light intensity might play in initiating the UV-induced self-aggregation process.

The third theme researched in this work was on regrowth potential of *E. coli* and indigenous wastewater coliform after being exposed to UV radiation. An important

finding in this study was that regrowth of both *E. coli* and indigenous wastewater bacteria were higher after being irradiated at 40 mJ/cm² than at 15 mJ/cm². Although counterintuitive at first, when approached from a nutrient centric perspective, it became clear that more nutrients would become available at higher UV doses (hence, more regrowth would occur) due to a higher degree of cell lysis following the disinfection process. Even in the absence of any apparent nutrients, significant regrowth of *E. coli* was observed in PBS indicating that the lysis of UV-damaged cells was likely providing the food source for the surviving bacteria. Moreover, addition of nutrients did not boost dark repair of *E. coli* under the conditions tested but greatly increased its regrowth. These findings highlight the importance of evaluating regrowth and reactivation potentials of bacteria separately as possible control strategies and consequences would differ greatly.

With respect to the overarching goal of safer water and better protection of public health, many challenges remain. This research makes a contribution to the field of water and wastewater disinfection by addressing some of the major issues surrounding UV disinfection efficacy. The following recommendations for future research are based on the results and conclusions presented in this thesis.

One suggestion for future research is to investigate how well disinfectants other than UV irradiation would perform under the bioflocculation conditions tested in this study. Other disinfectants can be evaluated alone or in combination with UV. A detailed study of sequential disinfection's role in promoting the efficacy of UV irradiation in the presence

of particles and flocs would be a valuable contribution to the field of water and wastewater disinfection. Additional future work can also be undertaken to further investigate UV-induced aggregation in different water matrices than the one studied in this work. For instance, whether UV irradiation propels attachment of microbes onto particles, in addition to self-aggregating, in a particle rich medium can be examined. Finally, molecular methods can be used to measure residual cell activities, such as membrane integrity, respiratory activity and transport activity, following UV irradiation to determine the time frame of cell lysis in conjunction with regrowth studies.

APPENDIX A: ADDITIONAL DATA FOR CHAPTER 5

Table A.1: Number concentrations of very large flocs.

Calcium Concentration	Starting Particle Size		
	3.2 μm	11 μm	25 μm
	flocs > 10 μm (#/mL)	flocs > 17 μm (#/mL)	flocs > 33.5 μm (#/mL)
0 mM	6	9	112
5 mM	13	23	149
10 mM	241	244	284
15 mM	395	329	238